

**CHEMICAL CHARACTERIZATION AND SPECIATION OF THE MACRO
NUTRIENTS IN THE ATMOSPHERIC PARTICLES DRY AND WET
DEPOSITION MODES OVER THE EASTERN MEDITERRANEAN:
SOURCE AREAS, BIO-AVAILABILITY AND IMPACT OF ATMOSPHERIC
INPUTS ON MARINE PRODUCTIVITY**

A THESIS SUBMITTED TO
THE GRADUATE SCHOOL OF MARINE SCIENCES
OF
MIDDLE EAST TECHNICAL UNIVERSITY

BY

MÜNEVVER NEHİR

IN PARTIAL FULFILLMENT OF THE REQUIREMENTS
FOR
THE DEGREE OF MASTER OF SCIENCE
IN
OCEANOGRAPHY

SEPTEMBER 2016

Chemical Characterization and Speciation of the Macro Nutrients in the Atmospheric Particles, Dry and Wet Deposition Mode over the Eastern Mediterranean: Source Areas, Bio-Availability and Impact of Atmospheric Inputs on Marine Productivity

Submitted by **MÜNEVVER NEHİR** in partial fulfillment of the requirements for the degree of **Master of Science in Oceanography, Institute of Marine Sciences, Middle East Technical University** by,

Prof. Dr. Ahmet Kıdeys _____

Director, Graduate School of Marine Sciences, METU

Prof. Dr. Süleyman Tuğrul _____

Head of Department, Oceanography Dept., METU

Assist. Prof. Dr. Mustafa Koçak _____

Supervisor, Oceanography Dept., METU

Examining Committee Members:

Assist. Prof. Dr. Mustafa Koçak _____

Oceanography Dept., METU

Prof. Dr. Cemal Saydam _____

Environmental Engineering, Hacettepe University

Prof. Dr. Zahit Uysal _____

Marine Biology and Fisheries Dept., METU

Date: **09.09.2015**

I hereby declare that all information in this document has been obtained and presented in accordance with academic rules and ethical conduct. I also declare that, as required by these rules and conduct, I have fully cited and referenced all material and results that are not original to this work.

Name, Last name : Münevver NEHİR

Signature :

ABSTRACT

CHEMICAL CHARACTERIZATION AND SPECIATION OF THE MACRO NUTRIENTS IN THE ATMOSPHERIC PARTICLES, DRY AND WET DEPOSITION MODES OVER THE EASTERN MEDITERRANEAN: SOURCE AREAS, BIO-AVAILABILITY AND IMPACT OF ATMOSPHERIC INPUTS ON MARINE PRODUCTIVITY

NEHIR, Münevver

M.Sc. in Oceanography

Supervisor: Assist. Prof. Dr. Mustafa Koçak

Middle East Technical University

September 2016, 96 pages

Two stage aerosol (coarse: PM_{10-2.5} and fine: PM_{2.5}) and rainwater samples were collected at a rural site (Erdemli) located on the coast of the eastern Mediterranean, between January 2014 and April 2015. Concentrations of the water-soluble nitrogen species (organic nitrogen (WSN), nitrate, ammonium, total nitrogen (WSTN) and urea) were measured in a total of 740 aerosol and 23 rainwater samples. Among the nitrogen species, WSN ($24.6 \pm 16.3 \text{ nmol N m}^{-3}$) denoted the highest arithmetic mean and followed by ammonium and nitrate concentrations in aerosol samples. Approximately 61% of the WSN was associated with coarse particles though the remaining fraction (39%) was accompanied with fine particles. Correspondingly, WSN contributions to WSTN in coarse and fine mode were found to be around 47.6 and 28.1 %. The volume weighted mean concentration of WSN was around $21.5 \mu\text{M N}$ in rainwater. Relative contribution of WSN to WSTN ($73.5 \mu\text{M N}$) was 29.3 % in rainwater. The urea mean concentration in coarse mode with standard deviations of $2.7 \pm 2.7 \text{ nmol N m}^{-3}$ and in fine mode $1.7 \pm 1.7 \text{ nmol N m}^{-3}$. Around 61 % of the urea was associated with coarse mode aerosol, whilst the remaining 39 % was associated with fine mode aerosol. Urea relative contributions to WSTN in coarse and fine mode were 8.5 and 4.9 %, and to WSN in coarse and fine mode were 18 and 18 %, respectively.

The daily variability in the concentration of water-soluble nitrogen species including WSN and urea may be an order of magnitude. The lowest concentrations of water-soluble nitrogen species were found to be associated with rainy days.

Relatively higher values of these water-soluble species were observed in summer and these concentrations might be attributed to the lack of wet deposition and re-suspension of cultivated soil. However, water-soluble organic nitrogen and urea exhibited the highest concentrations when air masses back trajectories originated from desert regions located at North Africa and the Middle East. For instance, one of the highest WSON ($66.1 \text{ nmol N m}^{-3}$) and urea ($19.8 \text{ nmol N m}^{-3}$) concentrations were observed on March 2, 2014 when the air mass back trajectories originated from Sahara and the Middle East deserts.

Monthly mean concentrations of WSON and urea in coarse mode indicated inverse correlations with rain amount which suggested that these particles were removed from atmospheric compartment efficiently by wet deposition. Moreover, WSON and urea in coarse particles demonstrated inverse relationship with temperature and it might be ascribed to re-suspension of cultivated soil.

During the study period 45 dusty days were determined by a sharp increase in the concentration of nns-Ca^{2+} . Regarding dust and non-dust event, WSON and urea demonstrated 1.3 and 2 times higher concentrations during dust events compared to those of observed for non-dust events, respectively. The mineral dust episodes also affected the relative distributions of particles, coarse mode being dominant during the dust-events.

The lowest WSON concentration was associated with air masses originated from Russia while the highest values were observed airflow from the Middle East and North Africa. The calculated $\text{PM}_{10-2.5}/\text{PM}_{2.5}$ ratios of WSON for these airflows were higher than 1.15, denoting dominance of coarse fraction. The lowest urea concentrations were found when airflow derived from Russia, Northern Turkey and Middle East, with concentrations of 2.7, 2.9 and $2.3 \text{ nmol N m}^{-3}$, respectively. Whereas, there was a distinct difference between their $\text{PM}_{10-2.5}/\text{PM}_{2.5}$ ratio, suggesting airflow from Russia and Northern Turkey was equally influenced by fine and coarse particles whilst air masses from Middle East was mainly dominated by coarse particles. It might be argued that airflow originating from Middle East had more natural sources compared to anthropogenic sources.

Positive matrix factorization (PMF) analysis was applied to clarify sources of WSON and urea. Results denoted that 77 % and 10 % of the WSON was derived from

the re-suspension of cultivated soil and sea-salt particles, respectively. Nevertheless, 27 % of the urea was held by re-suspension of cultivated soil while 49 % of urea was found to be associated with nitrate, implying reaction between alkaline urea and acidic nitrate.

Atmospheric fluxes of WSON and nitrate were almost equally influenced by dry and wet deposition, whereas ammonium flux was dominated by wet deposition (92 %). Annually, the atmospheric fluxes of WSON and nitrate were calculated 20.5 and 21.6 mmol m⁻² yr⁻¹, respectively, whilst the atmospheric ammonium flux was found 15.6 mmol m⁻² yr⁻¹. Based upon to detected new production in the surface waters of the Eastern Mediterranean, the atmospheric water-soluble nitrogen fluxes were determined to assist 33 % of the production in coastal waters and 76 % of the production in open waters. The observed new production between June and October when stratification occurs was found to be around 2 C mg m⁻² day⁻¹. During this period, atmospheric nitrogen can support new production in the Cilicia Basin up to 6 times.

Keywords: aerosol, wet deposition, water-soluble nitrogen species, mineral dust, long range transport, atmospheric input, marine productivity, Eastern Mediterranean.

ÖZ

DOĞU AKDENİZ'DEKİ ATMOSFERİK PARÇACIKLARIN, KURU VE YAŞ ÇÖKELLERİNDE MAKRO BESİN TUZU İÇERİKLERİNİN BELİRLENMESİ VE TÜRLEŞTİRİLMESİ: KAYNAK BÖLGELER, BİYO-KULLANILABİLİRLİK VE ATMOSFERİK GİRDİLERİN DENİZSEL ÜRETİME ETKİSİ

NEHİR, Münevver

Yüksek Lisans Tezi, Oşinografi Anabilim Dalı

Tez Yöneticisi: Yrd. Doç. Dr. Mustafa Koçak

Orta Doğu Teknik Üniversitesi

Eylül 2016, 96 Sayfa

İki kademeli aerosol (İri: $PM_{10-2.5}$ ve İnce: $PM_{2.5}$) ve yağmur suyu örnekleri, Ocak 2014 ve Nisan 2015 tarihleri arasında, Doğu Akdeniz'in kıyısındaki Erdemli kırsal bölgesinde toplanmıştır. Toplam 740 aerosol ve 23 yağmur suyu örneğinde suda-çözünebilir azot türleri (organik azot (SÇOA), nitrat, amonyum, toplam azot (SÇTA) ve üre) konsantrasyonları belirlenmiştir. Azot türleri arasında, en yüksek aritmetik ortalamayı SÇOA ($24.6 \pm 16.3 \text{ nmol N m}^{-3}$) gösterirken sırasıyla amonyum ve nitrat takip etmiştir. SÇOA'nın yaklaşık % 61'i iri parçacıklara eşlik ederken, kalan % 39'u ince parçacıklarla ilişkilendirilmiştir. SÇOA'nın SÇTA'ya katkısı iri ve ince parçacıklarda sırasıyla % 47.6 ve % 28.1'dir. Yağmur suyunda belirlenen SÇOA'un hacim ağırlıklı ortalama konsantrasyonu $21.5 \mu\text{M N}$ 'dir. Göreceli katkılar düşünüldüğünde yağmur suyu örneklerinde SÇTA'nın ($73.5 \mu\text{M N}$) % 29.3'ünün SÇOA'dan kaynaklandığı tespit edildi. İri ve ince parçacıklarda belirlenen ortalama üre konsantrasyonu sırasıyla $2.7 \pm 2.7 \text{ nmol N m}^{-3}$ ve $1.7 \pm 1.7 \text{ nmol N m}^{-3}$ 'dir. Ürenin % 61'i iri parçacıklarla ilişkiliyken, kalan 39 %'u ince parçacıklarla ilişkilidir. SÇTA'a ürenin göreceli katkısı iri parçacıklarda % 8.5, ince parçacıklarda % 4.9 ve SÇOA'ya ürenin göreceli katkısı hem iri hem ince parçacıklarda %18 olarak hesaplanmıştır.

Suda-çözünebilir azot türlerinin, SÇOA ve üre de dahil olmak üzere, konsantrasyonlarındaki günlük değişim bir kaç mertebeyi bulabilir. Bu türlerin en düşük derişimleri yağmurlu günlerle ilişkili bulunmuştur. Suda-çözünebilir azot türlerinde göreceli yüksek derişimlerin yazın gözlenmesi, yağ çökelpmenin olmamasında ve ekilen toprağın yeniden süspansiyeye olmasına atfedilmiştir. Ne ki,

SÇOA ($66.1 \text{ nmol N m}^{-3}$) ve üre ($19.8 \text{ nmol N m}^{-3}$) için en yüksek konsantrasyonlar Kuzey Afrika ve Orta Doğu çöl bölgelerinden kaynaklanan hava kütlelerinde gözlenmiştir. Örneğin, en yüksek SÇOA ($66.1 \text{ nmol N m}^{-3}$) ve üre ($19.8 \text{ nmol N m}^{-3}$) konsantrasyonlarından biri 2 Mart 2014'te, Sahra ve Orta Doğu çöllerinden kaynaklanan hava kütlesi geri yörüngeleriyle ilişkilendirilmiştir.

İri parçacıklarda belirlenen aylık ortalama SÇOA ve üre konsantrasyonlarının yağmur miktarı ile ters ilişkili olması bu parçacıkların atmosferik kompartmandan yağmur ile etkili bir şekilde uzaklaştırıldığını göstermektedir. Yine iri parçacıklarda belirlenen aylık ortalama SÇOA ve üre konsantrasyonlarının sıcaklık ile ters ilişkili olması ekili toprağın yeniden süspansiyeye olmasına atfedilebilir.

Çalışma süresince, nss-Ca^{2+} konsantrasyonundaki ani artışlar ile 45 adet toz olayı tespit edilmiştir. Tozsuz günlere kıyasla, SÇOA ve üre konsantrasyonları toz epizodlarında sırasıyla 1.3 ve 2 kat artış göstermiştir. Mineral toz olayı ayrıca parçacıkların iri ve ince modlarda göreceli dağılımlarını da etkilemiştir, toz etkinliklerinde parçacıkların çoğu iri modda bulunmuştur.

En düşük SÇOA derişimleri Rusya'dan gelen hava kütlesiyle ilişkilendirilirken, en yüksek SÇOA derişimleri Orta Doğu ve Kuzey Afrika'dan gelen hava kütlelerinde gözlenmiştir. Bu hava kütlelerinde SÇOA için, $\text{PM}_{10-2.5} / \text{PM}_{2.5}$ oranı, 1.15'ten yüksek olarak hesaplanmış ve iri parçacıkların baskın olduğunu belirlenmiştir. En düşük üre konsantrasyonları Rusya, Kuzey Türkiye ve Orta Doğu'dan kaynaklanan hava kütleleriyle ilişkiliyken sırasıyla konsantrasyonlar 2.7, 2.9 ve $2.3 \text{ nmol N m}^{-3}$ 'dir. Oysa, $\text{PM}_{10-2.5} / \text{PM}_{2.5}$ oranları belirgin bir fark gösterirken; Rusya ve Kuzey Türkiye'den gelen hava kütleleri iri ve ince parçacıklardan eşit olarak, Orta Doğu kaynaklı hava kütleleri daha çok iri parçacıklardan etkilenmiştir. Orta Doğu'dan gelen hava kütlelerinin antropojenik kaynaklara kıyasla daha çok doğal kaynaklardan etkilendiği ileri sürülebilir.

SÇOA ve ürenin kaynaklarını belirlemek için Pozitif Matriks Faktörizasyon (PMF) uygulanmıştır. Elde edilen sonuçlar, SÇOA'nın % 77'sinin ekili toprağın yeniden süspansiyeye olmasından ve % 10'unun deniz-tuzu parçacıklarından kaynaklandığını göstermiştir. Bununla beraber, ürenin % 27'si ekili toprağın yeniden süspansiyeye olmasına ve % 49'u asidik nitrat ve alkali üre arasındaki reaksiyona atfedilmiştir.

S COA ve nitratın atmosferik akıları kuru ve yař  kellerden neredeyse eřit olarak etkilenirken, amonyum akısı yař  kel tarafından domine edilmiřtir (%92). S COA ve nitratın yıllık atmosferik akısı sırasıyla 20.5 ve 21.6 mmol N m⁻² yıl⁻¹ olarak hesaplanırken amonyumun yıllık atmosferik akısı 15.6 mmol N m⁻² yıl⁻¹ olarak hesaplanmıřtır. Doęu Akdeniz'in kıyı ve a ık y zey sularında belirlenen yeni  retim, sırasıyla % 33 ve % 76'sının atmosferik azot akılarınca saęlanabileceęi hesaplanmıřtır. Tabakalařmanın g zlendięi Haziran ve Ekim ayları arasında yeni  retim yaklaşık olarak 2 C mg m⁻² g n⁻¹ bulunmuřtur. Bu d nemde, atmosferik azot Kilikya Havzası'nda yeni  retime 6 kata kadar destekleyebilir.

Anahtar kelimeler: aerosol, yař  kel, suda- z nebilir azot t rleri, mineral toz, uzun erimli tařınım, atmosferik girdi, denizsel  retim, Doęu Akdeniz.

Dörtnala gelip Uzak Asya'dan
Akdeniz'e bir kısrak başı gibi uzanan
bu memleket, bizim.

Bilekler kan içinde, dişler kenetli, ayaklar çıplak
ve ipek bir halıya benziyen toprak,
bu cehennem, bu cennet bizim.

Kapansın el kapıları, bir daha açılmasın,
yok edin insanın insana kulluğunu,
bu dâvet bizim....

Yaşamak bir ağaç gibi tek ve hür
ve bir orman gibi kardeşesine,
bu hasret bizim...

Nazım Hikmet Ran

To my dearest family;

Ebru - Adnan and Anıl Nehir

and my beloved grandmother Tülay Durma

ACKNOWLEDGEMENTS

I am heartily thankful to my supervisor, Assist. Prof. Dr. Mustafa Koçak for his guidance, endless encouragement, teaching, supervision, support at every phases of this work. He is more than a supervisor or a lecturer, a model human and scientist for me. It was my honor to work with him.

I thank to my jury members Prof. Dr. Cemal Saydam and Prof. Dr. Zahit Uysal for their valuable comments and suggestions.

I am grateful to my colleagues, Ersin Tutsak for supplying cluster analysis of air mass back trajectories and Gültekin Yılmaz for his companionship.

I extend my gratitude to Pınar Kalegeri for her endless support in the laboratory and her friendship, I am grateful to our technical staff Merve Yeşildağ, Ramazan Ülger and Mehmet Durmaz and thanks to crews of the LAMAS1 for their kind assistance.

My deepest thanks to my family for everything they added to my life.

My special thanks to Benedikt Pellengahr for his deep understanding, continuous support, kindness and helping me in every situation.

My sincerest thanks to Ayşe Gazihan for her supports, valuable advices and cheerfulness.

I would also like to acknowledge all the friends in Setüstü.

This work was supported by The Scientific and Technological Research Council of Turkey (TUBITAK). Required data were collected within the framework of the TUBITAK 113Y107 project. This study was also supported by the DEKOSIM (Center for Marine Ecosystem and Climate Research) Project (BAP-08-11-DPT.2012K120880) funded by Ministry of Development of Turkey.

Many thanks to Mersin Meteorology Station for supplying daily rain dataset.

I also acknowledge to the GIOVANNI, MODIS and OMI mission scientists and associated NASA personnel for the production of the data used in this research effort.

TABLE OF CONTENTS

ABSTRACT	v
ÖZ	viii
ACKNOWLEDGEMENTS	xii
TABLE OF CONTENTS	xiii
LIST OF FIGURES	xv
LIST OF TABLES	xviii
1. INTRODUCTION	1
1.1. Aim of the Study	1
1.2. Overview of Atmospheric Aerosols	2
1.3. Long Range Transport of Atmospheric Aerosols to the Ocean	5
1.4. Removal of Water-Soluble Nitrogen Species from Atmospheric Compartment	6
1.5. Sources of Atmospheric Nitrogen	7
1.6. Mediterranean Sea and Potential Impacts of Atmospheric Inputs on Marine Productivity	8
2. MATERIALS AND METHODS	11
2.1. Sampling Sites Description	11
2.2. Atmospheric Sampling	12
2.2.1. Aerosol Collection	12
2.2.2. Wet and Dry Deposition Collection	13
2.3. Preparation of Samples for Analysis	14
2.4. Aerosol Chemical Analysis	15
2.4.1. Analytical Techniques	15
2.5. Formulas and Calculations	17
2.5.1. Estimation of Water-Soluble Organic Nitrogen (WSO _N)	17
2.5.2. Precision of Water-Soluble Organic Nitrogen (WSO _N)	18
2.5.3. Relative Contributions for Fine and Coarse Particles	18
2.5.4. Blank Contributions and Detection Limits for Water-Soluble Nitrogen Species	18
2.5.5. Settling Velocity	20

2.5.6. Calculation of Atmospheric Nitrogen Species Fluxes.....	20
2.5.7. Air Mass Back Trajectories.....	21
2.5.8. Application of Positive Matrix Factorization (PMF) for Source Apportionment.....	21
3. METEOROLOGY OF ERDEMLİ SAMPLING SITE AND AIR-MASSES BACK TRAJECTORIES.....	22
3.1. Meteorology.....	23
3.2. Air mass back trajectories and Cluster Analysis.....	26
4. WATER-SOLUBLE NITROGEN SPECIES IN AEROSOL AND RAINWATER IN THE EASTERN MEDITERRANEAN: SOURCES AND INFLUENCE OF THE MINERAL DUST EPISODE ON OBSERVED CONCENTRATIONS	29
4.1. General Characteristics of the Data.....	30
4.2. Comparison of Aerosol and Rainwater Water-Soluble Nitrogen Species concentrations with data from Literature	33
4.3. Daily variations of Water-Soluble Nitrogen Species in Aerosol and Rainwater at Erdemli	41
4.4. Seasonal variations of Water-Soluble Nitrogen Species in Aerosol at Erdemli	52
4.5. Influence of Mineral Dust Episodes on the Water-Soluble Nitrogen Species.....	63
4.6. Influence of Air Flow on Water-Soluble Nitrogen Species.....	71
4.7. Correlation between Water-Soluble Nitrogen Species and Major Ions	73
4.8. Application of PMF to Determine the Sources of WSON and Urea	79
4.9. Atmospheric Depositions of N-Species and Implications Regarding Marine Production.....	79
5. CONCLUSION AND RECOMMENDATIONS FOR FUTURE RESEARCH	82
REFERENCES	86

LIST OF FIGURES

Figure 1. 1. The origins of atmospheric aerosols on a global scale, estimated fluxes (Tg year ⁻¹) and particle size (Seinfeld and Pandis, 1998).	5
Figure 1. 2. The Mediterranean Sea, SeaWiFS image (Turley, 1999).	10
Figure 1. 3. Potential impacts of atmospheric input to nutrient (a) non-limited and (b) limited marine environments.	10
Figure 2. 1. Location of the rural sampling site Erdemli (36° 33' 54" N and 34° 15' 18" E) situated at the on the coastline of the Eastern Mediterranean.	11
Figure 2. 2. The relative blank contributions determined for water-soluble nitrogen species. Coarse particles (a) and fine particles (b).	19
Figure 3. 1. The rain rate (mm day ⁻¹) between 1998-2007 (Mehta and Yang, 2008).	24
Figure 3. 2. The number of rainy days per month (a), the amount of rainfall (b), and average temperature (c) between 2000 and 2015 obtained from Mersin meteorology station.	25
Figure 3.3. a. Cluster analysis of 3-days air mass back trajectories and air flow reaching Erdemli site at 1000 m altitude between January 2014 and April 2015.	27
Figure 3.3. b. Cluster analysis of 3-days air mass back trajectories and air flow reaching Erdemli site at 1000 m altitude between January 2014 and April 2015.	27
Figure 3.3. c. Cluster analysis of 3-days air mass back trajectories and air flow reaching Erdemli site at 3000 m altitude between January 2014 and April 2015.	28
Figure 3.3. d. Cluster analysis of 3-days air mass back trajectories and air flow reaching Erdemli site at 4000 m altitude between January 2014 and April 2015.	28
Figure 4. 1. The locations of stations used for literature comparison and corresponding concentrations for water-soluble (a), (b) nitrate and (c) ammonium (nmol N m ⁻³). Locations of sampling sites in the Black Sea, in the Eastern Mediterranean and in the Europe, MED -Cruise (Medinets 1996), A and F refers to Antalya (Güllü et al. 1998); and Finokalia (Kouvarakis et al. 2001), respectively, Amasra (Karakaş et al. 2004), Black Sea (BS-Cruise, Kubilay et al. 1995), Zmiinyi Island (Western Black Sea, Medinets and Medinets 2012), Sinop (Koçak et al., 2016) and Erdemli (current study).	37

Figure 4. 2. The daily variations in the concentrations of (a) water-soluble organic nitrogen (WSON), (b) nitrate (NO_3^-), (c) ammonium (NH_4^+), (d) water-soluble total nitrogen (WSTN) (nmol N m^{-3}), rain amount (mm) and determined concentrations of nitrogen species in rainwater ($\mu\text{M N}$) between January 2014 and April 2015 for PM_{10} aerosol samples.....	42
Figure 4. 3. 3-day backward trajectories (1, 2, 3 and 4 km height) and OMI (Ozone Mapping Instrument) Aerosol Index (AI) of air masses arriving at the Erdemli sampling site on 2 th of March 2014.	44
Figure 4. 4. 3-day backward trajectories (a, 1, 2, 3 and 4 km height) and OMI (Ozone Mapping Instrument) Aerosol Index (b, AI) of air masses arriving at the Erdemli sampling site on 19 th of November 2014.	45
Figure 4. 5. The daily variability of urea concentrations in PM_{10} (nmol N mol^{-3}) and observed rain amounts (mm) at Erdemli.	47
Figure 4. 6. 3-day backward trajectories (a, 1, 2, 3 and 4 km height) and OMI (Ozone Mapping Instrument) Aerosol Index (b, AI) of air masses arriving at the Erdemli sampling site on 8 th of March 2014.	48
Figure 4. 7. 3-day backward trajectories (a, 1, 2, 3 and 4 km height) and OMI (Ozone Mapping Instrument) Aerosol Index (b, AI) of air masses arriving at the Erdemli sampling site on 18 th February 2014.	49
Figure 4. 8. 3-day air masses back trajectories corresponding to (a) 23 rd and (b) 24 th October 2014.	51
Figure 4. 9. 3-day air masses back trajectories corresponding to March 15, 2015. ...	52
Figure 4. 10. Monthly variation of average concentrations of WSON in fine and coarse particles (nmol N m^{-3}).	53
Figure 4. 11. Monthly mean concentrations for NH_4^+ (nmol N m^{-3}) in coarse and fine particles.	55
Figure 4. 12. Monthly mean concentrations for NO_3^- (nmol N m^{-3}) in coarse and fine particles.	55
Figure 4. 13. Monthly mean concentrations for urea (nmol N m^{-3}) in coarse and fine particles.	56
Figure 4. 14. The relationship between WSON (nmol N m^{-3}) and rain (mm) for both (a), (b) coarse and (c) fine particles.	58
Figure 4. 15. The relationship between WSON (nmol N m^{-3}) and temperature ($^\circ\text{C}$) for both (a), (b) coarse and (c) fine particles.	59

Figure 4. 16. (a) The relationship between water-soluble ammonium (nmol N m^{-3}) and rain (mm) and (b) temperature ($^{\circ}\text{C}$) for PM_{10}	60
Figure 4. 17. (a) The relationship between water-soluble nitrate (nmol N m^{-3}) and rain (mm) and (b) The relationship between water-soluble nitrate (nmol N m^{-3}) when high monthly mean values are removed and rain (mm) for PM_{10}	61
Figure 4. 18. The relationship between water-soluble nitrate (nmol N m^{-3}) and temperature ($^{\circ}\text{C}$) for PM_{10}	62
Figure 4. 19. The relationship between (a) urea (nmol N m^{-3}) and rain amount (mm) (b) urea (nmol N m^{-3}) and temperature ($^{\circ}\text{C}$) in coarse mode (c) urea (nmol N m^{-3}) and rain amount (mm) and (d) urea (nmol N m^{-3}) and temperature ($^{\circ}\text{C}$) in fine mode.	63
Figure 4. 20. Observed nssCa^{2+} (dust threshold $> 2000 \text{ ng m}^{-3}$) concentration (ng m^{-3}) values between January 2014 and April 2015.	65
Figure 4. 21. 3-day air-mass back trajectories arriving at 1, 2, 3 and 4 km and OMI-AI corresponding to 24 th of February 2014.	66
Figure 4. 22. (a) 3-day air-mass back trajectories arriving at 1, 2, 3 and 4 km and (b) OMI-AI for 15 th of November 2014, (c) 3-day air-mass back trajectories arriving at 1, 2, 3 and 4 km and (d) OMI-AI for 16 th of November 2014.	67
Figure 4. 23. The possible impacts of atmospheric nitrogen to the new production in the coastal and open marine environment.	81

LIST OF TABLES

Table 1. 1. Global nitrogen oxide (NO _x) budget (Finlayson-Pitts and Pitts, adapted from 2000).....	5
Table 2. 1. The collected sample types, number of samples and dates during this study.	13
Table 2. 2. The summary of methods applied by Ion Chromatography for urea, water-soluble ammonium and water-soluble nitrate.	16
Table 2. 3. The blank contributions and detection limits of water-soluble nitrogen species and the uncertainties of WSON for coarse and fine blank filters (nmol N m ⁻³).	19
Table 4. 1. The statistical summary of the WSON, NO ₃ ⁻ , NH ₄ ⁺ and WSTN for aerosol (nmol N m ⁻³) and rainwater (μmol N L ⁻¹) samples at Erdemli during the period of January 2014 and April 2015.	32
Table 4. 2. The statistical summary of the urea for aerosol (nmol N m ⁻³) and rainwater (μmol N L ⁻¹) samples at Erdemli during the period of January 2014 and April 2015.	33
Table 4. 3. Comparison of WSON concentrations in aerosol (nmol N m ⁻³) and rainwater (μmol N L ⁻¹) samples for different sites of the World.	35
Table 4. 4. Volume-weighted mean concentrations for nitrate (NO ₃ ⁻) and ammonium (NH ₄ ⁺) in rainwater during the study period along with documented values obtained from literature.	39
Table 4. 5. The arithmetic mean concentrations of urea in aerosol and rainwater samples collected from different sites located around the Mediterranean, Atlantic and Pacific regions.	41
Table 4. 6. The statistical summary of aerosol species for (a) dust events (b) non-dust events at Erdemli.	70
Table 4. 7. The statistical summaries for WSON and urea mean concentrations (nmol N m ⁻³) according to the origination of air masses for non-dust events.	72
Table 4. 8. Correlation coefficients for (a) coarse (PM _{10-2.5}) and (b) fine (PM _{2.5}) particles for dust episodes.	75
Table 4. 9. Correlation coefficients for (a) coarse (PM _{10-2.5}) and (b) fine (PM _{2.5}) particles for non-dust events.	77

Table 4. 10. The results of PMF analysis that is used to determine the origins of WSON and urea.79

Table 4. 11. Summary of the WSON, NO_3^- , NH_4^+ and WSTN fluxes (F_d) in PM10 samples and WSON, NO_3^- , NH_4^+ contributions to WSTN in dry and wet depositions at Erdemli during the period of January 2014 and April 2015.80



1. INTRODUCTION

1.1. Aim of the Study

Aerosols play a central role in many global processes (such as biogeochemistry, atmospheric chemistry and climate) and public health (Arimoto, 2001, Satheesh and Moorthy, 2005; Chen et al., 2007; Herut et al., 2005, Paytan et al., 2009). From oceanographers point of view the atmospheric nutrient deposition has been considered as a vital source of the new primary production particularly for oligotrophic waters (Markaki et al., 2003; Herut et al., 2005, Paytan et al., 2009).

Determinations of the deposition of nitrogen species in the atmosphere were mainly based on inorganic nitrogen compounds, i.e., nitrate and ammonium. However, in 1990s studies were extended to include organic nitrogen compounds (Cornell et al., 1995; Russell et al., 1998; Paerl, 1993; Seitzinger and Sanders, 1999). It has been reported that atmospheric water-soluble organic nitrogen (WSON) is much more abundant than assumed, being approximately 30 % of total nitrogen deposition (Jickells, 2006). Furthermore, Duce et al. (2008) estimated that anthropogenic emission of atmospheric reactive nitrogen species including WSON might increase around 4-fold in total atmospheric nitrogen deposition to the ocean and around 11-fold in total nitrogen deposition in atmosphere from 1860 to 2030.

It is important to identify the origin and magnitude of atmospheric WSON since it can play a vital role in marine productivity. Aims of the current study were to; (a) enhance our knowledge about the possible impacts of atmospheric nitrogen inputs on coastal and open waters of the Eastern Mediterranean, (b) find out the soluble and bio-available fractions of atmospheric nitrogen species associated with atmospheric samples, (c) determine the origin of water-soluble organic nitrogen and urea in atmospheric samples.

1.2. Overview of Atmospheric Aerosols

The atmosphere is the layer of gases that surrounds the fragile Earth and makes conditions suitable for living organisms. The content and composition of the atmosphere can be divided into three main groups as follows: (i) Primary (major), (ii) Secondary (minor) and (iii) Trace. As it is well known, nitrogen (78 %) and oxygen (21 %) are primary or major components of the atmosphere whilst carbon dioxide, water vapor, argon, etc. are secondary or minor constituents. On the other hand, trace compounds, despite identifying very low quantities, (gases; such as ozone and atmospheric particles; for example mineral dust) might be originated from both natural and anthropogenic sources which influence human health and biogeochemical processes (Rosenfeld, 2000; Ramanathan et al., 2001; Arimoto 2001; Kleanthous et al., 2014).

Atmospheric Particles (Aerosols or Particulate Matter): Aerosol is referred to as a suspension of solid and liquid particles in gas. It is used to refer to the suspended particles. Another way of referring to the atmospheric particles or aerosols is particulate matter (PM) and PM_x defines the mass of the particles with an aerodynamic diameter lower than $X \mu\text{m}$. Generally, atmospheric particles have been divided into two classes according to their size: namely coarse ($d: 10\text{-}2.5 \mu\text{m}$) and fine ($d < 2.5 \mu\text{m}$). The coarse mode aerosol contains primarily sea salt and mineral dust derived from mechanical erosion of soils and desert sands.

When the mechanism and the origin of atmospheric particles are considered, atmospheric particles can be divided two groups; (a) Primary, (b) Secondary or (1) Natural and (2) Anthropogenic, respectively. Primary aerosols are formed by mechanical processes (i.e. suspension and/or breakup of particles from bulk material by the wind such as the mineral dust and sea salt) whilst secondary aerosols are characterized by gas to particle conversion (i.e. oxidation of gaseous sulfur dioxide to particle sulfate). Natural aerosols which are formed by mechanical processes or biological activities explain 92 % of atmospheric particles. The contribution of anthropogenic aerosols (motor vehicles, ships, fossil fuels, industrial activities, etc.) to atmospheric particles is 8 % (Figure 1.1). Atmospheric particles are complex mixtures of soluble and insoluble species that arise from natural sources like soil dust, sea salt and volcanoes and from anthropogenic activities such as combustion of fossil fuels.

Conceptually, atmospheric particles can be categorized into five main groups based on their chemical composition:

- a. Mineral Dust:** Mineral dust is one of the major components of the global atmospheric aerosol in terms of mass fluxes, radiative and climate impact, and nutrient deposition onto the oceans. It is lifted directly from soils in the source regions by winds. Soil particles are produced by the chemical weathering of rocks and by mechanical processes. Mineral dust mainly originates from desert areas of the world. The abundance of mineral in dust is also highly variable and reflects the source region. For example, particles from the Saharan desert indicated great variability in their mineralogical composition according to source area. Mineral dust aerosols are rich in crustal elements like Ca, Si, Al and Fe.
- b. Sea Salt:** Sea salt aerosols are enriched in Na^+ , Mg^{2+} , Cl^- and SO_4^{2-} . Sea salt aerosol is produced at the sea surface by the bursting of air bubbles resulting from air induced by wind (Blanchard and Cipriano, 1983) and account almost 25 % of the atmospheric aerosol burden. The production of sea salt aerosol and its size distribution is strongly related to wind speed. For example, sea salt size ranged from 0.05 to 150 μm in diameter under the wind speed up to 17 m s^{-1} (O' Dowd et al., 1997 and references therein).
- c. Nitrogen Containing Species:** Lightning, biological material (oxidation of organic nitrogen compounds) and nitrification-denitrification processes are natural sources whereas the combustion of fossil fuels, fertilizers, motor vehicles and nitric acid production are anthropogenic sources of nitrate (Prospero et al., 1996). Important precursors of aerosol nitrate are nitrogen monoxide (NO) and nitrogen dioxide (NO_2). The sum of NO and NO_2 is expressed as nitrogen oxides (NO_x). The main sink of NO_x is oxidation to nitric acid (HNO_3). Since HNO_3 is extremely soluble in water and highly reactive, it is rapidly removed from the atmosphere via precipitation and by direct deposition to surfaces. NO_x 's are important in terms of potential affect to air quality and climate. Tropospheric NO_x controls the ozone budget and at the same time it leads the amount of hydroxyl radical and formation of aerosol nitrate. NO_x can arise as a result of both anthropogenic and natural originated processes. Anthropogenic sources might be summarized as respectively, combustion of fossil fuels, combustion of bio-fuels

(mainly power plants), transportation (cars, ships and aircraft) and industrial activities. The main origin of NO_x is combustion processes however it can also be formed with the reaction between nitrogen in the air and oxygen during the high temperature combustion. The major component of NO_x which is formed in this way is NO and also NO_2 is formed in small amount by oxidation of NO. Natural sources of NO_x can be listed as soil, burning of vegetation and lightning. 60 % of NO_x is originated from anthropogenic activities whereas the contributions of terrestrial biogenic and burning of vegetation are 18 % and 15 %, respectively (Table 1.1).

- d. Sulfates:** Sulfates (SO_4^{2-}) are among the most important aerosol compounds in the atmosphere. The major precursors for sulfate aerosols are sulfur dioxide (SO_2) emitted from fossil fuel combustion and volcanoes, and oceanic emissions of biogenic dimethyl sulfide (DMS). SO_4^{2-} has many sources both natural and anthropogenic (Saltzman et al., 1986; Savoie et al., 1994; Mihalopoulos et al., 1997; Kouvarakis and Mihalopoulos, 2002; Kubilay et al., 2002). The anthropogenic sources of SO_4^{2-} are burning of coal, petroleum products, smelting of non-ferrous ores, manufacture of sulfuric acid, the conversion of pulp into paper, and refuse incinerators whilst natural sources are volcanic eruptions, sea-salt spray and soil dust sulfate emissions, biogenic emissions from oceans, plants, wetlands and soils and biomass burning. The term non-sea-sulfate (nssSO_4^{2-}) is used to distinguish between aerosol sulfate derived from seawater and from gypsum ($\text{CaSO}_4 \cdot 2\text{H}_2\text{O}$), biogenic and anthropogenic sulfates.
- e. Carbonaceous Particles:** Carbon-containing aerosols over the oceans are derived from a wide range of natural and anthropogenic processes and originate from both marine and continental environments. Black carbon and organic material are two main components of carbonaceous particles in the atmosphere. Black carbon can be derived from combustion processes. Organic matter can be directly emitted from sources or produced from atmospheric reaction with gaseous organic precursors (Seinfeld and Pandis, 1998; Raes et al., 2000).

Table 1. 1. Global nitrogen oxide (NO_x) budget (Finlayson-Pitts and Pitts, adapted from 2000).

Sources	NO _x (Tg year ⁻¹)
Anthropogenic	72
Burning of Vegetation	18
Terrestrial Biogenic	22
Oceans	0.01
Total	122

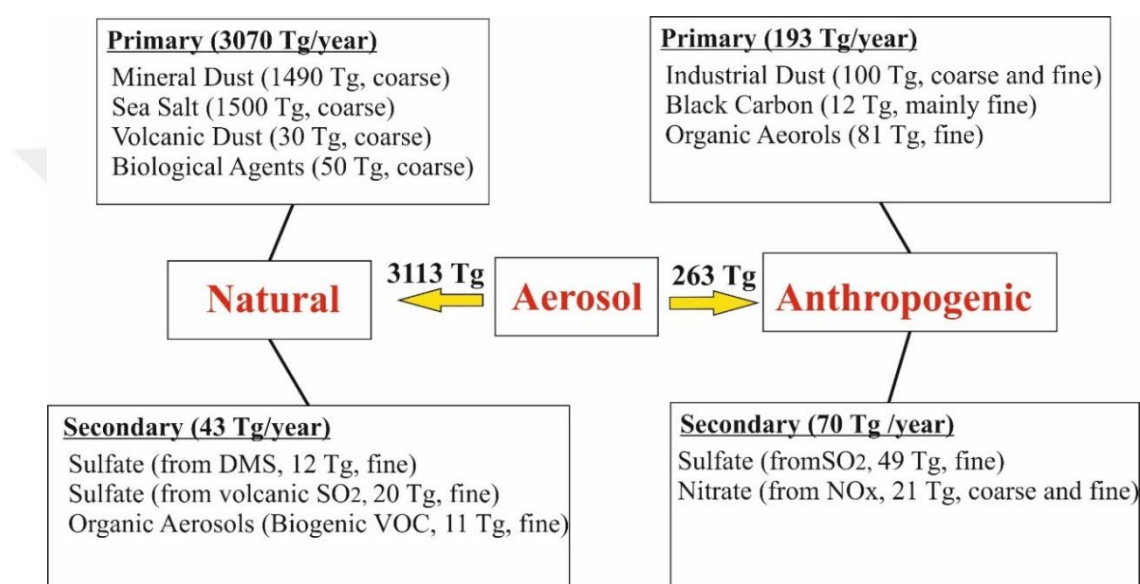


Figure 1. 1. The origins of atmospheric aerosols on a global scale, estimated fluxes (Tg year⁻¹) and particle size (Seinfeld and Pandis, 1998).

1.3. Long Range Transport of Atmospheric Aerosols to the Ocean

Aerosols originated from natural and anthropogenic sources contribute to the atmospheric particle burden on a global scale, traveling thousands of kilometers (Koçak, 2006). For instance, pollutants from continental regions might be determined in the Polar areas located at the Northern (Tuomi et al., 2003 and references therein) and Southern (Lowenthal et al., 2000; Mishra et al., 2004) hemispheres. Desert regions are the main sources of mineral dust particles. The extent of Saharan dust has been detected for various regions, including the North Atlantic (Carlson and Prospero, 1972), Europe (Borbely-Kiss et al., 1999), the Western Mediterranean (Loye-Pilot et al., 1986; Rodriguez et al., 2001) and Eastern Mediterranean (Kubilay and Saydam, 1995; Kubilay et al., 2000, 2005; Herut et al., 2001; Koçak et al., 2004a).

During long-range transport, atmospheric aerosols may react with gaseous, liquid species (O₃ organic gases, nitrogen, sulfur and sulfuric/nitric acids) and other particles because they provide reaction surfaces which cause the phase shift of many species (Mamane and Gottfried, 1989, 1992; Dentener et al., 1996; Usher et al., 2003). Through these reactions, the physical and chemical properties of aerosols altered which modify their solubility, optical, ice and cloud condensation nuclei properties (Spokes et al., 1994; Arimoto, 2001).

1.4. Removal of Water-Soluble Nitrogen Species from Atmospheric Compartment

Atmospheric particles can be removed from atmospheric compartment by (a) wet and (b) dry deposition. The measurements of organic nitrogen in precipitation were firstly made in the 1800s (Neff et al., 2002 and references therein). These early studies have shown that water-soluble nitrogen species were determined in both wet and dry deposition in various locations (Hendry and Brezonik, 1980; Lewis, 1981; Rendell et al., 1993; Cornell et al., 1995; Eklund et al., 1997). It has been determined that aerosols which contain macro and micro nutrients such as P, N and Fe can influence biogeochemical cycles of marine and coastal ecosystems by dry and wet depositions (Avila., et al., 1998; Guerzoni et al., 1999).

(a) Wet Deposition: The settling of atmospheric particles to Earth's surface by precipitation (rain, snow etc.) in cloud or below cloud is expressed as wet deposition (Seinfeld and Pandis, 1998). The precipitation below cloud depends on the efficiency of rainfall to collect atmospheric particles. Similar to dry deposition, the efficiency of collection of wet deposition is showing a decrease through a fine particle accumulation mode. However, precipitation in cloud is formed by combination of particles after collision to cloud/ice particles or by participating in cloud condensation nucleus and ice core.

(b) Dry Deposition: The settling of atmospheric particles to Earth's surface by the effect of gravitation is referred as dry deposition (Seinfeld and Pandis, 1998). Dry deposition usually described with settling velocities. The smallest dry deposition settling velocities are observed for a set of accumulation. Dry deposition rate increases as particle size decreases. Smaller particles have higher deposition rates

due to the Brownian motions (a random motion of particles due to the collision with molecules and atoms in gases). Dry deposition rate especially shows a considerable increase depending on the gravity for particles larger than 1 μm and plays a major role in the removal of coarse particles.

1.5. Sources of Atmospheric Nitrogen

Two main components of atmospheric nitrogen are inorganic and organic nitrogen. Nitrate (NO_3^-) and ammonium (NH_4^+) are the most discussed two species of inorganic nitrogen. NO_3^- is dominated by the reaction of gaseous nitric acid with alkaline sea salt and mineral dust particles whilst NH_4^+ is dominated by the reaction between gaseous alkaline ammonia and acidic sulfuric acid (Jickells et al., 2016). It has been shown that there are various possible sources of WSON originated from both natural and anthropogenic sources including organic nitrates, reduced organic N, dust and biological organic N (Neff et al., 2002; Cornell et al., 2003).

Nitrogenous end-products of marine species lead the natural sources of WSON (Antia et al., 1991). Neff et al. (2002) pointed out that oceans can be an important source of WSON for instance amino acids in aerosols derived from sea spray and gas phase amines released by marine species (Yang et al., 1994). In addition, agricultural fertilizers might be a significant source of WSON within these urea was the focus of previous studies (Glibert et al., 2005). Nitrogen species derived from agricultural fertilizers can enter the atmosphere with windblown and/or biomass burning. As population increase, the use of transportation vehicles and industrial processes are also increased which release large amounts of anthropogenic organic nitrogen to the atmosphere (Chen and Preston, 2004).

WSON is the most bio-available form of organic nitrogen in aquatic systems and it is possibly mineralized by marine microorganisms (Chen 2010, and references therein). It has been depicted that some forms of WSON might be directly used as a nutrient by primary producers (Antia et al., 1991; Murphy et al., 2000), some forms can be degraded to produce bio-available nitrogen and other forms can be harmful and toxic to some species (Chen and Preston, 1998; Cornell et al., 2003). WSON may act as a cloud condensation nuclei (Jacobson et al., 2000) and WSON in fog and clouds

explains from 10 to 17 % of the total dissolved nitrogen (Decesari et al., 2000; Collett et al., 2008).

Similar to WSON, urea can be originated from diverse natural and anthropogenic sources (Gilbert et al., 2005). Agricultural practices are one of the most important source of the urea since it is used as a nitrogen fertilizer and it may arise from industrial activities including manufacture of resins, glues, medicines, cosmetics and cleaning products (Violaki and Mihalopoulos, 2011 and references therein). Besides, it may result from metabolic processes of humans and marine species (Violaki and Mihalopoulos, 2011 and references therein).

1.6. Mediterranean Sea and Potential Impacts of Atmospheric Inputs on Marine Productivity

The Mediterranean is surrounded by two contrasting regions. The Northern Mediterranean shore is envired by industrialized and semi-industrialized regions, whilst the Southern and Eastern Mediterranean shores are bordered by arid and desert regions. The Mediterranean Sea is unique, being a semi-enclosed, with a narrow connection with the Atlantic Ocean through the Strait of Gibraltar; the connection is made to the Red Sea via the Suez Canal and the narrow Bosphorus strait connecting it to the smaller enclosed Black Sea (Turley, 1999). The Mediterranean Sea has low chlorophyll-a concentration when it is compared with Black Sea and chlorophyll-a concentration is decreasing from Western Mediterranean to Eastern Mediterranean (see Figure 1.2.).

The Mediterranean Sea is characterized by its oligotrophic (deficit in macro nutrients) surface waters and low primary productivity, defining as low nutrient and low chlorophyll (LNLC) region (Ediger et al., 2005 and references there in). When primary production and nutrients are considered, Mediterranean Sea can be defined as the desert of the world's oceans. The oligotrophy of Mediterranean is primarily resulted by its anti-estuarine circulation and hence the nutrient deficiency in the basin increases from west to east along with decreasing primary productivity (Krom et al., 2004, Pitta et al., 2005). The molar N/P ratio in the Eastern Mediterranean (25-28) is found to be higher than those of observed for Western Mediterranean (22) and the normal oceanic Redfield ratio of 16. Studies in the literature have shown the

significance and influence of atmospheric deposition of desert dust on the biogeochemistry of the Mediterranean Sea (Ridame and Guieu, 2002; Saydam and Şenyuva, 2002; Carbo et al., 2005; Herut et al., 2005). For example, adding dust experiment which is done by Herut et al. (2005) have revealed that chlorophyll-a and primary production could increase to 5 times. It has been hypothesized that Saharan dust pulses can cause phytoplankton blooms in summer (Ridame and Guieu, 2002) or in events of daytime dust deposition in wet conditions (Saydam and Şenyuva, 2002). Moreover, atmospheric organic nitrogen deposition to seawater can increase primary productivity (Wedyan and Fandi, 2007 and references there in). In order to demonstrate the influence of atmospheric organic nitrogen on phytoplankton productivity, Peierls and Paerl (1997) have been performed bioassay urea addition experiment. These authors showed that the addition of urea to the west Atlantic Ocean surface waters stimulated carbondioxide fixation (indicating increase in primary production) as much as nitrate and ammonium biassay experiments. Likewise, Zohary et al. (2005) have been carried out microcosm experiment in the P-limited Eastern Mediterranean and concluded that the lack of response of phytoplankton to the mesoscale P-enrichment was because of their N-starvation and biomass did not increase if both nutrients (P and N) were not added. Thus, the Eastern Mediterranean might be considered as being limited by both phosphorus and nitrogen (Zohary et al., 2005).

The potential impacts of atmospheric input to nutrient (a) non-limited and (b) limited marine environments are presented in Figure 1.3. If there is no limitation by nutrients, ecosystem does not give any response to atmospheric inputs and it is in steady state. However, CO₂ absorption and biogenic sulfur emission increase when there is an atmospheric input to marine environment when it is limited by nutrients. As CO₂ absorption and biogenic sulfur emission increase, primary and secondary productions also increase.

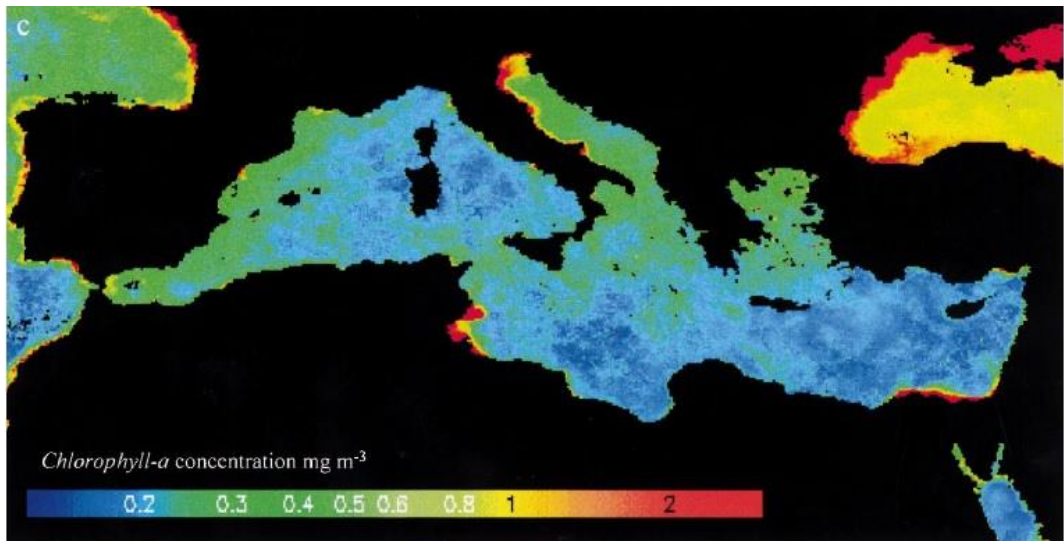


Figure 1. 2. The Mediterranean Sea, SeaWiFS image (Turley, 1999).

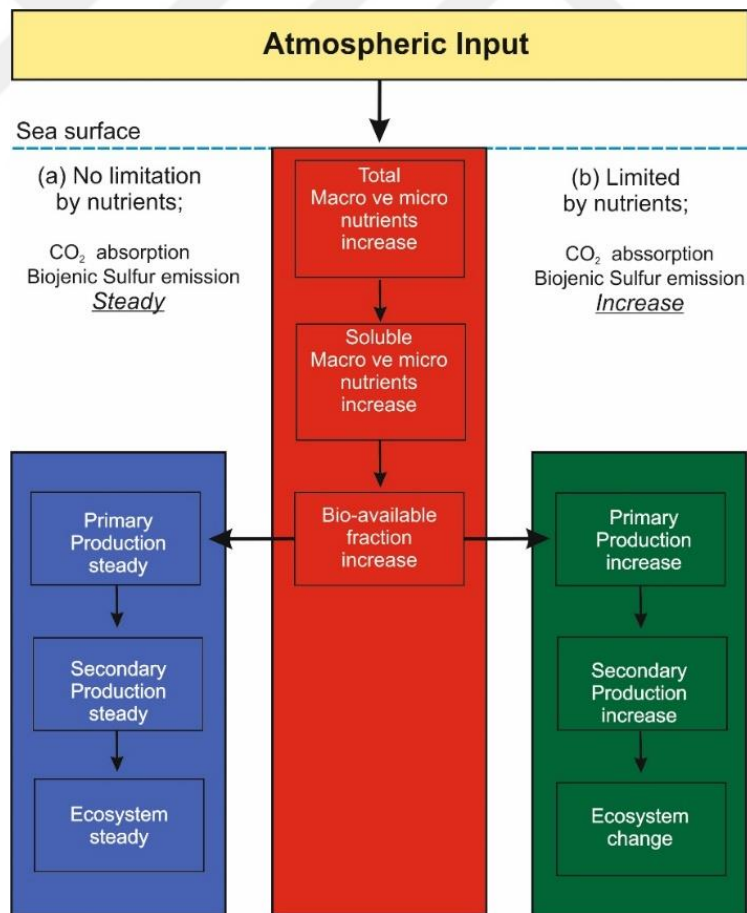


Figure 1. 3. Potential impacts of atmospheric input to nutrient (a) non-limited and (b) limited marine environments.

2. MATERIALS AND METHODS

2.1. Sampling Sites Description

Aerosol and rainwater sampling were carried out at a rural site located on the coastline of the Eastern Mediterranean, Erdemli, Turkey ($36^{\circ} 33' 54''$ N and $34^{\circ} 15' 18''$ E, Figure 2.1.). The sampling tower (above sea level ~ 22 m, ~ 10 m away from the sea) is situated at the Institute of Marine Sciences, Middle East Technical University (IMS-METU). Beginning from the north, the sampling tower is surrounded by lemon trees and cultivated land while from the south, it looks out over Northern Levantine Basin. Although it is not under direct influence of any industrial activities, the city of Mersin with a population of 800.000 is located 45 km to the east of the sampling site (Kubilay and Saydam, 1995, Koçak et al., 2012). The climate over the sampling location is similar to that observed for Mediterranean with a mild, humid winters and dry summers. The relatively long spring season (March-May) is characterized by unsettled winter type weather associated with North African cyclones (Kubilay et al., 2000) and the relatively short autumn season exhibits likewise unsettled weather conditions (Brody and Nestor, 1980).

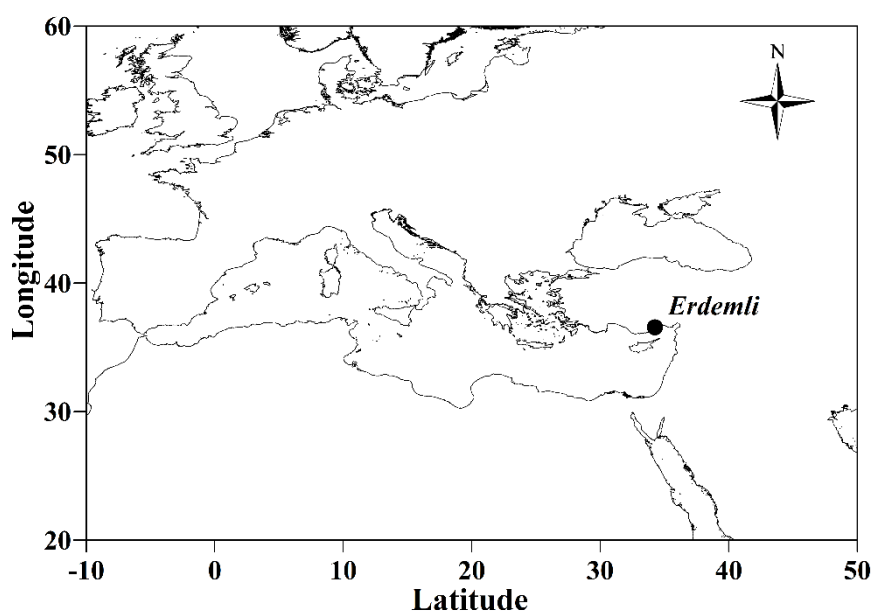


Figure 2. 1. Location of the rural sampling site Erdemli ($36^{\circ} 33' 54''$ N and $34^{\circ} 15' 18''$ E) situated at the on the coastline of the Eastern Mediterranean.

2.2. Atmospheric Sampling

The collected sample types, number of samples and sampling period for the current study is presented in Table 2.1.

2.2.1. Aerosol Collection

Atmospheric particles were collected from the atmosphere by filtration method. Thus, air was filtered through a filter by applying vacuum pump. A Gent type stacked filter unit (SFU) was used to collect aerosol filter samples in two size fraction namely, coarse (diameter between 10-2.5 μm) and fine (diameter less than 2.5 μm) (Hopke et al., 1997; Koçak et al., 2007). SFU was designed to load two size fraction filters consecutively. The first section of SFU was loaded with apiezon covered polycarbonate filter with pore size 8 μm (Whatman Track Etched 111114, circle diameter: 47 mm), whilst the apiezon covered polycarbonate filter with pore size 0.4 μm (Whatman Track Etched 111107, circle diameter: 47 mm) loaded to the second section. Filters are covered with apiezon by the company to prevent bouncing of particles from the surface. SFU was placed in the black cylinder which was designed to prevent the intrusion of particles larger than 10 microns, after setting a vacuum pump approximately 16.5 L min^{-1} vacuum, sampling was started. In order to minimize any possible contamination, the filter loading and unloading of SFU were achieved in a laminar air flow cabinet (clean dust free). To remove any possible particles from a laminar air flow cabinet, it was run for at least 15 minutes before the filter loading and unloading of SFU.

The sampling campaigns commenced in January 2014 and finished in April 2015. Over the sampling period a total of 740 aerosol samples, in two size fraction, were collected at Erdemli sampling site. The mean observational coverage of the aerosol sampling period was higher than 80 %. Sampling was stopped compulsorily from time to time due to technical malfunctions and cleaning of the apparatus.

2.2.2. Wet and Dry Deposition Collection

In addition to aerosol samples, wet and dry deposition samples were collected by using an automatic Wet/Dry sampler (Model ARS 1000, MTX Italy). The Wet/Dry sampler, which is equipped with rain sensor, worked automatically. The sampler device is designed to accommodate two identical buckets (0.0707 m² cylinders) and the lid is controlled by a rain sensor. The lid covered wet deposition bucket during the absence of rain while it tops dry deposition bucket in the course of rain. The influence of environmental factors were important on dry deposition whereas it had almost no impact on wet deposition samples. Although, the top of the dry deposition bucket was covered with 100 µm mesh to prevent intrusion of big particles and insects, the tiny bugs were found in dry deposition samples. The mesh was found to be broken into pieces by crows and corn cob pieces were also found in the buckets from time to time. Due to aforementioned factors, the dry deposition samples were prone to contamination, for example enormously high nutrient concentrations.

A total of 23 wet deposition samples were collected during sampling period. After each rain event, the rainwater samples were transferred into the laboratory for filtration (2 and 0.4 µm Whatman, polycarbonate filters). Dry deposition samples were diluted with 150 mL Milli-Q (18.2 Ω) water and the same inline filtration process was applied.

Table 2. 1. The collected sample types, number of samples and dates during this study.

Sample Type	Number of Samples	Date
Aerosol	740	January 2014 - April 2015
Coarse + Fine	370 coarse + 370 fine	
Dry Deposition	40	October 2014 - August 2015
Wet Deposition	23	October 2014 - April 2015

- (a) **Preparation of Filters:** The aerosol filters were retrieved equilibrated and weighed (0.01 mg sensitivity) after a 24 h collection period under well stabilized temperature and relative humidity (20 °C and 50 % RH).
- (b) **Storage of Atmospheric Samples:** Aerosol samples and subsamples of rainwater were kept frozen (-20 °C) directly after collection until analysis (not more than a month).
- (c) **Blank Filters:** Blank filters were taken during sampling period and they were treated just like sample filters without operating vacuum pump.

2.3. Preparation of Samples for Analysis

2.3.1. Preparation of Atmospheric Samples for Analysis

(a) **Preparation of Samples for Ion Chromatography Analysis:** For the determination of water-soluble ions in collected aerosol samples by ion chromatography instrument, one quarter of the filter was extracted for 60 minutes in 20 mL of ultra-pure water (18.2 Ωm) by mechanic shaker and about 100 µL chloroform was added as preservative to prevent biological activity after removing the filter (Bardouki et al., 2003, Koçak et al., 2007). On the other hand, collected subsamples of rainwater were kept in -20 °C until analysis.

(b) **Preparation of Samples for Water-Soluble Total Nitrogen Analysis:** 5 mL of the water-soluble samples were filtered with 0.4 µm pore size filters and prepared for analysis.

2.4. Aerosol Chemical Analysis

2.4.1. Analytical Techniques

2.4.1.1. Ion Chromatography (IC)

A various columns, executive phases, detectors and methods were used during the application of Ion Chromatography Instrument (Thermo-Dionex, ICS-5000). The summary of methods applied by Ion Chromatography for urea, water-soluble ammonium and water-soluble nitrate are presented in Table 2.2.

Water-Soluble Nitrogen Species: The concentrations of water-soluble nitrogen species were selected in the aqueous extracts of all aerosol, rainwater (wet deposition) and dry deposition samples. Water-soluble ammonium (NH_4^+) was detected electrochemically by using CS12-A separation column, MSA (20 mM) eluent and CSRS-300 (4 mm) suppressor while water-soluble nitrate (NO_3^-) was determined by applying AS11-HC separation column, KOH (30 mM) eluent and AERS-500 (4 mm) suppressor (Product Manual for Dionex IonPac AS11-HC-4m, IonPac CS12A Manual).

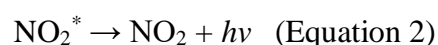
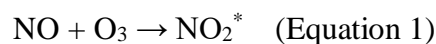
Urea: The urea concentrations were determined in the aqueous extracts of all aerosol rainwater (wet deposition) and dry deposition samples. Urea quantification was performed by Ion Chromatography (IC). MSA (20 mM) eluent, Dionex IonPac CS12 column, CS12 guard column and Variable Wavelength Detector were used at 190 nm wavelength.

Table 2. 2. The summary of methods applied by Ion Chromatography for urea, water-soluble ammonium and water-soluble nitrate.

Ion Chromatography	Urea (NH₂)₂CO	Water-Soluble Ammonium (NH₄⁺)	Water-Soluble Nitrate (NO₃⁻)
Guard Column	CG12	CG12A	AG11-HC
Separation Column	CS12	CS12A	AS11-HC
Loop	250 µL	15 µL	150 µL
Membrane Suppressor	-	CSRS (4mm)	ASRS (4 mm)
Eluent (Concentration) (Flow Rate)	MSA (20 mM) (0.5 mL/ min)	MSA (20 mM) (1.5 mL/ min)	KOH (30 mM) (1.5 mL/min)
Detector	Variable Wavelength (190 nm)	Conductivity	Conductivity

2.4.1.2. Water-Soluble Total Nitrogen (WSTN)

For the determination of water-soluble total nitrogen in aerosol and rainwater samples, the Torch Teledyne Tekmar TOC/TN instrument was used. While the sample was injected into the combustion furnace (750 °C), the N in the sample was converted to NO. Carrier gas (dry air with high purity) swept the sample gas to the PMT Chemiluminescence detector then the sample gas proceeded through the nitrogen module where NO interfered with ozone. NO₂ was comprised within the mobile phase (see Equation 1). When NO₂ turned to the quiet phase, extra energy was extracted as light ($h\nu$). This process was known as Chemiluminescence (see Equation 2). A light detector converted the light signals to electronic signals that allow amount determination. The Torch appointed the Chemiluminescence detector utilizing the light multiplexer line. The detected light quantity was directly proportional to the amount of NO in the sample gas. The last integrated area was then compared with the stored calibration data and the sample concentration in the unit of parts per million (ppm) was reported. The relative contributions of nitrogen species to WSTN will be given in the Chapter IV.



2.5. Formulas and Calculations

2.5.1. Estimation of Water-Soluble Organic Nitrogen (WSON)

Since there is no chemical analysis method to detect concentration of water-soluble organic nitrogen (WSON), it is calculated by subtracting water-soluble inorganic nitrogen (WSIN) from water-soluble total nitrogen (WSTN) (see Equation 3).

$$\text{WSON} = \text{WSTN} - \text{WSIN} \quad (\text{Equation 3})$$

WSIN refers to sum of NO₃⁻ and NH₄⁺.

2.5.2. Precision of Water-Soluble Organic Nitrogen (WSON)

WSON uncertainties were calculated by using formula (see Equation 4) suggested by Hansell (1993).

The calculated WSON uncertainties for fine particles, coarse particles and rainwater were 36.0 nmol N m⁻³, 40.0 nmol N m⁻³ and 90.0 μM N, respectively (see Table 2.3).

$$s_{\text{DON}} = (s_{\text{TDN}}^2 + s_{\text{TIN}}^2)^{1/2} \quad (\text{Equation 4})$$

2.5.3. Relative Contributions for Fine and Coarse Particles

Relative contributions (RC) for fine and coarse particles can be calculated by using the concentration of both fine and coarse concentrations (see Equation 5). It can be briefly expressed as follows:

$$\text{RC (\%)} = \left(\frac{\text{coarse or fine particle concentration}}{\text{coarse} + \text{fine particle concentration}} \right) \times 100 \quad (\text{Equation 5})$$

2.5.4. Blank Contributions and Detection Limits for Water-Soluble Nitrogen Species

The blank contributions and detection limits (standard deviation x 3) of water-soluble nitrogen species and the uncertainties of WSON for coarse and fine blank filters are presented in Table 2.3. The blank contributions for NO₃⁻, NH₄⁺, WSTN and urea were 0.31, 0.11, 2.2 and 0.02 nmol N m⁻³ whilst detection limits varied between 0.15, 0.05, 2.0 and 0.006 nmol N m⁻³ for coarse filters. For fine filters, the blank contributions were 0.13, 0.56, 2.3 and 0.02 nmol N m⁻³ with the detection limits 0.09, 0.39, 2.0 and 0.006 nmol N m⁻³ for NO₃⁻, NH₄⁺, WSTN and urea, respectively. In Figure 2.2., the relative blank contributions for NO₃⁻, NH₄⁺, WSTN and urea are presented for both coarse and fine particles.

Table 2. 3. The blank contributions and detection limits of water-soluble nitrogen species and the uncertainties of WSON for coarse and fine blank filters (nmol N m^{-3}).

Water-Soluble Nitrogen Species	Coarse Filters		Fine Filters	
	Blank	Detection Limit	Blank	Detection Limit
NO_3^-	0.31	0.15	0.13	0.09
NH_4^+	0.11	0.05	0.56	0.39
WSTN	2.2	2.0	2.3	2.0
Urea	0.02	0.006	0.02	0.006
	uncertainties		uncertainties	
WSON	36.0		40.0	

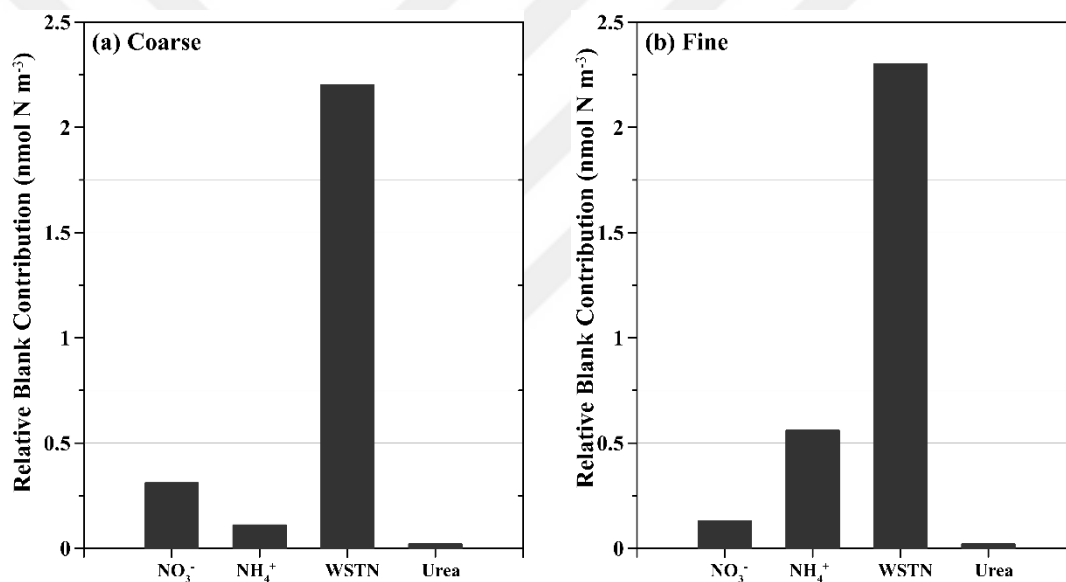


Figure 2. 2. The relative blank contributions determined for water-soluble nitrogen species. Coarse particles (a) and fine particles (b).

2.5.5. Settling Velocity

Settling velocity (V_d) is calculated as shown in the following equation (see Equation 6) (Koçak et al., 2010).

$$V_d = \left[\frac{C_f}{C_f + C_c} \right] \times 0.1 + \left[\frac{C_c}{C_f + C_c} \right] \times 2.0 \quad (\text{Equation 6})$$

C_f : mean concentration of species in fine particles

C_c : mean concentration of species in coarse particles

2.5.6. Calculation of Atmospheric Nitrogen Species Fluxes

The rain volume weighted average concentration (C_w) of nitrogen species can be calculated as follow:

$$C_w = \frac{\sum_{i=1}^n C_i \times Q_i}{\sum_{i=1}^n Q_i} \quad (\text{Equation 7})$$

where C_i is the nitrogen concentration and Q_i is the rainfall for the i_{th} precipitation event.

The wet and dry atmospheric fluxes of nitrogen species were calculated according to the procedure explained in Herut et al. (1999, 2002). The wet atmospheric deposition fluxes (F_w) were calculated from the annual amount of precipitation (P_{annual}) and the volume weighted mean concentration (C_w) of the substance of interest (see Equation 8).

$$F_w = C_w \times P_{annual} \quad (\text{Equation 8})$$

The dry deposition (F_d) of nitrogen species can be calculated as the product of atmospheric mean concentrations of species (C_d) and their settling velocities (V_d), where F_d is given in units of $\mu\text{mol m}^{-2} \text{yr}^{-1}$, C_d in units of $\mu\text{mol m}^{-3}$ and V_d in units of m yr^{-1} .

$$F_d = C_d \times V_d \quad (\text{Equation 9})$$

2.5.7. Air Mass Back Trajectories

3-days back trajectories of air masses arriving at the Erdemli station were computed by using the HYSPLIT Dispersion Model (HybridSingle Particle Lagrangian Integrated Trajectory; Draxler and Rolph, 2003). Four arrival elevations were selected: 1000, 2000, 3000 and 4000 meter altitudes. The cluster analysis of produced back trajectories were done by using K-means method in Statistica program in order to categorize trajectories (Cluster Analysis; Dorling et al., 1992).

2.5.8. Application of Positive Matrix Factorization (PMF) for Source Apportionment

In order to identify the sources of water-soluble nitrogen species at Erdemli, the receptor modeling tool *Positive Matrix Factorization* (PMF2 version 4.2, hereinafter referred to as 'PMF') has been applied. The tool which was developed by Paatero and Tapper (1994), with a detailed description in Paatero (2007), proved to be successful in assessing the source contribution to particulate matter (Paatero and Tapper, 1994; Huang et al., 1999; Lee et al., 1999; Viana et al., 2008; Koçak et al., 2009). The ability of PMF to constrain factor loadings and factor scores to non-negative values is important in regard to this study. Likewise, being able to process missing data and values below detection limits by adjusting the corresponding error estimates, has significance for it. Measured data constituting uncertainties has been assessed as the sum of the analytical uncertainties and 1/3 of the detection limit value. While values below the detection limit and missing data have been replaced by half of their detection limit and by their mean values. Below the detection limit uncertainties for values have been set at 5/6 of the detection limit whereas uncertainties of the missing data were adjusted to four times their mean concentrations (Polissar et al., 1998). The robust mode of PMF has been applied in this study to dataset since it can avoid extremely large values in the dataset, which can disproportionately affect the result.

3. METEOROLOGY OF ERDEMLİ SAMPLING SITE AND AIR-MASSSES BACK TRAJECTORIES

Both temporal and spatial variability of the atmospheric particles are significantly impacted by meteorological parameters namely rainfall, temperature, wind direction and air flow pattern (Kubilay and Saydam, 1995; Güllü et al., 1998; Mihalopoulos et al., 1997; Bardouki et al., 2003; Kubilay et al., 2002, 2005; Koçak et al., 2010). The removal of aerosols from the atmospheric compartment occur via combination of dry (not involving an aqueous deposition phase) and wet (precipitation scavenging) depositions. The dry deposition is a continuous mechanism in which the removal of aerosols is strictly regulated by particle size. On contrary, the wet deposition is a sporadic or rain specific process which is noticeably less dependent on the particle size, despite of the sequential removal of larger and smaller particles in single rain episode (Özsoy and Saydam, 2000). A number of studies in the atmosphere over the Eastern Mediterranean have clearly shown the influence of such parameters on aerosol chemical composition (Kubilay and Saydam, 1995; Mihalopoulos et al., 1997; Güllü et al., 1998; Kubilay et al., 2000; Bardouki et al., 2003; Koçak et al., 2004a, b). Aforementioned studies have demonstrated that lower concentrations of aerosol species in winter are related to wet precipitation scavenging however in the summer atmospheric particles are accumulated in the atmosphere as a consequence of (i) greater surface soil re-suspension and (ii) the lack of any significant rain events. Solar flux (or temperature) is also important meteorological parameter since, for instance, the elevated light levels resulted in high photochemical production of OH radicals and hence sulfate particles (Mihalopoulos et al., 2007). Furthermore, the history of air-masses affects the aerosol and rainwater chemical composition (Kubilay and Saydam, 1995; Özsoy and Saydam, 2000; Koçak et al., 2009, 2010). Elevated crustal dominated species (such as Al, Fe and Ca) in aerosol and rainwater is mainly associated with air flow from Sahara and the Middle East deserts whereas, high concentrations of pollution derived species (e.g., Ni and V) are chiefly connected with air flow originated from industrial countries located at Europe.

3.1. Meteorology

The climate of the Mediterranean is defined by mild, rainy winters and dry summers. Winter months (January, February and December) are dominated by rainfall whilst summer months (June, July and August) are described by dry and hot weather. The duration of the transitional seasons are different from each other. Although transition seasons are characterized by unsettled weather conditions, relatively longer spring season (March, April and May) is associated with North African cyclones (Kubilay et al., 2000) while autumn (October) is defined by weather change from summer to winter, lasting one month (Brody and Nestor, 1980).

As can be deduced from the Figure 3.1., the whole Mediterranean region is under the influence of rainfall during winter and autumn season (Mehta and Yang, 2008). Spring season has less rainfall when it is compared to autumn season. However, the Mediterranean Region is completely dry during the summer.

The number of rainy days per month, total rain amount and average temperature for a 15-year period (2000-2015) at Mersin is presented in Figure 3.2. It is determined that the seasonal cycle of the rainfall is similar to those observed for the whole Mediterranean. As expected, the local temperature exhibited an increase from winter months (10 °C) to spring and reached its maximum in July and August (28 °C). From September to November the temperature showed a gradual decline and in December it fell to expected seasonal levels. The number of rainy days had a similar pattern as rainfall. However, the decrease and/or increase between months were sharper for rainfall. It is observed that as the temperature increased, the rainfall and the number of rainy days decreased.

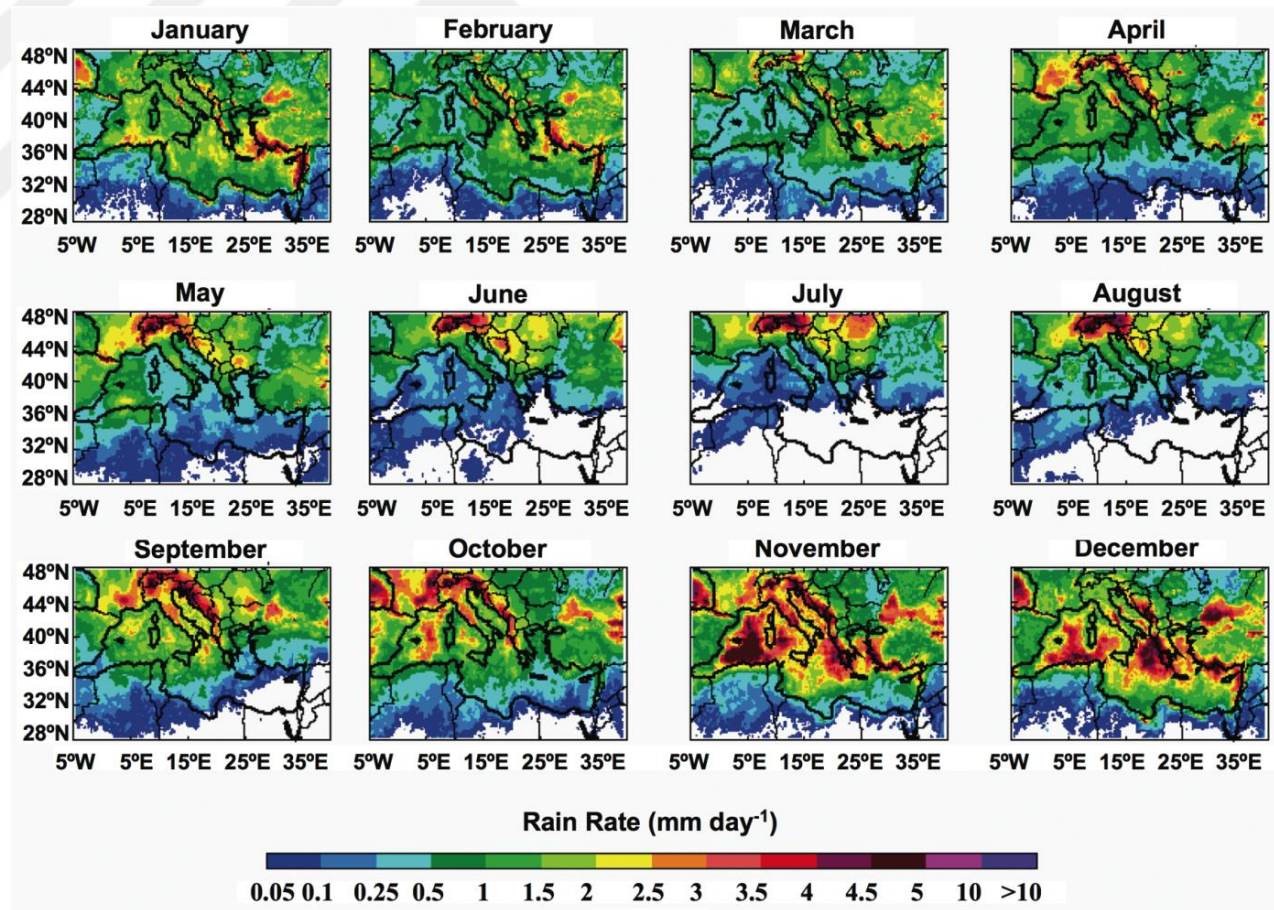


Figure 3. 1. The rain rate (mm day⁻¹) between 1998-2007 (Mehta and Yang, 2008).

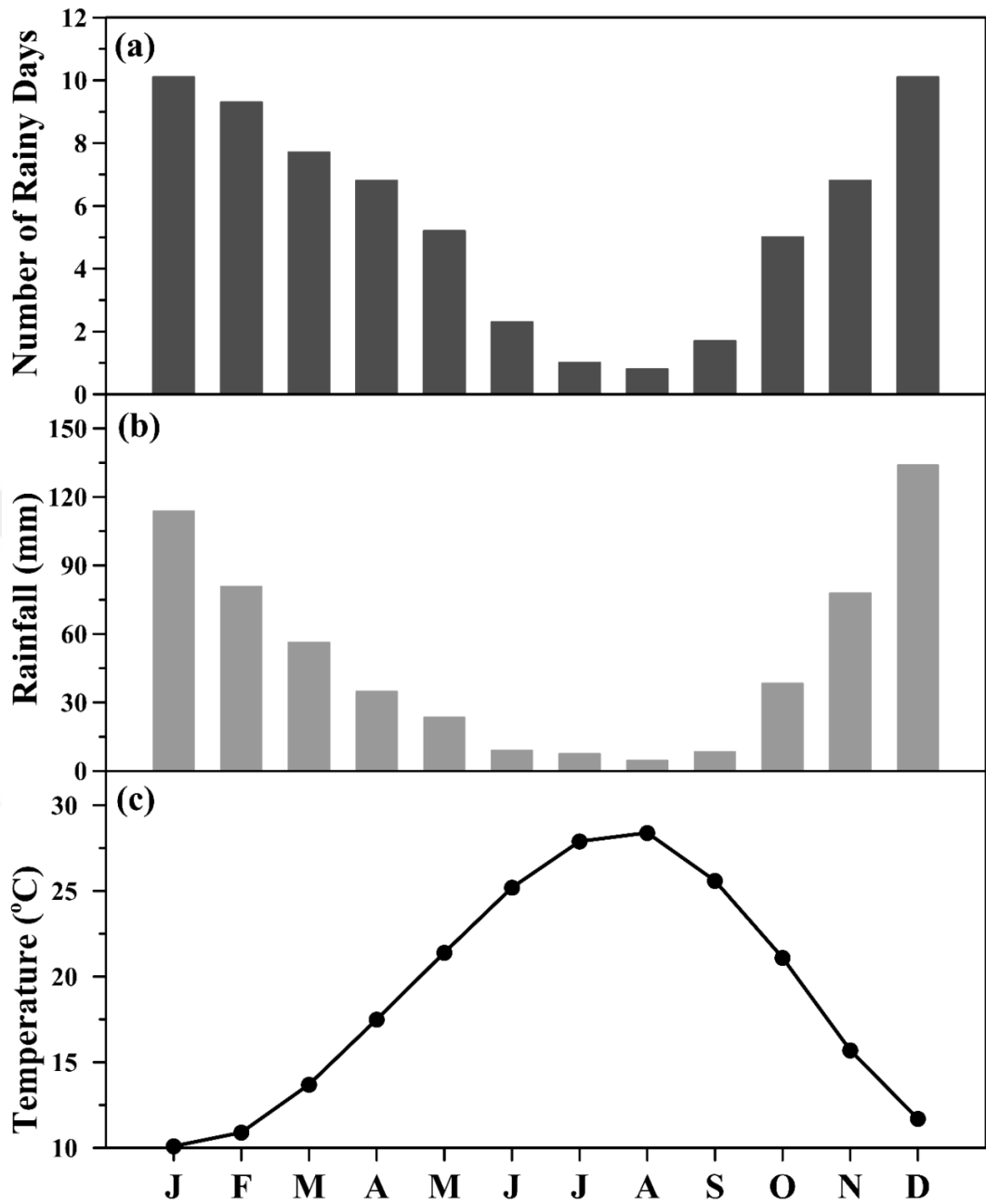


Figure 3. 2. The number of rainy days per month (a), the amount of rainfall (b), and average temperature (c) between 2000 and 2015 obtained from Mersin meteorology station.

3.2. Air mass back trajectories and Cluster Analysis

In order to cluster and compare the variability of air flow reaching at Erdemli site, 1000, 2000, 3000 and 4000 meter heights were selected. The Figures 3.3. a., b., c and d exhibit the means of clustered trajectories and calculated frequencies for each cluster between January 2014 and April 2015 for 1000, 2000, 3000 and 4000 meter altitudes, respectively.

Considering the air mass trajectories arriving at 1000 m altitude seven clusters can be defined. First cluster denoted air flow with low wind speed (short fetch) from West Turkey (WT), explaining 29.2 % of the air masses. The second cluster indicated trajectories from Western Mediterranean (WM), then passing through Italy, Greece and Aegean coast of Turkey, elucidating 7.8 % of the air flow. Air masses originating from Balkans (Cluster 3, NW) represented 8.7 % of the trajectories. The fourth cluster demonstrated air masses with high speed (long fetch) from North (NL), sweeping former Soviet Union/Black Sea and accounting for 4.1 % of the air flow. The fifth cluster represented trajectories with short fetch (low wind speed) from North Turkey (NT), elucidating 21.6 % of the air masses. The sixth and seventh clusters pointed out air flow from Middle East (ME) and Saharan desert (SAH), refining 16.5 % and 12.1 % of the air masses back trajectories, respectively.

When the classification for the trajectories arriving at different altitudes, namely 1000, 2000, 3000 and 4000 m compared a number of trend can be made. With the increasing altitude, the effect of distant sources, such as Saharan and European, increased. For instance, the % influence of Saharan air masses increased almost 4 times from 1000 m to 4000 m. On contrary, the % influence of local sources (e.g. short fetch trajectories from Turkey) decreased gradually with altitude. To illustrate, there was no air flow originating from Turkey at 4000 m height. The obtained results are in accordance with previous studies carried out in the region (Koçak et al., 2005).

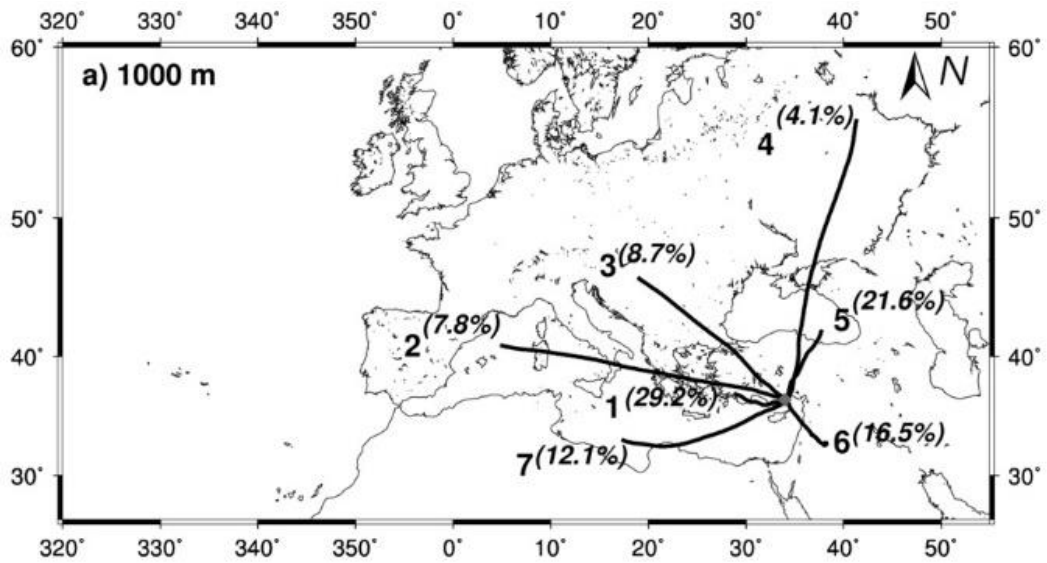


Figure 3.3. a. Cluster analysis of 3-days air mass back trajectories and air flow reaching Erdemli site at 1000 m altitude between January 2014 and April 2015.

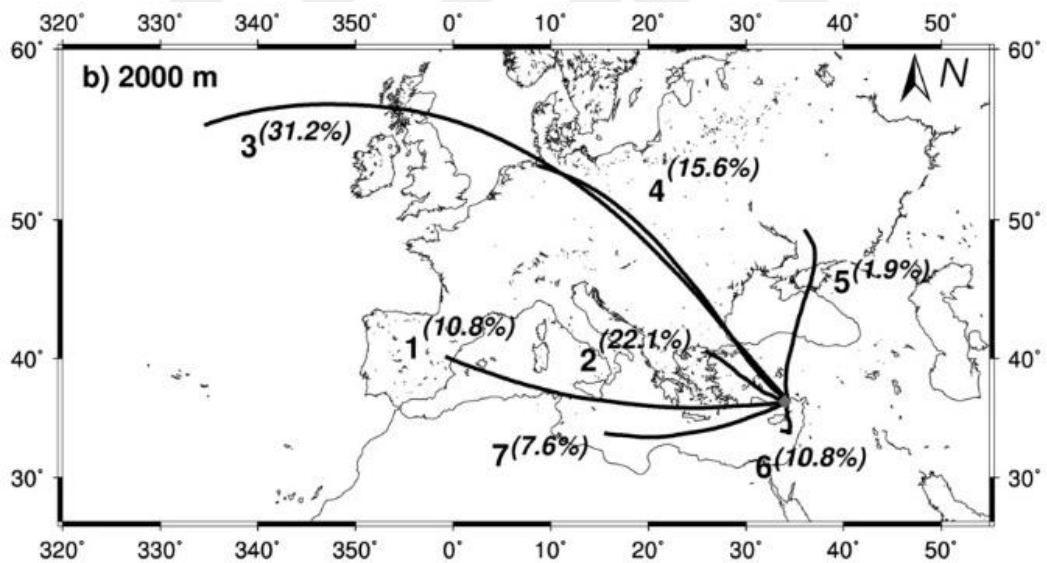


Figure 3.3. b. Cluster analysis of 3-days air mass back trajectories and air flow reaching Erdemli site at 1000 m altitude between January 2014 and April 2015.

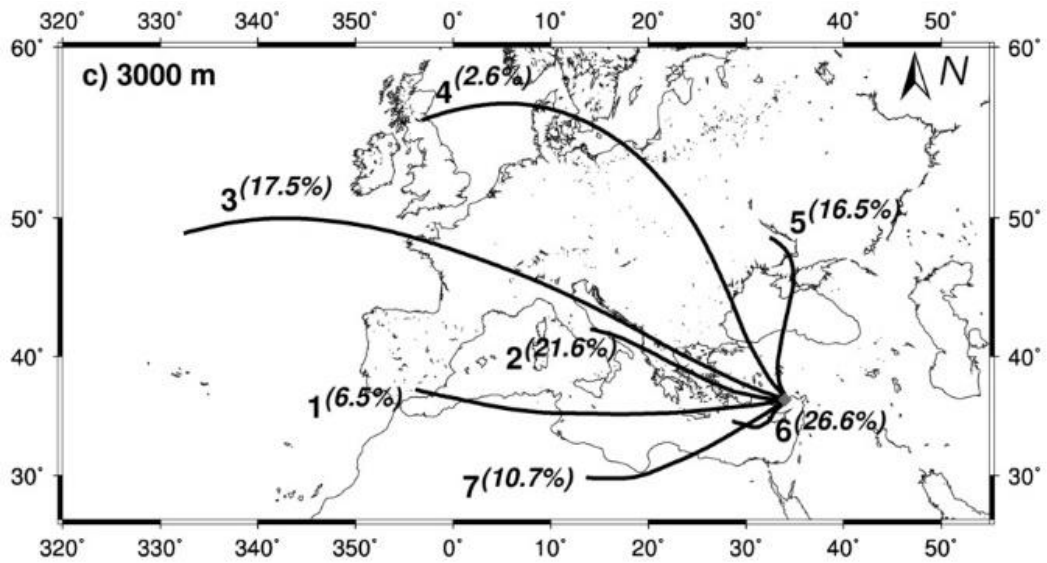


Figure 3.3. c. Cluster analysis of 3-days air mass back trajectories and air flow reaching Erdemli site at 3000 m altitude between January 2014 and April 2015.

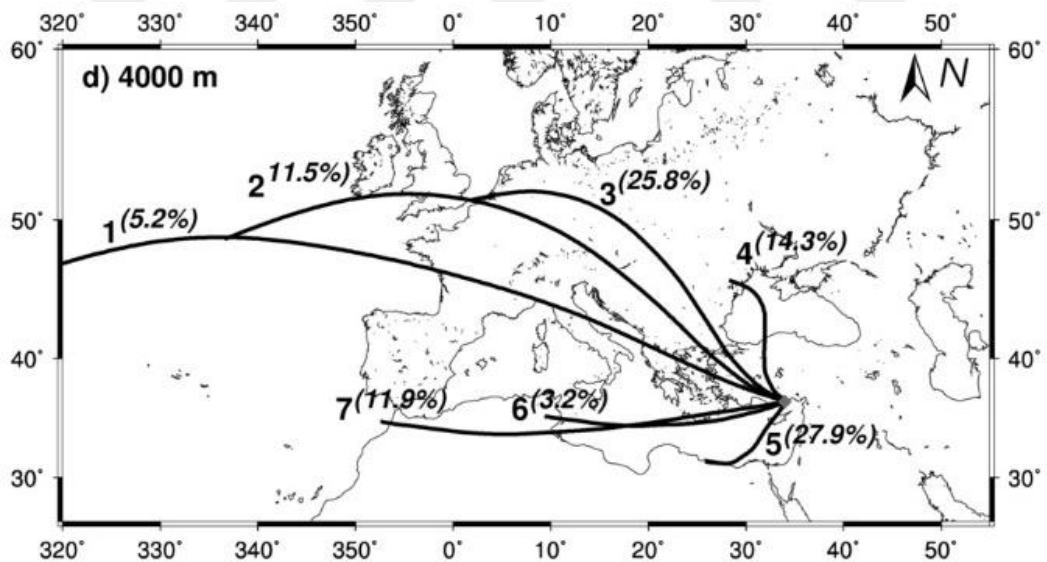


Figure 3.3. d. Cluster analysis of 3-days air mass back trajectories and air flow reaching Erdemli site at 4000 m altitude between January 2014 and April 2015.

4. WATER-SOLUBLE NITROGEN SPECIES IN AEROSOL AND RAINWATER IN THE EASTERN MEDITERRANEAN: SOURCES AND INFLUENCE OF THE MINERAL DUST EPISODE ON OBSERVED CONCENTRATIONS

A great number of data on inorganic nitrogen species (NO_3^- and NH_4^+) in aerosol and rainwater for the Eastern Mediterranean has been published (Mihalopoulos et al., 1997; Guerzoni et al., 1997, 1999; Herut et al., 1999; Kouvarakis et al., 2001; Bardouki et al., 2003; Markaki et al., 2003; Koçak et al., 2004a,b, 2010, 2015; Carbo et al., 2005). These studies have highlighted short (daily) and long term (seasonal) changes in the concentrations of water-soluble inorganic nitrogen species and the impact of atmospheric inorganic nitrogen inputs on marine productivity. Water-soluble nitrate and ammonium show a lower concentration during winter season because of wet precipitation and low gas-to-particle conversion. Nitrate and ammonium denote their peak values during summer season owing to elevated photochemistry and the lack of wet precipitation. Air-masses back trajectory clustering analysis has revealed that the lowest nitrate and ammonium concentrations in aerosol and rainwater were associated with air flow from the Mediterranean Sea (Koçak et al., 2010). It has been demonstrated that the atmospheric inorganic nitrogen fluxes in the Mediterranean accounts 60 % of the total nitrogen originating from continental sources (Guerzoni et al., 1999). Kouvarakis et al. (2001) illustrated that the atmospheric input of inorganic nitrogen species was more than enough to sustain the observed marine productivity, up to 8 times. Considering water-soluble organic nitrogen including urea, not only the number of studies is limited but the number of samples is insufficient. Based on our knowledge, there are only three publications about this subject in the Eastern Mediterranean.

4.1. General Characteristics of the Data

In this section the general characteristics of the Water-Soluble Organic Nitrogen (WSON), Nitrate (NO_3^-), Ammonium (NH_4^+) and Water-Soluble Total Nitrogen (WSTN) in aerosol and rainwater samples were discussed.

(a) Aerosol: The statistical summary for WSON, water-soluble inorganic nitrogen species, NO_3^- , NH_4^+ and WSTN determined in PM_{10} , $\text{PM}_{10-2.5}$ and $\text{PM}_{2.5}$ aerosol samples obtained from Erdemli between January 2014 and April 2015 are presented in Table 4.1. Among the nitrogen species, WSON denoted the highest arithmetic mean and followed by ammonium and nitrate concentrations. The concentration of WSON was estimated to reach up to 79 nmol N m^{-3} with mean value and standard deviation of $24.6 \pm 16.3 \text{ nmol N m}^{-3}$. Approximately 61 % of the WSON was associated with coarse particles though the remaining fraction (39%) was accompanied with fine aerosols. A number of studies have been reported the relative size distribution of WSON for Eastern Mediterranean (Finokalia, Violaki and Mihalopoulos, 2010) and remote marine sites (Hawaii, Cornell et al., 2001; Tasmania, Mace et al., 2003a). The aerosol WSON in Finokalia (68 %) and Hawaii was chiefly found in fine mode while WSON in Tasmania was mainly associated with coarse fraction. Water-soluble inorganic NO_3^- and NH_4^+ concentrations fluctuated between 0.2-88.4 and 0.5-164.4 with mean values (standard deviations) of $17.9 (\pm 15.7)$ and $23.3 (\pm 24.4) \text{ nmol N m}^{-3}$. As expected, NO_3^- was mainly associated with coarse particles, accounting 88 % of the observed mean value while NH_4^+ was dominated by fine mode, elucidating 96 % of the detected mean concentration. Similar results have been reported for Eastern Mediterranean in the previous studies (Bardouki et al., 2003; Koçak et al., 2007). The existence of NO_3^- in the coarse mode might be ascribed to a reaction of gaseous nitric acid or other nitrogen oxides with alkaline sea salt and mineral dust particles. On the other hand, the occurrence of NH_4^+ in fine particles is resulted from the reaction between gaseous alkaline ammonia and acidic sulfuric acid (Mihalopoulos et al., 2007).

WSTN concentrations in aerosol varied between 9.7 and $176.8 \text{ nmol N m}^{-3}$ with an arithmetic mean value and a standard deviation of 65.7 and 34.0, respectively. On average WSTN concentration was almost equally influenced by coarse and fine

particles, however, the contribution from the former (48 %) was slightly lower than that of latter (52 %).

The Table 4.1., also demonstrates relative contributions of water-soluble organic nitrogen, NO_3^- and NH_4^+ to WSTN in PM_{10} , $\text{PM}_{10-2.5}$ and $\text{PM}_{2.5}$. As can be deduced from the table, WSTN concentration in coarse mode was equally influenced by WSON and NO_3^- , each species explaining 47.6 and 49.8 %, respectively. On the other hand, NH_4^+ contribution to WSTN was found to be only 2.8 %. WSTN in fine particles was chiefly associated with NH_4^+ (65.5 %). WSON accounted to 28.1 % of the WSTN whereas NO_3^- contribution to fine WSTN was around 6.4 %.

The statistical summary, including arithmetic mean, standard deviation, median, minimum and maximum, for urea ($(\text{NH}_2)_2\text{CO}$) measured in PM_{10} , $\text{PM}_{10-2.5}$ and $\text{PM}_{2.5}$ aerosol samples collected from Erdemli during the study period (January 2014 April 2015) is depicted in Table 4.2. Arithmetic mean urea concentration was $4.4 \pm 3.5 \text{ nmol N m}^{-3}$, with a maximum value of $19.8 \text{ nmol N m}^{-3}$. Approximately, 65 % of the urea originated from coarse fractions, while 35 % of the urea derived from fine particles. The size distribution of urea has been documented for the Eastern Mediterranean (Finokalia: Violaki and Mihalopoulos, 2011), Atlantic (Hawaii: Cornell et al., 2001) and Pacific (Tasmania: Mace et al., 2003b). Urea in the atmosphere over the Pacific primarily derived from coarse particles whereas, urea at Finokalia (eastern Mediterranean, 76 %) and Hawaii (Atlantic) principally came from fine fraction. Table 4.2., also illustrates the relative contribution of urea to WSTN and WSON in PM_{10} , $\text{PM}_{10-2.5}$ and $\text{PM}_{2.5}$. Regarding both coarse and fine particles, WSON was equally influenced by urea contribution, elucidating 17 %. Nevertheless, urea contributions to WSTN in coarse and fine mode were 8 % and 4 %, respectively. Taking into account the values presented above, it should be noted that urea contributions to WSON and WSTN were considerable over the Eastern Mediterranean atmosphere.

(b) Rainwater

Volume-weighted-mean (VWM) concentrations of WSON, NO_3^- , NH_4^+ and WSTN in rainwater are presented in Table 4.1., along with minimum-maximum concentrations and relative contributions of WSON, nitrate and NH_4^+ to WSTN. As it can be seen from table, VWM concentrations of each species were more or less

comparable, yet NH_4^+ denoted the highest concentration with a value of $28.7 \mu\text{mol N L}^{-1}$. The VWM concentration of WSON and NO_3^- were around 21.5 and $23.3 \mu\text{mol N L}^{-1}$, respectively. Considering their relative contributions to WSTN, WSON and NO_3^- accounted for 29.3 and 31.7 % of the WSTN whilst NH_4^+ elucidated 39.0 % of the observed WSTN concentration in rainwater. On the other hand, the VWM concentration of urea in rainwater was $1.2 \mu\text{mol N L}^{-1}$, ranged between 0.1 and $13.4 \mu\text{mol N L}^{-1}$. In rainwater samples the relative contributions of urea to WSTN and WSON were around 2 and 6 %, respectively (Table 4.2.).

Table 4. 1. The statistical summary of the WSON, NO_3^- , NH_4^+ and WSTN for aerosol (nmol N m^{-3}) and rainwater ($\mu\text{mol N L}^{-1}$) samples at Erdemli during the period of January 2014 and April 2015.

Aerosol (nmol N m^{-3})	WSON	NO_3^-	NH_4^+	WSTN
<i>PM₁₀</i>				
Arithmetic Mean	24.6	17.9	23.3	65.8
Standard Deviation	16.3	15.7	24.4	34
Minimum	-27.9	0.2	0.5	9.7
Maximum	79	88.4	164.4	176.8
Relative Contribution*	37	27	35	
<i>PM_{10-2.5}</i>				
Arithmetic Mean	15.0	15.7	0.9	31.6
Standard Deviation	13.0	14.8	1.0	18.7
Minimum	-23.4	0.1	0.1	4.1
Maximum	66.5	86.4	6.9	118.4
Relative Contribution*	47.6	49.8	2.8	
<i>PM_{2.5}</i>				
Arithmetic Mean	9.6	2.2	22.4	34.2
Standard Deviation	11.5	2.3	24.2	23.6
Minimum	-40.2	0.1	0.1	1.7
Maximum	56.9	15.3	161.1	153.5
Relative Contribution*	28.1	6.4	65.5	
Rainwater ($\mu\text{mol N L}^{-1}$)				
VWM**	WSON	NO_3^-	NH_4^+	WSTN
	21.5	23.3	28.7	73.5
Minimum	-2.9	0.2	9.1	24.3
Maximum	257.2	74.6	122.6	356.2
Relative Contribution*	29.3	31.7	39.0	

* represents relative contribution of each nitrogen species (as percentage) to water soluble total nitrogen.

** VWM refers to volume weighted mean.

Table 4. 2. The statistical summary of the urea for aerosol (nmol N m^{-3}) and rainwater ($\mu\text{mol N L}^{-1}$) samples at Erdemli during the period of January 2014 and April 2015.

Aerosol (nmol N m^{-3})	UREA	WSON	WSTN	RC* to WSON	RC* to WSTN
<i>PM₁₀</i>					
Arithmetic Mean	4.4	24.6	65.8	18	7
Standard Deviation	3.7	16.3	34		
Minimum	0.1	-27.9	9.7		
Maximum	19.8	79	176.8		
<i>PM_{10-2.5}</i>					
Arithmetic Mean	2.7	15.0	31.6	18	9
Standard Deviation	2.7	13.0	18.7		
Minimum	0.1	-23.4	4.1		
Maximum	16.4	66.5	118.4		
<i>PM_{2.5}</i>					
Arithmetic Mean	1.7	9.6	34.2	18	5
Standard Deviation	1.7	11.5	23.6		
Minimum	0.1	-40.2	1.7		
Maximum	9.0	56.9	153.5		
Rainwater ($\mu\text{mol N L}^{-1}$)					
VWM**	UREA	WSON	WSTN		
	1.2	21.5	73.5	6	2
Minimum	0.1	-2.9	24.3		
Maximum	13.4	257.2	356.2		

*RC represents relative contribution (as percent).

** VWM refers to volume weighted mean.

4.2. Comparison of Aerosol and Rainwater Water-Soluble Nitrogen Species concentrations with data from Literature

The mean concentrations of WSON in aerosol and rainwater samples collected from different sites located around the Mediterranean, Atlantic and Pacific regions are illustrated in Table 4.3. Before assessing the present value and the reported values from the literature, it is worth noting that the WSON comparison is challenging not only because there are different sampling periods, sampling/measurement techniques and limited number of samples but also there is a high uncertainty explicitly resulted from the estimation of WSON. Furthermore, unfortunately, considering the published articles there is a lack of information about the uncertainty of WSON though there is a substantial statistical knowledge about arithmetic mean, standard deviation, minimum and maximum values. In addition, Keene et al. (2002) have particularly put an emphasis on the tendency in literature to neglect negative or usage of zero instead of negative values during the estimation of WSON from WSTN and WSIN. As these

authors have reasonably highlighted the omission or substitution of such values inevitably would result in positive bias in WSON concentration.

As can be deduced from the reported WSON values in, in general the lowest concentrations were found in remote or pristine marine environments. The WSON concentrations in the atmosphere over the Indian (Amsterdam Island: $1.0 \text{ nmol N m}^{-3}$, Violaki et al., 2015), Atlantic (Barbados: $1.3 \text{ nmol N m}^{-3}$, Zamora et al., 2011) and Pacific Ocean (Hawaii, Oahu: $4.1 \text{ nmol N m}^{-3}$, Cornell et al., 2001, Tasmania: $5.3 \text{ nmol N m}^{-3}$, Mace et al., 2003b), which were at least 4 times less than those observed for Mediterranean region (Erdemli: $24.6 \text{ nmol N m}^{-3}$, this study, Finokalia: $17.1 \text{ nmol N m}^{-3}$, Violaki and Mihalopoulos, 2010), were found to be varied between 1 and 4 nmol N m^{-3} . These low values might be attributed to (i) the absence of the strong anthropogenic sources in the vicinity of the sampling sites and/or (ii) the dilution of the WSON originating from long range transport via both dry and wet deposition. The highest WSON concentrations emerged particularly over China (Ho et al., 2015, concentration of WSON measured in $\text{PM}_{2.5}$) and Taiwan (Chen et al., 2010) with values above 70 nmol N m^{-3} . As already have been stated in Chen et al. (2010) WSON concentrations at these sampling sites were markedly influenced by anthropogenic activities such as fossil fuel combustion and man induced biomass burning. The mean WSON concentration at Erdemli ($24.6 \text{ nmol N m}^{-3}$) was comparable to that reported previously for the same site (29 nmol N m^{-3} , Mace et al., 2003a). On the other hand, the present WSON concentration was almost 1.5 times higher than that of observed at Finokalia and this difference might be attributed to the characteristic of the sites, the former being rural and the latter being background.

Similar to aerosols, the reported WSON values for rainwater samples also exhibited the lowest concentrations in remote or pristine marine environments, such as Tasmania (below the detection limit). The highest VWM urea concentrations were found at China ($103 \text{ } \mu\text{M N}$) and Norwich ($33 \text{ } \mu\text{M N}$), respectively. These high values attributed to the anthropogenic activities. On the other hand, the VWM urea concentration over the Mediterranean was at least four times lower than that reported for China. Erdemli had 1.2 times higher urea concentration in rainwater than that observed at Finokalia.

Table 4. 3. Comparison of WSON concentrations in aerosol (nmol N m⁻³) and rainwater (μmol N L⁻¹) samples for different sites of the World.

Aerosol (nmol N m ⁻³)	WSON	RC	NS	SP	Reference
Mediterranean Sea					
<i>Erdemli, Turkey</i>	24.6	37	740	2014-2015	This Study
<i>Erdemli, Turkey</i>	29	26	39	2000	Mace et al. [2003a]
<i>Finokalia, Crete</i>	17.1	13	65	2005-2006	Violaki and Mihalopoulos [2010]
Pacific Ocean					
<i>Hawaii</i>	4.1	33	16	1998	Cornell et al. [2001]
<i>Tasmania</i>	5.3	-	24	2000	Mace et al. [2003b]
<i>Taiwan</i>	75.9	26	77	2006	Chen et. al. [2010]
<i>Xi'an, China (PM_{2.5})</i>	300	44	65	2008-2009	Ho et. al. [2015]
Atlantic Ocean					
<i>Barbados</i>	1.3	12	57	2007-2008	Zamora et al. [2011]
<i>Amazon, dry season</i>	61	-	37	1999	Mace et al. [2003c]
<i>Amazon, wet season</i>	3.5	-	27	1999	Mace et al. [2003c]
Indian Ocean					
<i>Amsterdam Island</i>	1	-	42	2005	Violaki et al. [2015]
Rainwater (μmol N L ⁻¹)	WSON	RC	NS	SP	Reference
Mediterranean Sea					
<i>Erdemli, Turkey</i>	21.5	29	23	2014-2015	This Study
<i>Erdemli, Turkey</i>	15	17	18	2000	Mace et al. [2003a]
<i>Finokalia, Crete</i>	18	23	18		Violaki et al. [2010]
Pacific Ocean					
<i>Tahiti*</i>	4.8		8		Cornell et al. [1998]
<i>Hawaii</i>	2.8		17	1998	Cornell et al. [2001]
<i>Tasmania</i>	7.2		6		Mace et al. [2003b]
<i>North China Plain, China</i>	103	25	15	2003-2005	Zhang et al. [2008]
<i>Kilauea, Hawaii</i>	6.5		20	1998	Cornell et al. [2001]
Atlantic Ocean					
<i>Bermuda</i>	5.6	42	5	1994	Cornell et al. [1998]
<i>Mace Head</i>	3.3	37	7		Cornell et al. [1998]
<i>Norwich, UK</i>	33	35	12		Cornell et al. [1998]
<i>Virginia, US</i>	3.1	65	83	1996-1999	Keene et al. [2002]
<i>Delaware, US</i>	4.2	78	50	1997-1999	Keene et al. [2002]
<i>New Hampshire, US</i>	0.6	26	12	1997	Keene et al. [2002]

RC, NS and SP refer to relative contribution of WSON to WSTN, number of samples and sampling period, respectively.

Figure 4.1.a, b, and c display stations used for literature comparison and corresponding concentrations for water-soluble nitrate and ammonium, respectively. Water-soluble nitrate and ammonium concentrations at Erdemli were found to be comparable to those reported for Finokalia. Considering historic values documented for Mediterranean region, it should be highlighted that the recent values were at least 2 times lower compared to previous concentrations. Water-soluble nitrate at Erdemli was 2 times higher than the concentration reported for Sinop, whereas water-soluble ammonium concentration at Erdemli was comparable to the value reported for Sinop. Water-soluble nitrate and ammonium levels observed for Erdemli were almost equal to concentrations documented for Atlantic and Europe. During the last two decades, dramatic decrease in the concentrations of nitrate and ammonium over Europe has been noted (EMEP, 2013). This considerable reduction from 1990's to 2010's might be ascribed to decline in (a) fertilizer practices and (b) NO_x . Not only the decrease in fertilizer usage but also the abatement in NO_x emissions in the region (EMEP, 2013) may also lead to the significant decline from 1990's to 2010's. The highest mean nitrate was found at Tel Shikmona and this huge value might be resulted from (a) aridity of region, (b) higher incoming solar flux and (c) type of filter (in this case Whatman-41 cellulose). It is obvious that the first two peculiarities might affect the nitrate concentration; however, type of the filter is also important considering volatile species. Laboratory experiments have been shown that positive nitrate and ammonium artifact can result the adsorption of gaseous species such as HNO_3 and NH_3 on filter surfaces or on already collected particles (Wieprecht et al., 2004 and references therein). Furthermore, field campaigns have supported aforementioned findings (Koçak et al., 2010). During this study, aerosol samples were simultaneously collected on Whatman-41 cellulose and polycarbonate filters. Comparison between cellulose and polycarbonate filters revealed that nitrate and ammonium concentrations were distinctly different for each filter type, the results from former being at least 2.0 and 1.7 times higher than those observed for nitrate and ammonium in polycarbonate filters, respectively.

Volume-weighted mean concentrations for nitrate and ammonium in rainwater during the study period along with documented values obtained from literature is presented in Table 4.4. VWM concentrations for nitrate and ammonium in rainwater

collected from Erdemli were 40 % and 30 % lower than those historic values documented for same sampling site. As stated before, such decrease in the concentrations of inorganic nitrogen species over the Europe has been reported by The European Monitoring and Evaluation Programme (EMEP, 2016). Similar reduction in the water-soluble aerosol nitrate and ammonium was presented in the previous section (see Section 4.1.). The VWM concentration of nitrate at Erdemli was two times lower than those reported for Tel Shikmona and Ashdod. The lowest VWM concentrations of nitrate and ammonium were observed at Heraklion, being 30 % and 38 % less than those detected for Erdemli, respectively. This difference might be ascribed to the green houses and cultivated soil around the vicinity of the Erdemli sampling site.

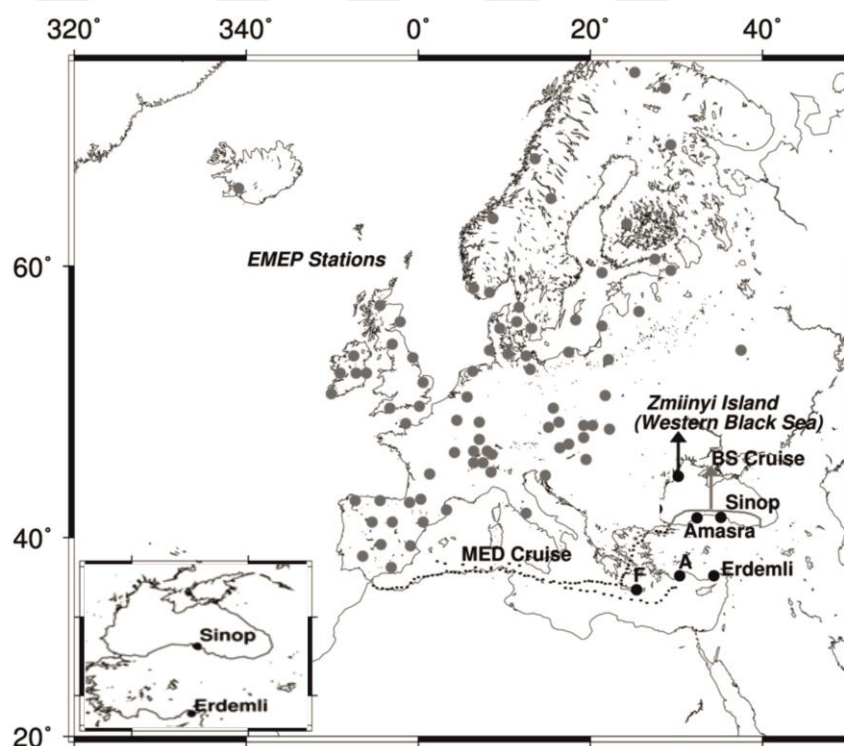


Figure 4. 1. The locations of stations used for literature comparison and corresponding concentrations for water-soluble (a), (b) nitrate and (c) ammonium (nmol N m^{-3}). Locations of sampling sites in the Black Sea, in the Eastern Mediterranean and in the Europe, MED -Cruise (Medinets 1996), A and F refers to Antalya (Güllü et al. 1998); and Finokalia (Kouvarakis et al. 2001), respectively, Amasra (Karakaş et al. 2004), Black Sea (BS-Cruise, Kubilay et al. 1995), Zmiinyi Island (Western Black Sea, Medinets and Medinets 2012), Sinop (Koçak et al., 2016) and Erdemli (current study).

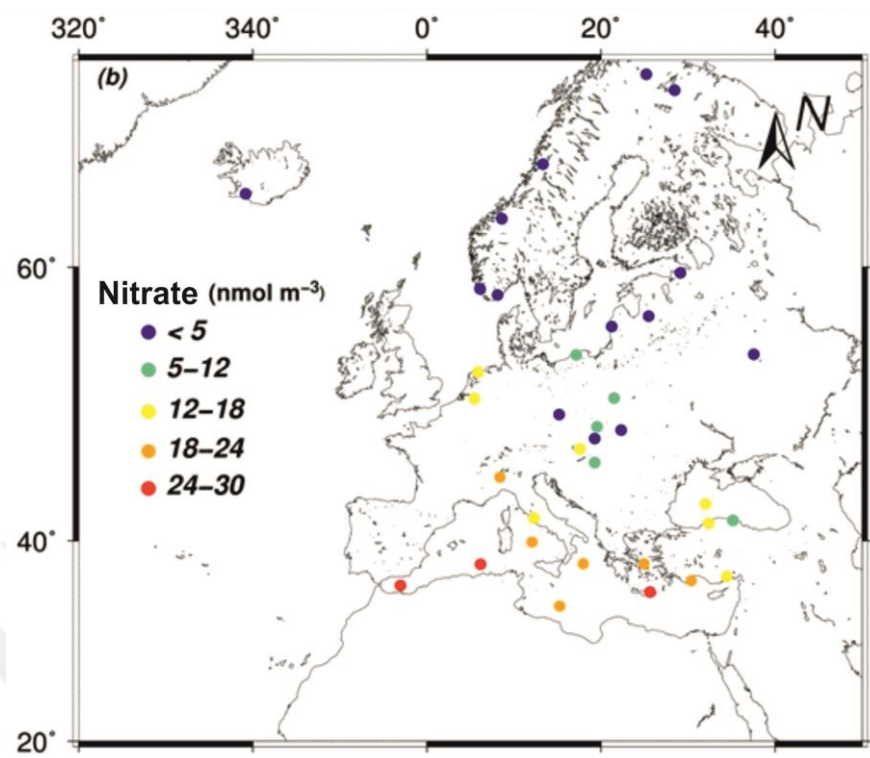


Figure 4.1. Continued.

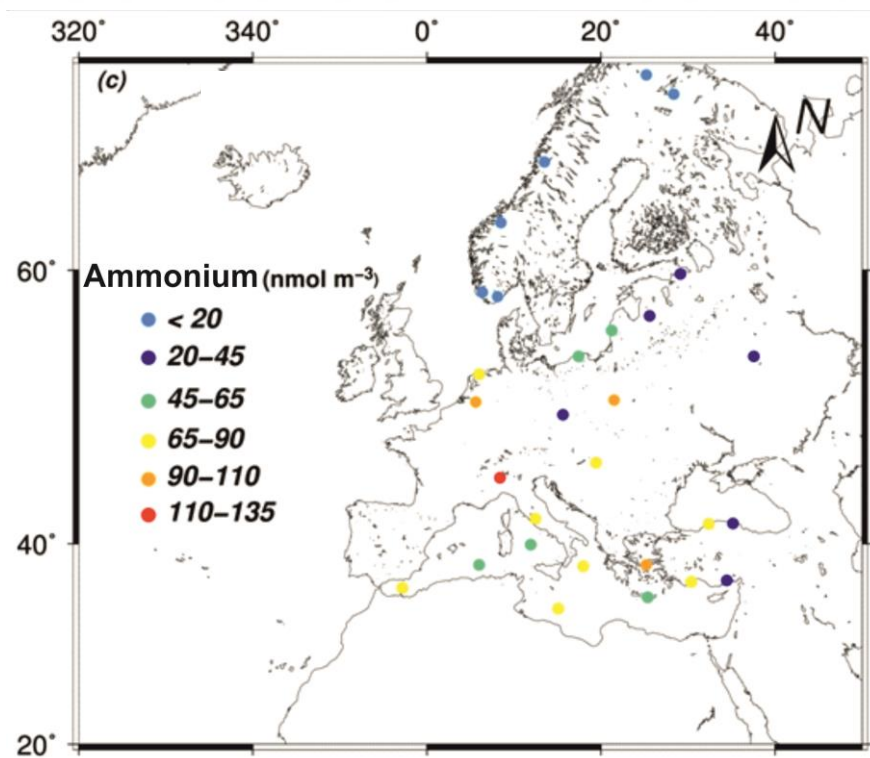


Figure 4.1. Continued.

Table 4. 4. Volume-weighted mean concentrations for nitrate (NO_3^-) and ammonium (NH_4^+) in rainwater during the study period along with documented values obtained from literature.

Rainwater VWM ($\mu\text{mol N L}^{-1}$)	NO_3^-	NH_4^+	Reference
Erdemli, Turkey	23	29	This study
Erdemli, Turkey	37	41	Koçak et al. [2010]
Heraklion, Crete	18	21	Markaki et al. [2003]
Tel Shikmona, Israel	41	25	Herut et al. [1999]
Ashdod, Israel	57	45	Herut et al. [1999]

The arithmetic mean concentrations of urea in aerosol and rainwater samples collected from different sites located around the Mediterranean, Atlantic and Pacific regions are illustrated in Table 4.5. In general, the lowest mean urea concentrations were observed at the remote and/or pristine sampling areas. The mean concentrations of urea in atmospheric particles over the Pacific Ocean (Hawaii: $1.8 \text{ nmol N m}^{-3}$, Cornell et al., 2001; Tasmania: $0.9 \text{ nmol N m}^{-3}$, Mace et al., 2003b) were at least 1.7 times lower than those observed for Mediterranean (Erdemli $4.4 \text{ nmol N m}^{-3}$, this study; Finokalia: $3.1 \text{ nmol N m}^{-3}$, Violaki and Mihalopoulos, 2011). The minimum values detected at remote and/or pristine sites might be attributed to (i) the absence of strong pollutant and anthropogenic sources and/or (ii) the dilution of the urea during the long range transport via dry and wet depositions (Mace et al., 2003b). The highest concentration ($6.2 \text{ nmol N m}^{-3}$) of urea was observed at Rondonia, locating at the Amazon basin, since the sampling site was significantly influenced by massive biomass burning during the dry season (Mace et al., 2003c). The urea concentration at Erdemli was 30 % higher than that of Finokalia. Elevated urea concentrations at Erdemli compared to Finokalia might be inscribed to (i) closer proximity of the former site to the desert regions (particularly the Middle East desert) and/or (ii) agricultural activities around the vicinity of the Erdemli site. Interestingly, there was a dramatic difference between the current urea concentration and the historic value reported by Mace et al., 2003a, for the same sampling site. The current value for urea was in any case thirty times higher than that of documented previously. This distinct difference might be resulted from (i) the previous samples were not frozen at $-20 \text{ }^\circ\text{C}$ until analysis, (iii) the previous sampling were carried out by using glass fiber filters and this substrate may cause huge absorbance at 190 nm just before the urea peak.

The volume weighted mean (VWM) concentration of urea at Erdemli was comparable to that of historic value; whilst Erdemli had almost two times lower urea concentration than Finokalia. This difference might be due to the episodic nature of rainwater samples and also the location of sampling station. The highest VWM urea concentrations were observed at Norwich ($3.7 \mu\text{mol N L}^{-1}$) and Tahiti ($3.1 \mu\text{mol N L}^{-1}$). It should be underlined that Norwich station was strongly influenced from urban activities and Tahiti station was highly impacted by agricultural activities.



Table 4. 5. The arithmetic mean concentrations of urea in aerosol and rainwater samples collected from different sites located around the Mediterranean, Atlantic and Pacific regions.

Aerosol (nmol N m⁻³)	UREA	WSON	RC	NS	SP	Reference
Mediterranean Sea						
<i>Erdemli, Turkey</i>	4.4	24.6	18	740	2014-2015	This Study
<i>Finokalia, Crete</i>	3.1	11.8	26	28	2006	Violaki and Mihalopoulos [2011]
Pacific Ocean						
<i>Bellows, Oahu</i>	1.8	3.3	55		1998	Cornell et al. [2001]
<i>Tasmania</i>	0.9	3.6	25	19	2000	Mace et al. [2003b]
<i>Japan</i>	1.1					Simoneit et al. [2004]
Amazon						
<i>Rondonia</i>	6.2					Mace et al. [2003c]
Rainwater (μmol N L⁻¹)	UREA	WSON	RC	NS	SP	Reference
Mediterranean Sea						
<i>Erdemli, Turkey</i>	1.2	21.5	0.6	23	2014-2015	This Study
<i>Erdemli, Turkey</i>	1.6	15	11		2000	Mace et al. [2003a]
<i>Finokalia, Crete</i>	2.5		20		2006	Violaki et al. [2011]
Pacific Ocean						
<i>Tahiti</i>	3.1	4.8	65			Cornell et al. [1998]
<i>Bellows, Oahu</i>	1.1					Cornell et al. [2001]
<i>Tasmania</i>	bld	7.2				Mace et al. [2003b]
<i>Kilauea, Hawaii</i>		6.5			1998	Cornell et al. [2001]
Atlantic Ocean						
<i>Bermuda</i>	bld	5.6			1994	Cornell et al. [1998]
<i>Mace Head</i>	bld	3.3			1998	Cornell et al. [1998]
<i>Norwich, UK</i>	3.7	33	11			Cornell et al. [1998]

RC, NS and SP refer to relative contribution of urea to WSON, number of samples and sampling period, respectively. bld refers to below the detection limit.

4.3. Daily variations of Water-Soluble Nitrogen Species in Aerosol and Rainwater at Erdemli

Figure 4.2. illustrated daily variation of the water-soluble nitrogen species in aerosol samples together with daily rain amount from January 2014 to April 2015. The same figure also shows concentrations in rainwater samples obtained between October 2014 and April 2015.

(a) Aerosol: As can be depicted from the figure, WSON concentrations indicated large variations from one day to another day. The daily variability in the concentration of WSON may be an order of magnitude. Such variability has been reported for Atlantic (Zamora et al., 2010), Pacific (Chen et al., 2010) and Mediterranean (Violaki and Mihalopoulos, 2010). These studies have been demonstrated that the daily change in the concentrations of WSON might arise from (a) meteorological parameters (such as rain, temperature and wind speed/direction), (b) chemical reactions, (c) history of air masses back trajectories and (d) emission strength.

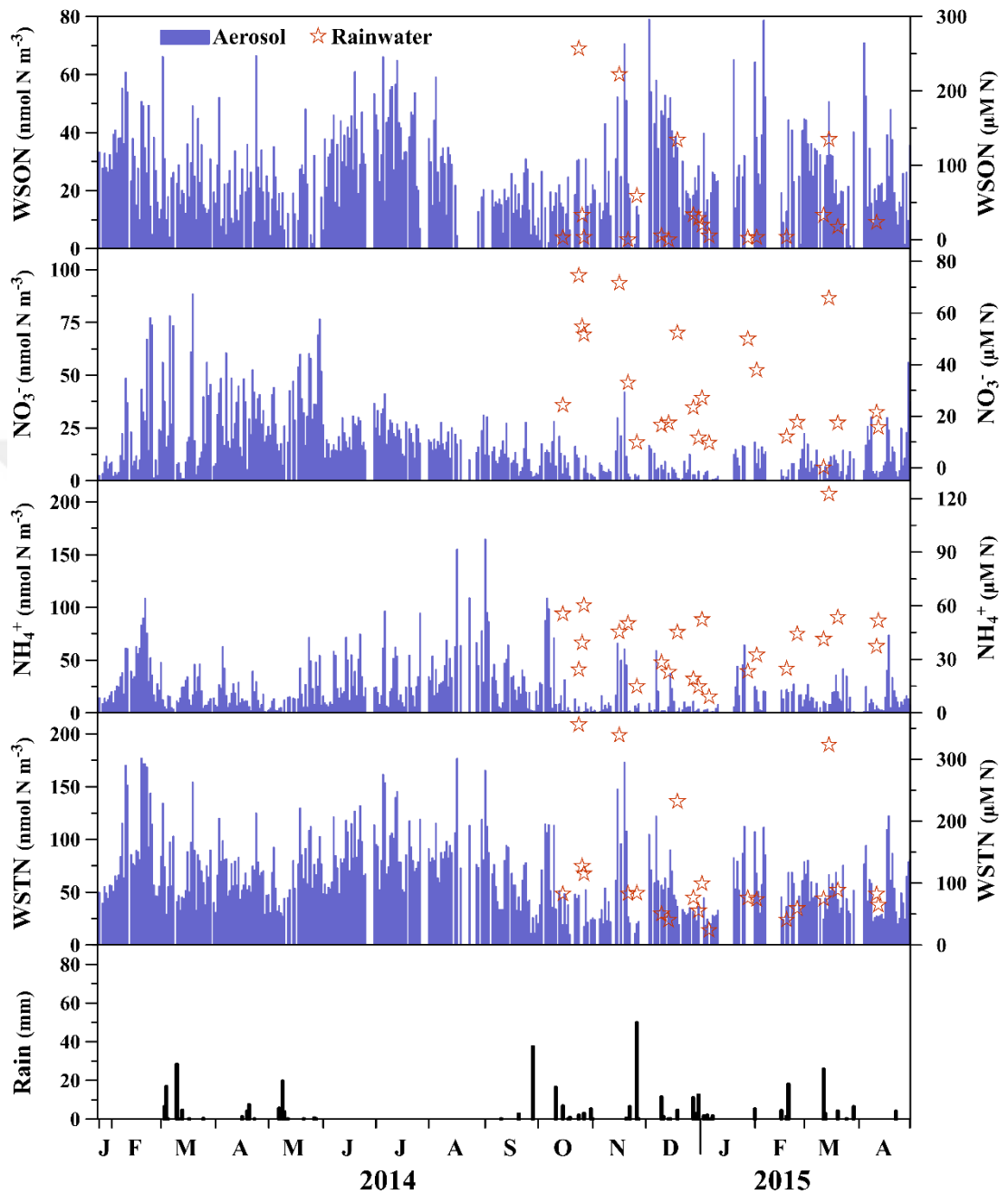


Figure 4. 2. The daily variations in the concentrations of (a) water-soluble organic nitrogen (WSON), (b) nitrate (NO_3^-), (c) ammonium (NH_4^+), (d) water-soluble total nitrogen (WSTN) (nmol N m^{-3}), rain amount (mm) and determined concentrations of nitrogen species in rainwater ($\mu\text{M N}$) between January 2014 and April 2015 for PM_{10} aerosol samples.

In general, lower concentrations of WSON were found to be associated with rainy days. To illustrate, one of the lowest WSON concentration was observed on 6th of March 2014, after three day consecutive rain event, with a value of 3.98 nmol N m⁻³. On the other hand, one of the highest WSON concentrations (66.1 nmol N m⁻³) was found on 2nd of March 2014 when the air mass back trajectories associated with south/south westerly airflow. 3-day backward trajectories (1, 2, 3 and 4 km height) and OMI (Ozone Mapping Instrument) Aerosol Index (AI) of air masses arriving at the Erdemli sampling site on 2nd of March 2014 is shown in Figure 4.3. As it can be seen from the figure, all air masses (except 1 km) originated from south whereas the back trajectory for 1 km altitude showed airflow from the Middle East (Southeasterly airflow). Back trajectories suggest that the sampling site was under the influence mineral dust transport originating from deserts regions located at the Middle East and North Africa. OMI-AI satellite image also supports the mineral dust intrusion into the Eastern Mediterranean. OMI-AI diagram clearly indicates a large dust plume over the Eastern Mediterranean between coordinates 20-45 °N and 15-40 °E. Aerosol Index was found to be very high over the Northeastern Mediterranean, ranging from 2.0 to 4.5. During this dust episode, % 85 of the WSON was affiliated with coarse fraction, which further supports the mineral dust as a main source of water-soluble organic nitrogen. The observed concentration of WSON on 5th of July 2014, with a value 66 nmol N m⁻³. The % 94 of the WSON concentration was originated from coarse mode, however, during this event there was no dust intrusion neither from Sahara nor from the Middle East deserts. This high value might be attributed to re-suspension of the soil particularly affected by intense agricultural activities. Another high WSON concentration was marked on 19th of November 2014 (see Figure 4.4) during the mineral dust episode with a value of 56.32 nmol N m⁻³. About % 78 of the observed concentration of the WSON was derived from coarse particles. The highest WSON concentration was monitored on 3rd of December 2014 was also found to be high with a value of 79 nmol N m⁻³. Although the dust intrusion was clarified during this event, most of the WSON was originated from fine particles which dictates the impact of man-made sources on the water-soluble organic nitrogen.

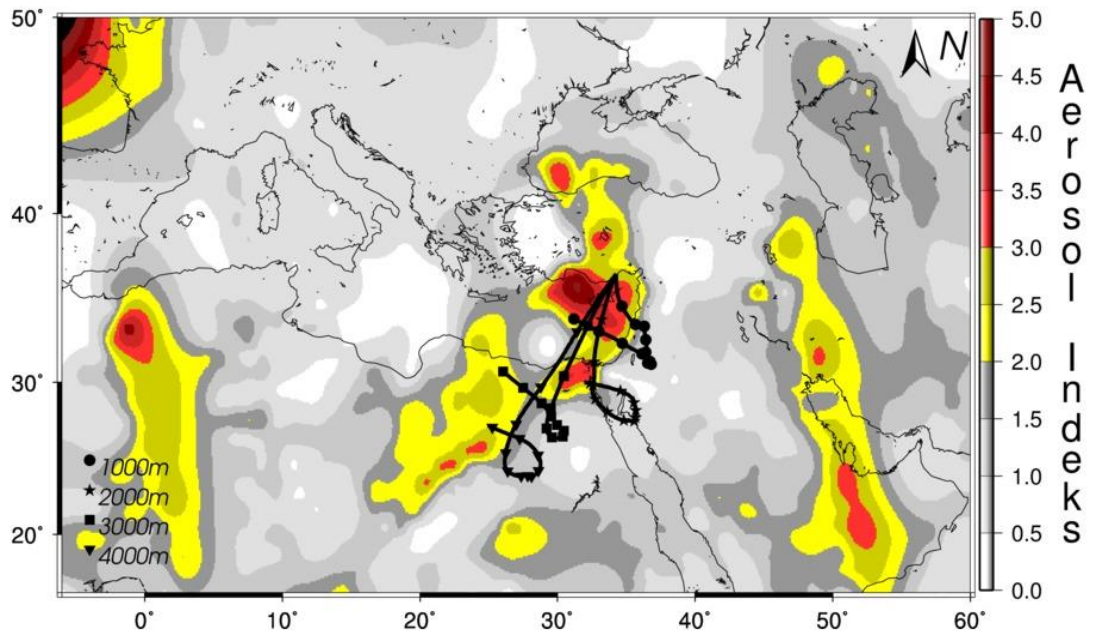
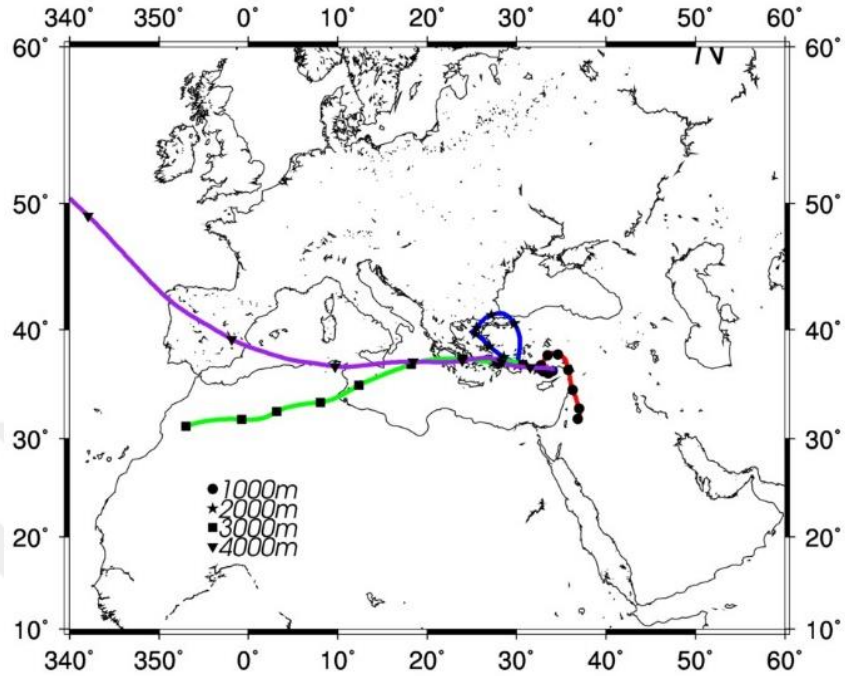


Figure 4. 3. 3-day backward trajectories (1, 2, 3 and 4 km height) and OMI (Ozone Mapping Instrument) Aerosol Index (AI) of air masses arriving at the Erdemli sampling site on 2th of March 2014.

(a)



(b)

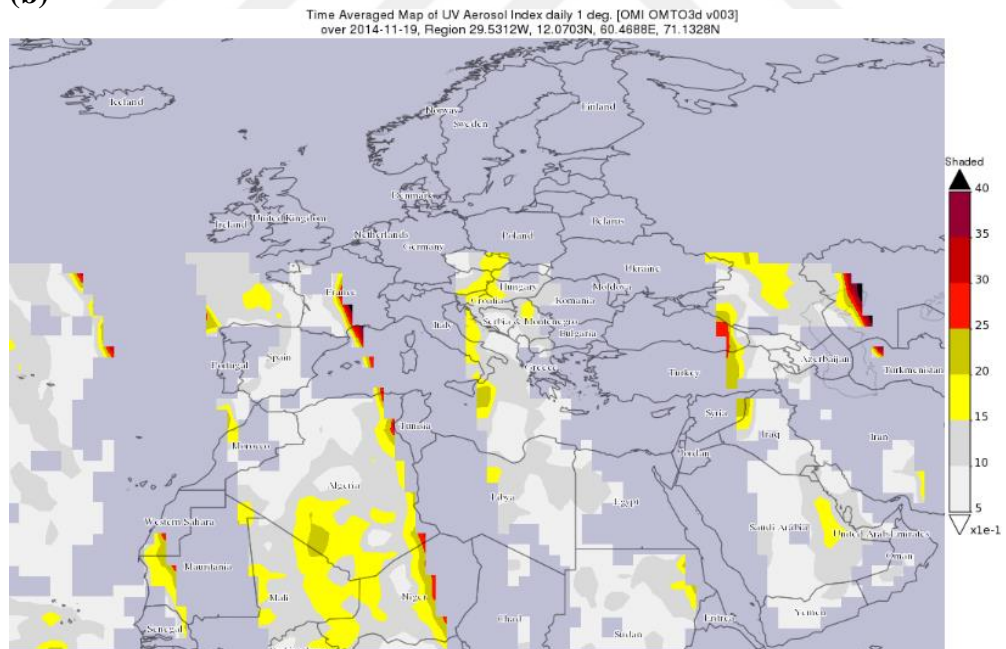


Figure 4. 4. 3-day backward trajectories (a, 1, 2, 3 and 4 km height) and OMI (Ozone Mapping Instrument) Aerosol Index (b, AI) of air masses arriving at the Erdemli sampling site on 19th of November 2014.

As can be seen from the Figure 4.5, urea concentration aerosols indicated a large variability, with values varying by up to an order of magnitude from day to day during the study period. Similar variability has been documented for Amazon (Cornel et al., 2011), Pacific (Mace et al., 2003b) and Mediterranean (Violaki and Mihalopoulos, 2011). As envisaged, the lowest urea concentrations were observed during rainy days. During rain events, urea values were found to be as low as 0.006 nmol N m⁻³. Throughout the study period, the highest urea concentration was inspected on 2nd of March 2014 with a value of 19.8 nmol N m⁻³. As stated before, during this day there was an intense mineral dust episode and 83 % of the urea concentration was held by coarse mode which dictates that the mineral dust was a main source of urea on 2nd of March. The second highest urea value was detected on 8th of March 2014 with a value of 18.7 nmol N m⁻³. OMI (Ozone Mapping Instrument) Aerosol Index (AI) and 3-day backward trajectories (1, 2, 3 and 4 km height) of air masses arriving at the Erdemli sampling site on 8th of March 2014 is depicted in Figure 4.6. All back trajectories illustrated from North Africa transport into to the Eastern Mediterranean. OMI-AI and the contribution of coarse fraction (>80 %) to urea concentration also propose the mineral dust episode over the sampling site. Similar events were frequently observed throughout the study period, indicating covariation between mineral dust episodes and elevated urea concentrations. Above all, it should be highlighted that the sources of urea are quite diverse. For instance, on 14th of July 2014 urea concentration was found to be 10.7 nmol N m⁻³, coarse mode elucidating 72 % of the observed value. During this day, there was no mineral dust plume over the study region, whereas, re-suspension of cultivated soil might be ascribed as a source of urea. Another interesting event was detected on 18th of February 2014 when the sampling site was under the weak dust episode. Correspondingly, urea concentration and contribution of fine particles were 6.8 nmol N m⁻³ and 66 %. As it is well documented in the literature mineral dust particles can serve as reaction surfaces (Krueger et al., 2004). Because of this peculiarity, an enhancement in the concentrations of pollutants might be monitored during the dust episodes. Such an increase might be ascribed to several processes namely; a) anthropogenic species emitted from local sources may mix with mineral dust during air mass transport from desert regions, b) anthropogenic species may be scavenged with and/or on to mineral dust particle surfaces when air

masses from desert areas passes through populated/industrialized regions (Choi et al., 2001; Guo et al., 2004; Vukmirovic et al., 2004; Koçak et al., 2012). Air masses back trajectories and OMI-AI for 18th of February 2014 is shown in the Figure 4.7. Trajectory analysis indicated that Erdemli was influenced by from North Africa (specifically Western Sahara) and mineral dust reaching the site after sweeping populated and industrialized regions such as Po Valley, Balkans, Istanbul and Marmara. Thus, the origin of urea might be attributed to both anthropogenic and mineral dust.

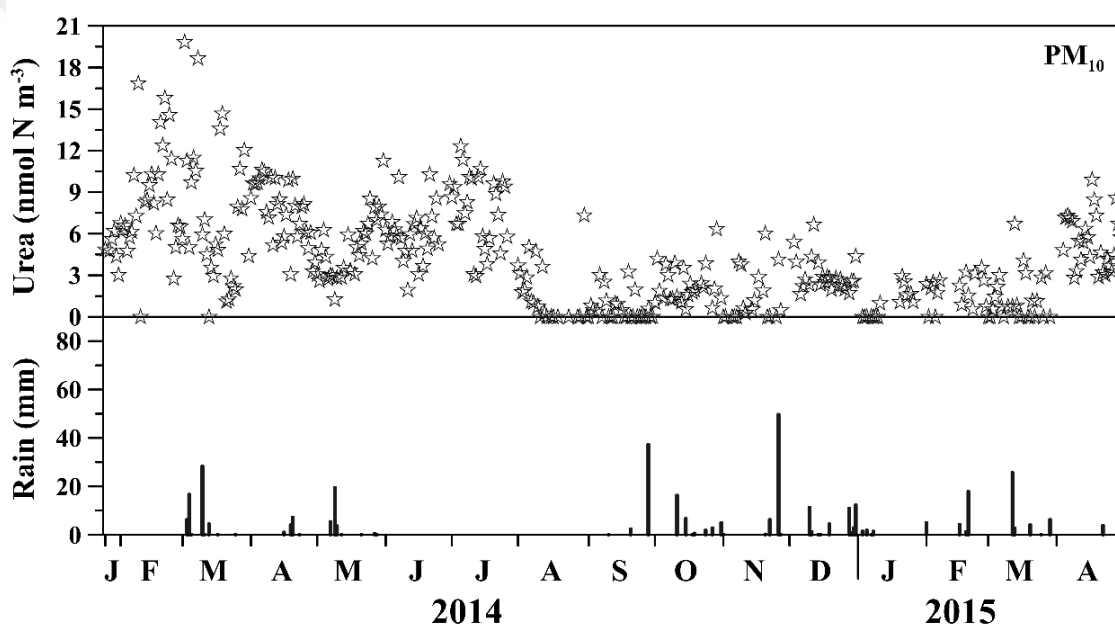
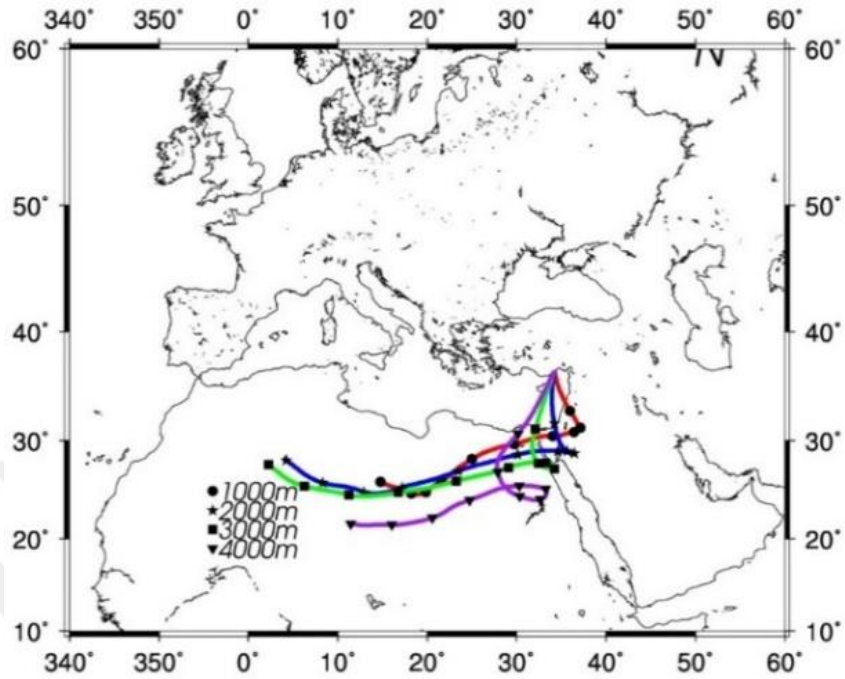


Figure 4. 5. The daily variability of urea concentrations in PM10 (nmol N mol⁻³) and observed rain amounts (mm) at Erdemli.

(a)



(b)

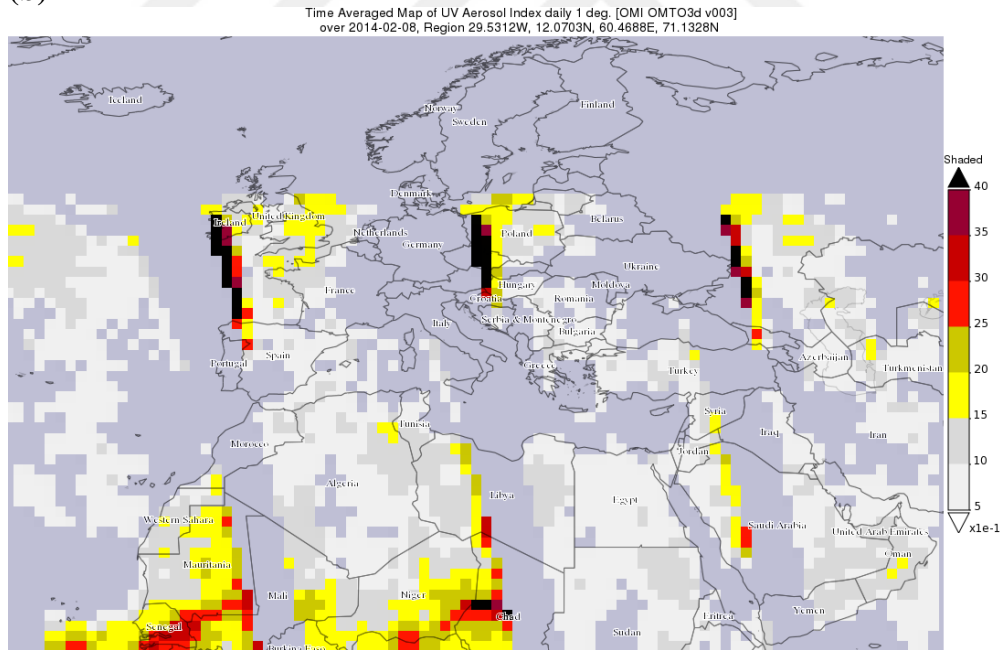
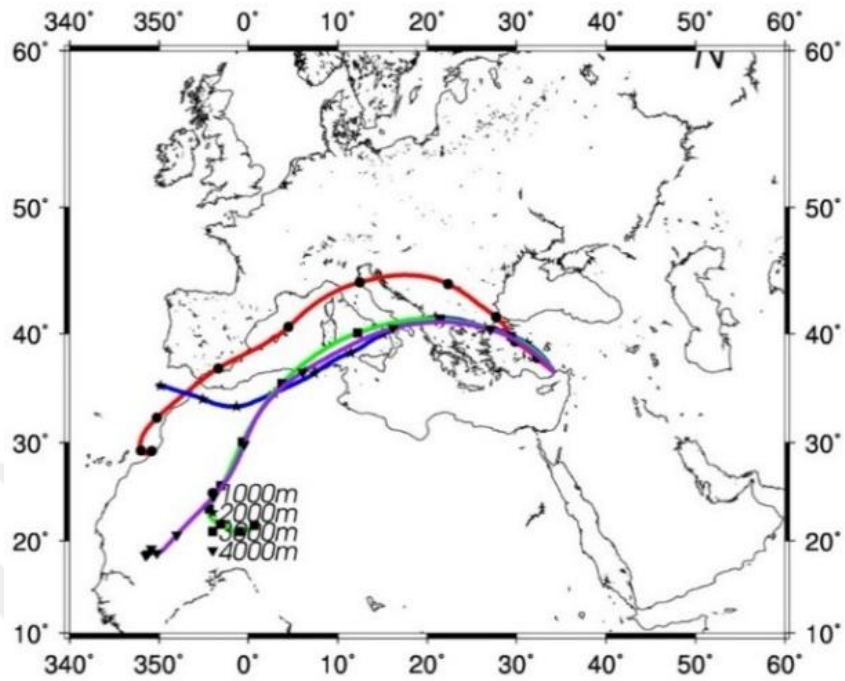


Figure 4. 6. 3-day backward trajectories (a, 1, 2, 3 and 4 km height) and OMI (Ozone Mapping Instrument) Aerosol Index (b, AI) of air masses arriving at the Erdemli sampling site on 8th of March 2014.

(a)



(b)

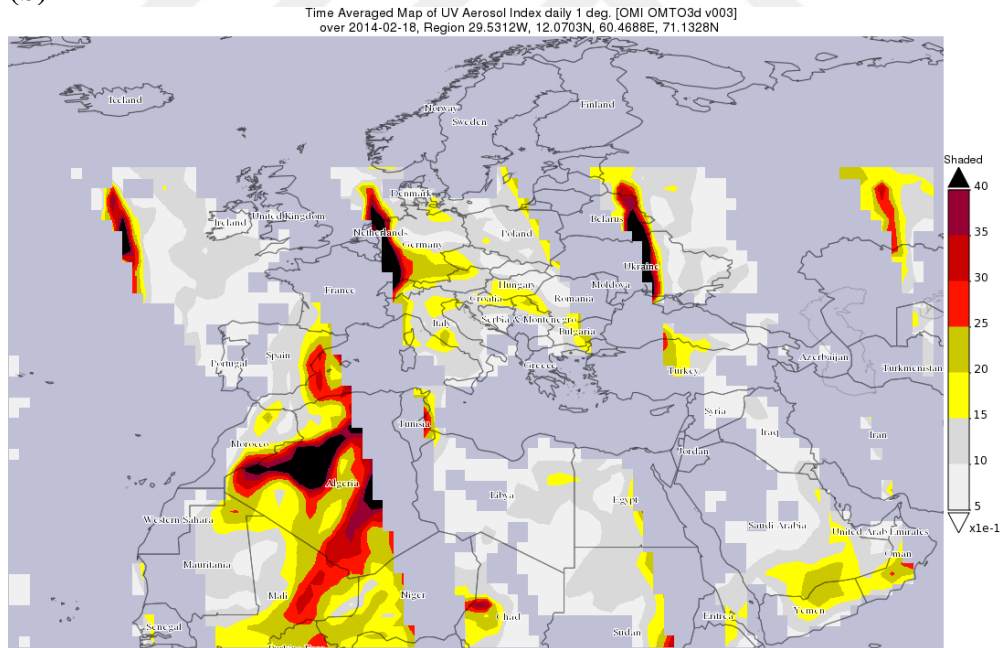


Figure 4. 7. 3-day backward trajectories (a, 1, 2, 3 and 4 km height) and OMI (Ozone Mapping Instrument) Aerosol Index (b, AI) of air masses arriving at the Erdemli sampling site on 18th February 2014.

(b) Rainwater: The calculated concentrations of WSON in the rainwater denoted a great variability from one rain episode to another one. The WSON concentrations ranged between $1 \mu\text{mol N L}^{-1}$ and $260 \mu\text{mol N L}^{-1}$. The highest WSON value was inspected on 24th of October 2014. The air masses back trajectories corresponding to 23rd and 24th of October 2014 are presented in Figure 4.8.a and b. Until the rain event, the sampling site was under the influence of completely different air masses. On 23rd of October, air mass back trajectories (1, 2 and 3 km) demonstrated airflow from Eastern Europe, sweeping arid desert regions before reaching at Erdemli. On 24th of October, Erdemli station was influenced by airflow coming from North Africa and the Middle East.

The detected urea concentrations in the rainwater demonstrated a large variability from one rain event to another one, ranging from $0.1 \mu\text{mol N L}^{-1}$ from $13 \mu\text{mol N L}^{-1}$. The highest urea concentration in rainwater was observed on 15th of March 2015. Air masses back trajectories are depicted in Figure 4.9. Trajectories showed that the sampling site impacted by dust transport from Saharan Desert.

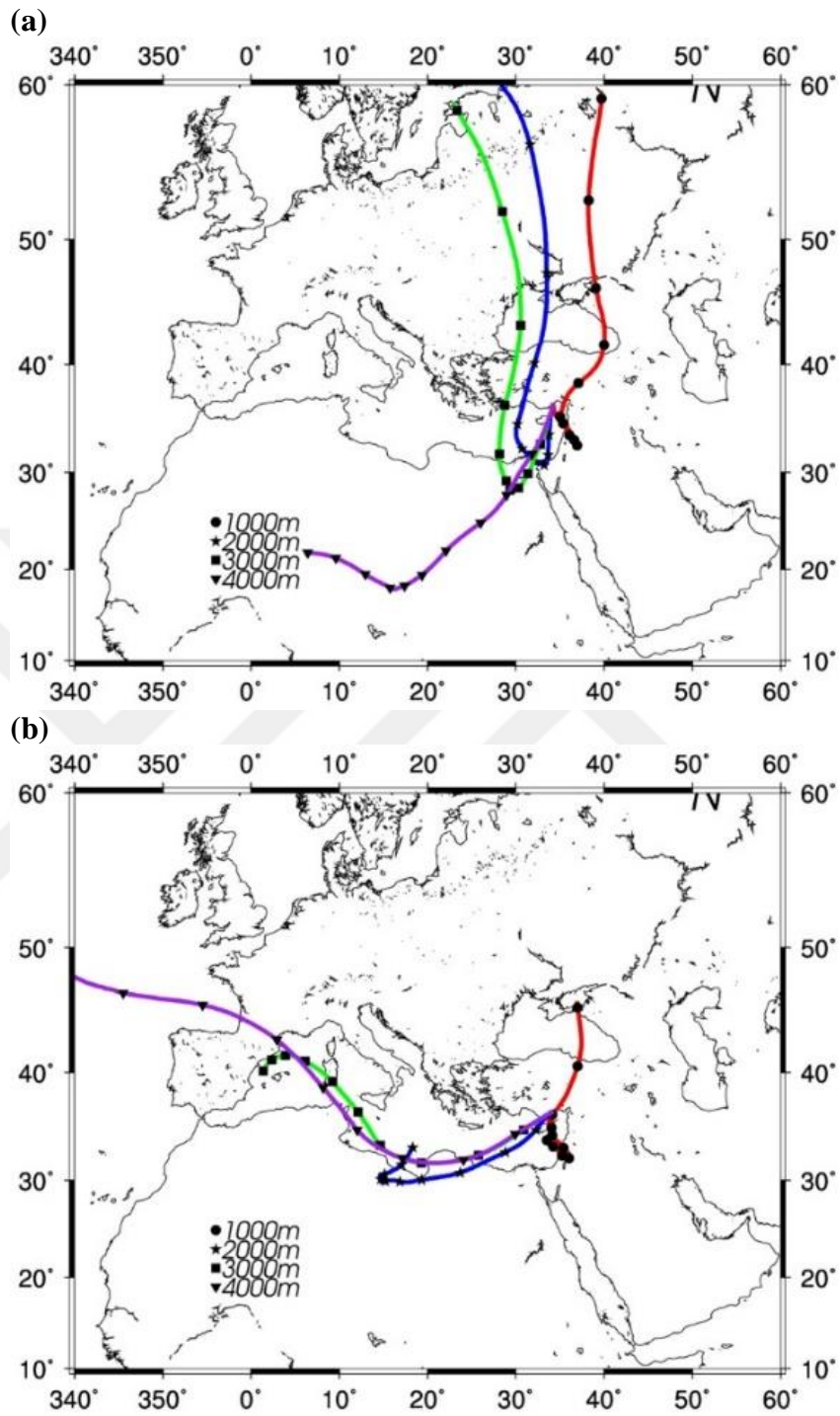


Figure 4. 8. 3-day air masses back trajectories corresponding to (a) 23rd and (b) 24th October 2014.

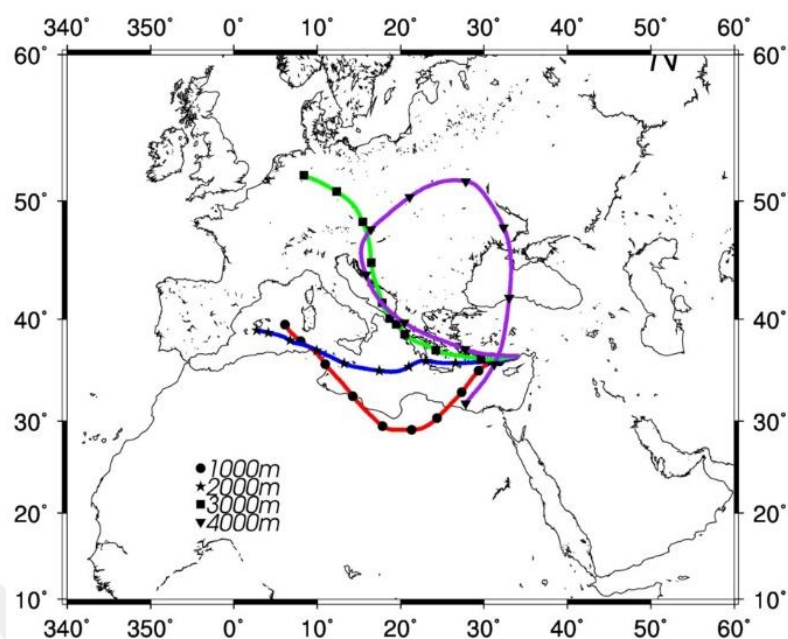


Figure 4. 9. 3-day air masses back trajectories corresponding to March 15, 2015.

4.4. Seasonal variations of Water-Soluble Nitrogen Species in Aerosol at Erdemli

Monthly variation of average concentrations of WSON in fine and coarse particles is depicted in Figure 4.10. As can be deduced from the monthly variation, WSON was found to denote complex seasonality. It illustrated bimodal seasonality with two maximum in winter and summer. The arithmetic mean concentrations of WSON in winter were comparable to those observed for summer, fluctuating from 30 to 40 nmol m^{-3} . However, there was distinct difference in the relative contribution of fine and coarse particles. During the winter season, the WSON was mainly found to be associated with fine particles, elucidating more than 60 % of the calculated concentrations. Based on considerable contribution of fine mode, it might be suggested that the WSON was predominated by anthropogenic derived aerosol. On contrary, WSON was chiefly affiliated with coarse particles, explaining more than %80 of the arithmetic mean concentrations of WSON. These high values in summer might be resulted from the absence of rain and re-suspension of cultivated soil.

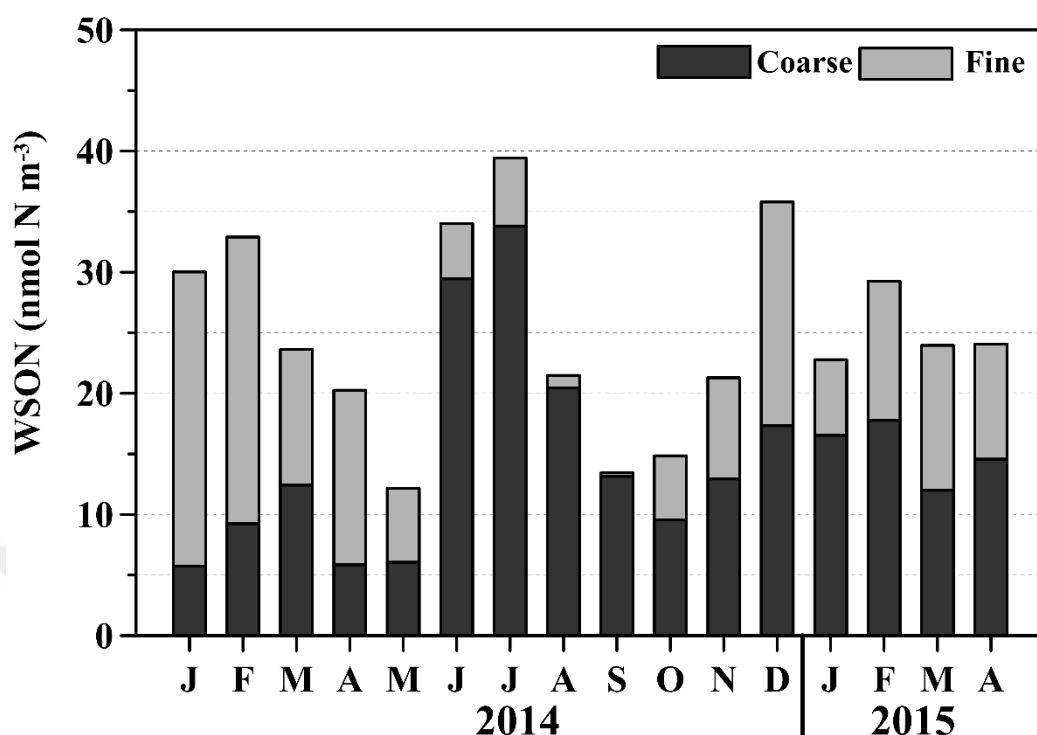


Figure 4. 10. Monthly variation of average concentrations of WSON in fine and coarse particles (nmol N m⁻³).

Water-soluble ammonium (see Figure 4.11.) exhibited the lowest concentrations chiefly in winter months whereas they depicted the highest concentrations in summer months. For example, in December, ammonium concentration was decreased down to 200 ng N m⁻³. On the other hand (except February 2014), it demonstrated an increase from winter to transition season and also it revealed gradual increase in concentration from transition season to summer. The main reasons for these low values might be ascribed to the efficient removal of particles by wet scavenging and decrease in photochemical reactions (Mihalopoulos et al., 2007). As it is well known, decrease in temperature and solar flux cause to reduction in photochemistry (Bardouki et al., 2003; Koçak et al., 2004a, b). The mean concentrations determined in the late summer months were 2 times higher than the average. The increase from winter to summer might be attributed to the following parameters: photochemistry, rain and the change in the air masses (Bardouki et al., 2003; Koçak et al., 2004a, b). For example, in a study over the eastern Mediterranean, Erduran and Tuncel (2001) indicated that the conversion of gaseous to particle was low in winter and high in summer, denoting a strong seasonal cycle. On the other hand,

during dry summer season, the life time of particles increased due to the absence of wet scavenging. Considering all seasons, it should be highlighted that more than 90 % of the ammonium was associated with fine particles.

Water-soluble nitrate (see Figure 4.12.) exhibited different seasonal cycle compared to the other water-soluble nitrogen species. It denoted relatively high concentrations both transitional and summer seasons whereas the lowest values were observed in rainy winter season. Higher mean concentrations were observed in summer months than that of winter. Both field and laboratory studies specified that nitrogen gases might react with alkaline sea salt and mineral dust (Mamane and Gottlieb, 1992, Underwood et al., 2001, Aymoz et al., 2004, Koçak et al., 2004a, b). Especially HNO_3 (nitric acid) and N_2O_5 might give heterogeneous reaction with alkaline sea salt and mineral dust particles. During sampling period, the correlation coefficient between nitrate and calcium in coarse particles was 0.60 which indicated the enrichment of nitrate in coarse mode. On the other hand, in the summer season the correlation coefficient between alkaline sea salts and nitrate for coarse particles was 0.70 which pointed out the reaction between acidic nitrogen species and alkaline sea salts and might be the reason of the relatively high concentrations found in transitional and summer months. As can be deduced from the figure, nitrate was dominated by coarse particles regardless of month (>80 %).

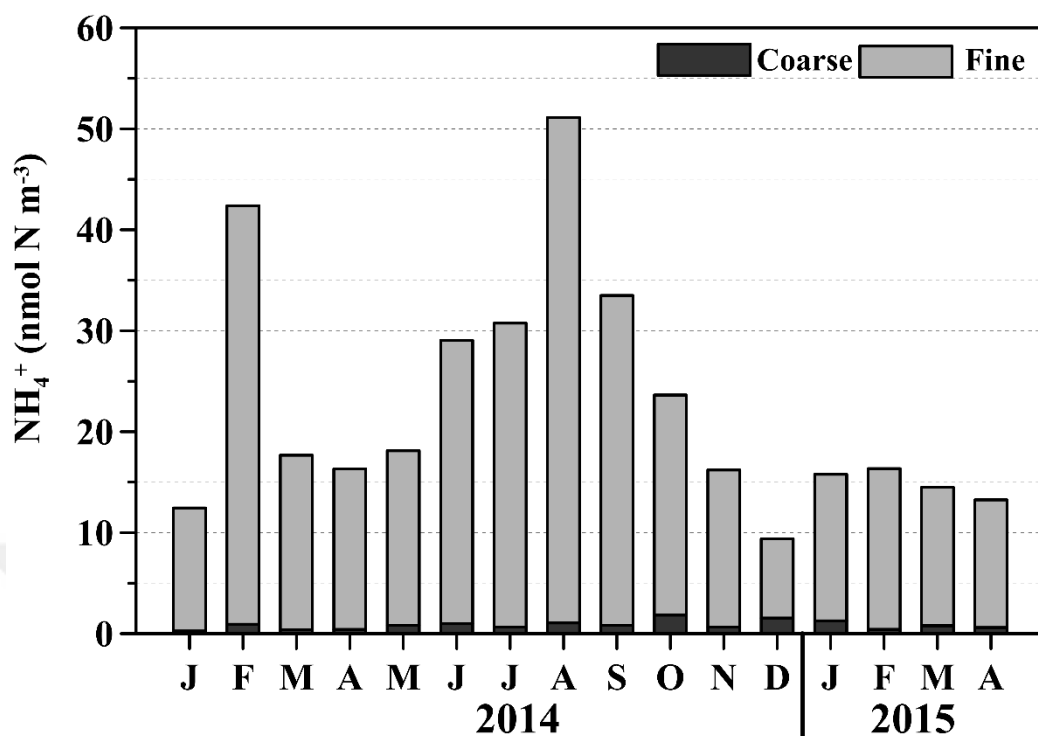


Figure 4. 11. Monthly mean concentrations for NH_4^+ (nmol N m^{-3}) in coarse and fine particles.

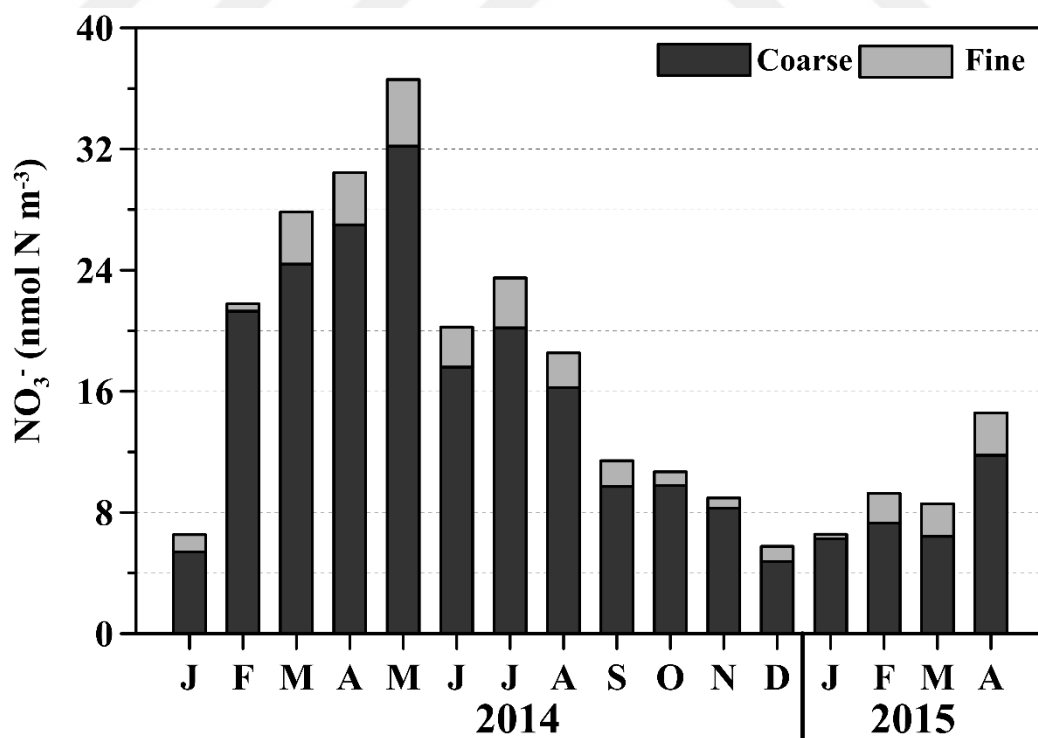


Figure 4. 12. Monthly mean concentrations for NO_3^- (nmol N m^{-3}) in coarse and fine particles.

Monthly mean concentrations for urea (nmol N m^{-3}) in coarse and fine particles are presented in Figure 4.13. Urea demonstrated complex seasonal variability. From this point of view, seasonality of urea was similar to those observed for WSON. Coarse and fine contributions to urea also exhibited variability, being highly influenced by coarse fraction during dust period (such as April, March, May) and summer. In general, during winter period urea was mainly associated with fine particles, implying dominance of anthropogenic sources.

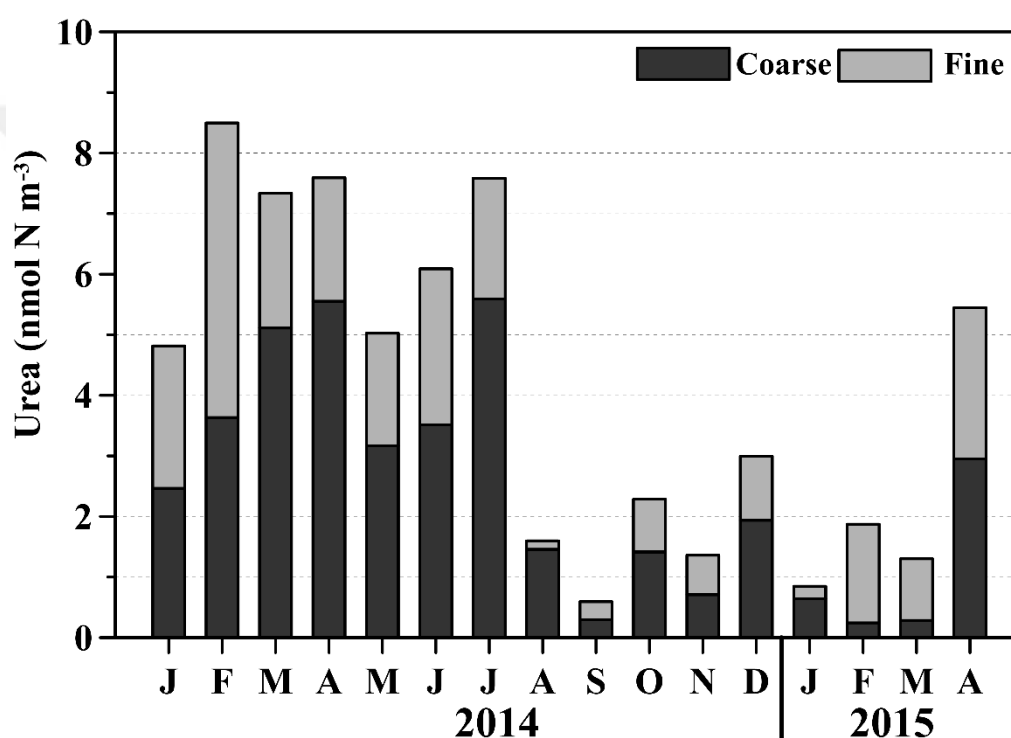


Figure 4. 13. Monthly mean concentrations for urea (nmol N m^{-3}) in coarse and fine particles.

As stated before, the particles are efficiently removed from the atmospheric compartment by wet scavenging. Whereas, the increase in temperature in summer results in rigorous photochemical reactions and evaporation of some species from soil. However, the relationship between water-soluble nitrogen species and temperature/rain amount might be complex because of air masses back trajectory history, emission strength and local winds.

In order to determine the influence of temperature and rain amount on the monthly mean concentrations, the relationship between monthly arithmetic means for each size (fine and coarse) and temperature/rain amount was explored.

Figure 4.14.a, b and c show the relationship between WSON and rain for both coarse and fine particles. Although, the monthly mean concentrations in coarse mode indicated sharp decline with the rain amount up to 50 mm, WSON concentrations increased in November and December despite of high rain amount (~ 100 mm). The main reason of this trend might be attributed to the long range transport of mineral dust particles into the Eastern Mediterranean from desert regions located at North Africa and the Middle East. In contrast, there was no relationship between monthly concentrations of WSON in fine mode and the rain amount. As expected, the wet precipitation removes coarse WSON more efficiently than fine WSON particles. Monthly WSON concentrations in coarse mode demonstrated linear decrease from 8 to 20 °C whilst it indicated dramatic increase temperature over 20 °C (see Figure 4.15.a and b). As the temperature increases along with absence of rain, the soil turns into less humid and eventually becomes dry and thus prone to re-suspension. These high values might be related to the re-suspension of cultivated soil. On the other hand, monthly arithmetic mean concentrations in fine particles pointed out inverse relationship to temperature, diminishing with increasing temperature (see Figure 4.15.c).

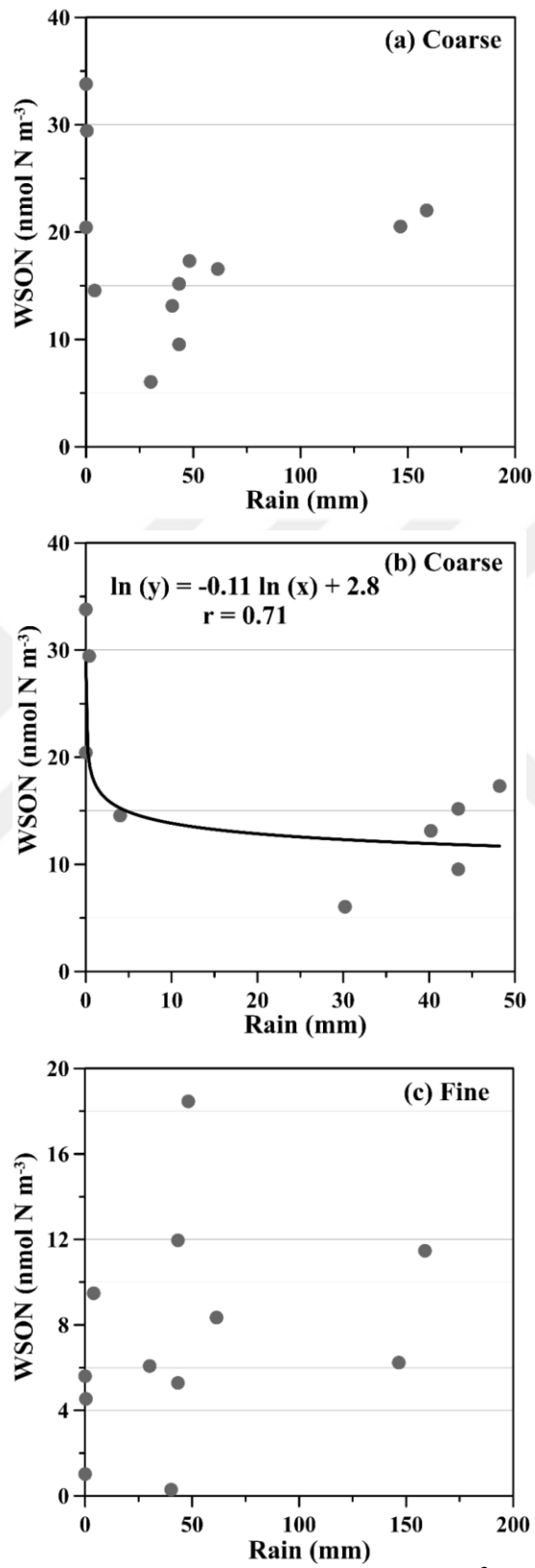


Figure 4. 14. The relationship between WSON (nmol N m⁻³) and rain (mm) for both (a), (b) coarse and (c) fine particles.

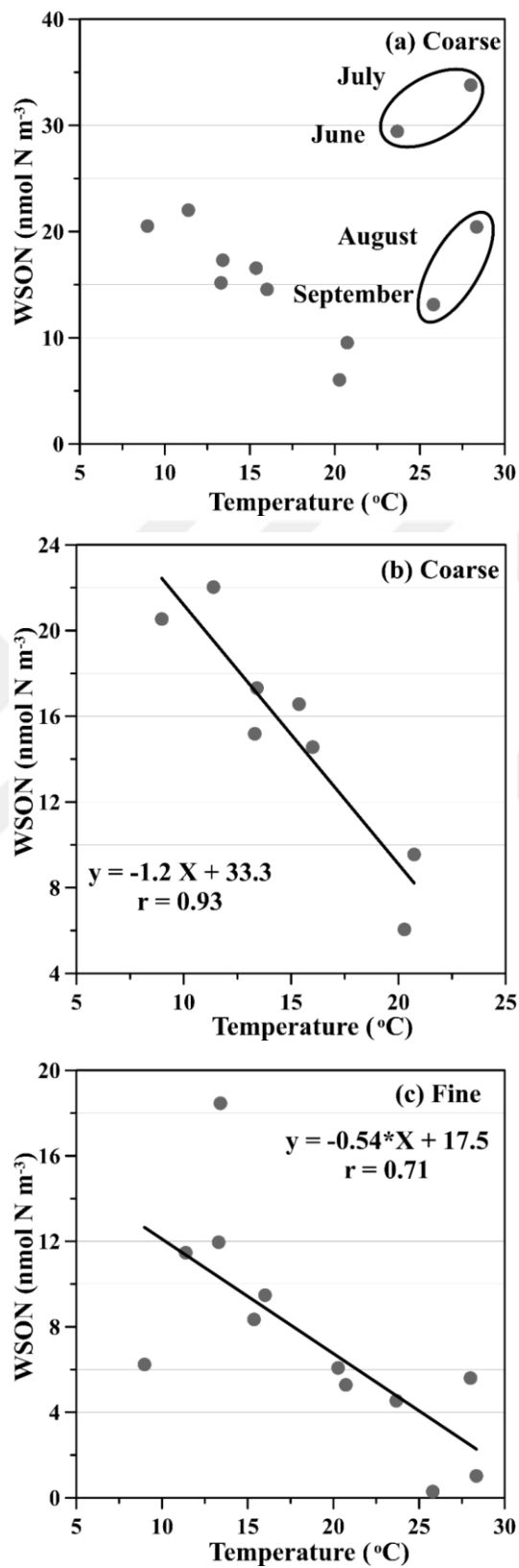


Figure 4. 15. The relationship between WSON (nmol N m⁻³) and temperature (°C) for both (a), (b) coarse and (c) fine particles.

As illustrated in the Figure 4.16.a., water-soluble ammonium in PM₁₀ showed an inverse correlations with rain amount. This specified that ammonium particles were removed from atmospheric compartment effectively by rain. The logarithmic relationship between concentration and rain amounts suggests sharp decrease of particles by wet scavenging. The correlation coefficients of water-soluble ammonium with rain amount was 0.74. The relationships between temperature (i.e., radiation) and water-soluble ammonium in PM₁₀ was presented in Figure 4.16.b. Between temperature and ammonium strong correlation coefficients has been identified with a value of 0.85. The observed strong correlation coefficient clearly indicated that gas to particle conversion of secondary ammonium particles were under the influence of photochemistry (particle concentration increased with increasing temperature).

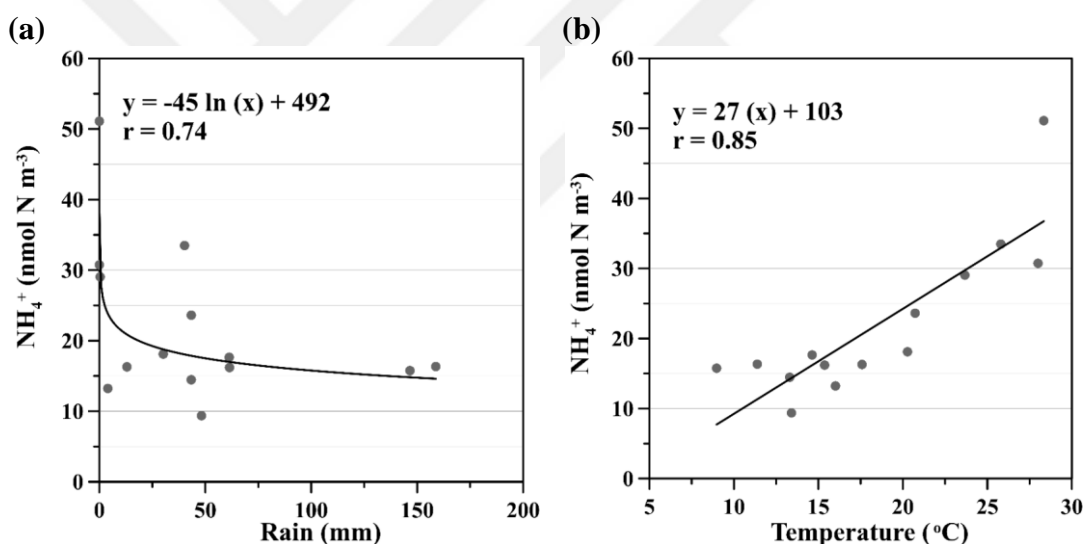


Figure 4. 16. (a) The relationship between water-soluble ammonium (nmol N m⁻³) and rain (mm) and (b) temperature (°C) for PM₁₀.

The monthly mean nitrate concentrations in PM₁₀ decreased with rain (see Figure 4.17.a.). Despite of rain, it exhibited high monthly means ($r = 0.32$) especially in March, April and May. The correlation coefficient between rain amount and nitrate may reach 0.92 if these two values are removed (see Figure 4.17.b.) Similar conclusion can be drawn relationship between monthly nitrate concentrations in PM₁₀ and temperature, expect for March, April and May (see Figure 4.18.) As mentioned previously, the majority of nitrate was accompanied with coarse particles due to acid and base reactions. During March, April and May, it might be argued that the possibility of nitrate concentrations' increase in mineral dust and sea salt were due to precursor gases and fluxes of air masses. Enrichments over mineral dust will be shown in the following sections (see statement above).

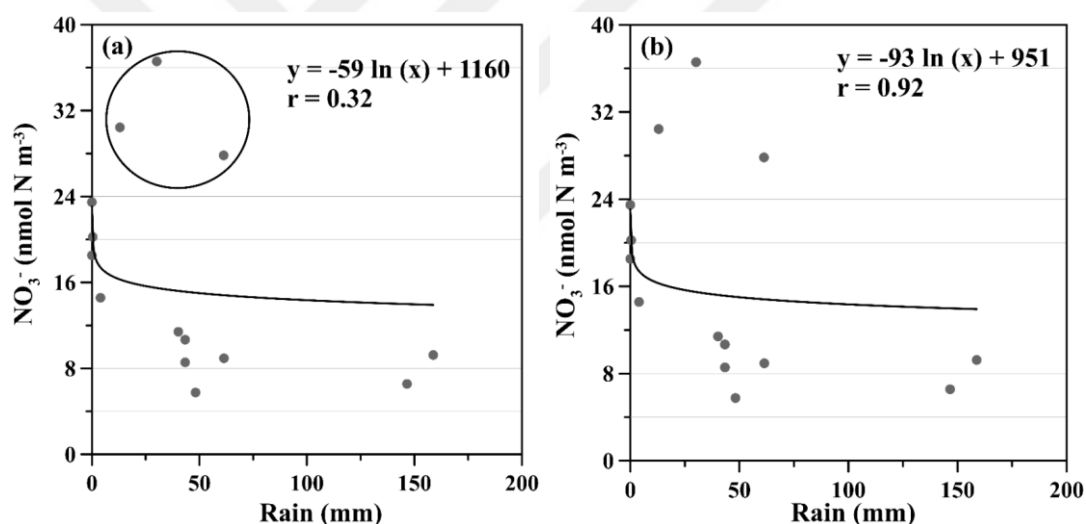


Figure 4. 17. (a) The relationship between water-soluble nitrate (nmol N m^{-3}) and rain (mm) and (b) The relationship between water-soluble nitrate (nmol N m^{-3}) when high monthly mean values are removed and rain (mm) for PM₁₀.

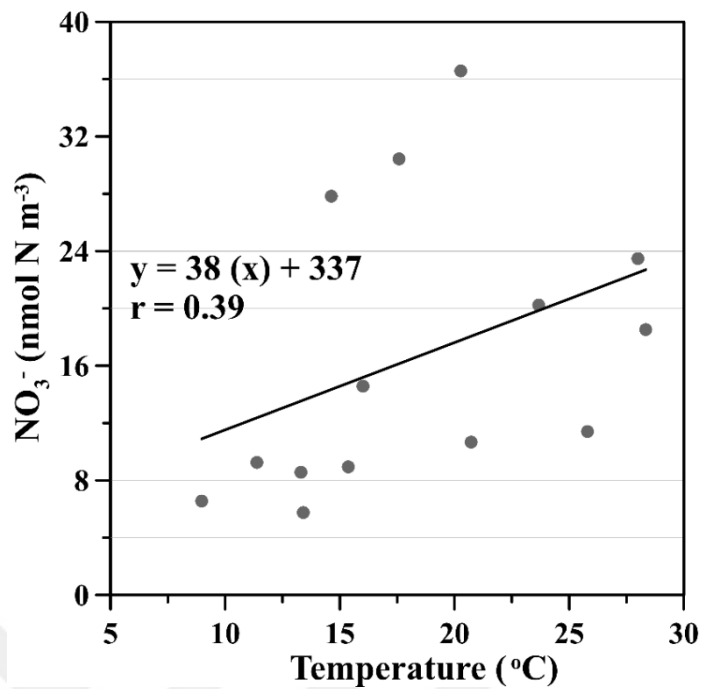


Figure 4. 18. The relationship between water-soluble nitrate (nmol N m⁻³) and temperature (°C) for PM10.

Figure 4.19.a, and b illustrate relationship between monthly mean urea and rain amount / temperature for coarse though Figure 4.19.c and d present relationship between monthly mean urea and rain amount / temperature for fine particles. As can be inferred from figures, there were no statistically significant correlation urea and rain amount/temperature, except for coarse urea. Urea in coarse mode indicated inverse correlations with rain amount ($r=0.67$). This suggested that coarse urea particles were removed from atmosphere efficiently by rain. The logarithmic relationship between concentration and rain amounts suggests sharp reduction of particles by precipitation. There was an inverse relationship between urea concentrations and temperature similar to the relationship between WSON concentrations and temperature.

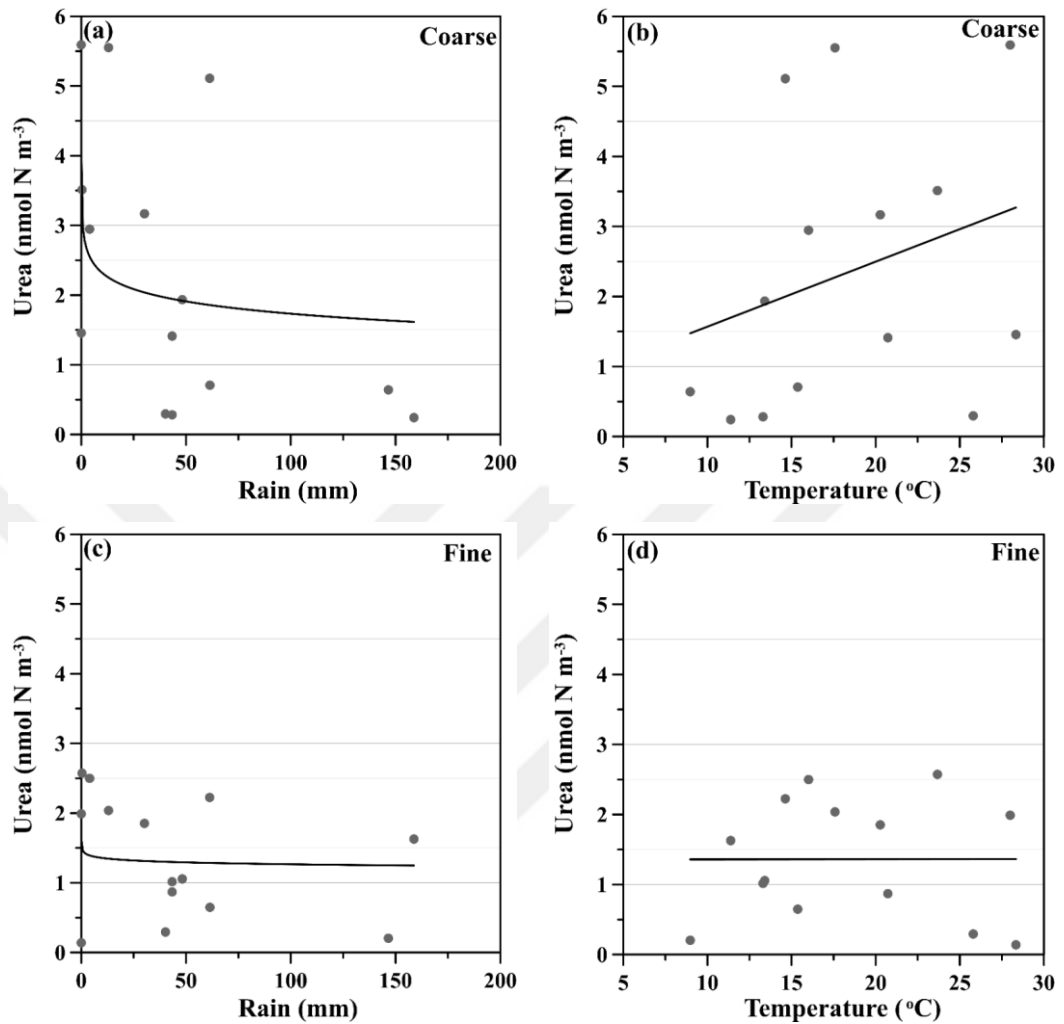


Figure 4. 19. The relationship between (a) urea (nmol N m⁻³) and rain amount (mm) (b) urea (nmol N m⁻³) and temperature (°C) in coarse mode (c) urea (nmol N m⁻³) and rain amount (mm) and (d) urea (nmol N m⁻³) and temperature (°C) in fine mode.

4.5. Influence of Mineral Dust Episodes on the Water-Soluble Nitrogen Species

As it is well documented, the eastern Mediterranean Sea is heavily impacted by mineral dust episodes originating from Sahara and the Middle East deserts (Kubilay and Saydam, 1995; Kubilay et al., 2000, Koçak et al., 2004a, b and 2012). For the current study water-soluble calcium concentrations were higher than 2000 ng N m⁻³ (as a threshold values, corresponding air mass back trajectories and OMI-AI were applied in order to clarify mineral dust events at Erdemli between February 2014 and April 2015. Observed nssCa²⁺ (dust threshold > 2000 ng m⁻³) concentration (ng m⁻³) values between January 2014 and April 2015 were presented in Figure 4.20. During

the study period, 45 dusty days were determined by an abrupt increase in the concentration of calcium. These dusty days were characterized by 25 distinct mineral dust episodes with varying periods from one day to 5 days. These dust episodes were applied as an example. First dust episode was observed from 21st to 24th of February 2014 with a mean nssCa²⁺ concentration of 3350 ng m⁻³. The highest nssCa²⁺ (4989 ng m⁻³) value was determined on 24th of February. Figure 4.21. shows 3-day air-mass back trajectories arriving at 1, 2, 3 and 4 km and OMI-AI. Trajectories reaching at 1 and 2 km indicated air flow from the Middle East whilst air-masses arriving at 3 and 4 km denoted long range transport originating from Sahara desert. On 24th of February, OMI-AI demonstrated dust could particularly over the Middle East with values reaching up to 2.5. Furthermore, OMI-AI indicated that the Levantine Basin was completely under the influence of mineral dust particles. The strongest dust episode was observed between 2nd and 3rd of March 2014. Correspondingly, nssCa²⁺ concentrations were 17100 ng m⁻³ and 9263 ng m⁻³ on 2nd and 3rd of the March (see Figure 4.20). The third dust episode was characterized with mean nssCa²⁺ concentration of 5120 ng m⁻³ from 15th to 16th November 2014. For this dust episode the highest nssCa²⁺ (6658 ng m⁻³) was detected on 16th of November. Air-mass back trajectories for 15th and 16th of November along with OMI-AI are presented in Figure 4.22.a and d. Back trajectories and OMI-AI suggested that the sampling site was under the influence of mineral dust particles both originating from the Middle East and Sahara desert.

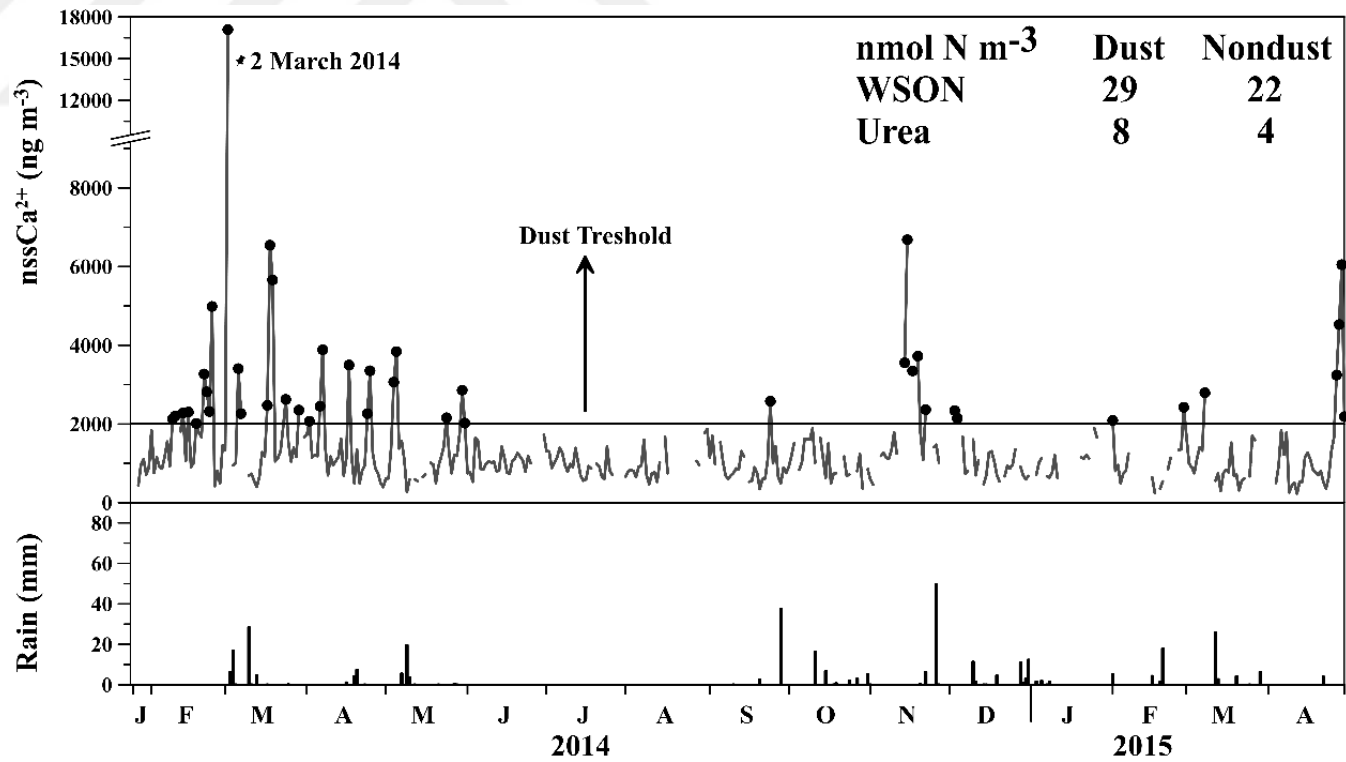


Figure 4. 20. Observed nssCa^{2+} (dust threshold $> 2000 \text{ ng m}^{-3}$) concentration (ng m^{-3}) values between January 2014 and April 2015.

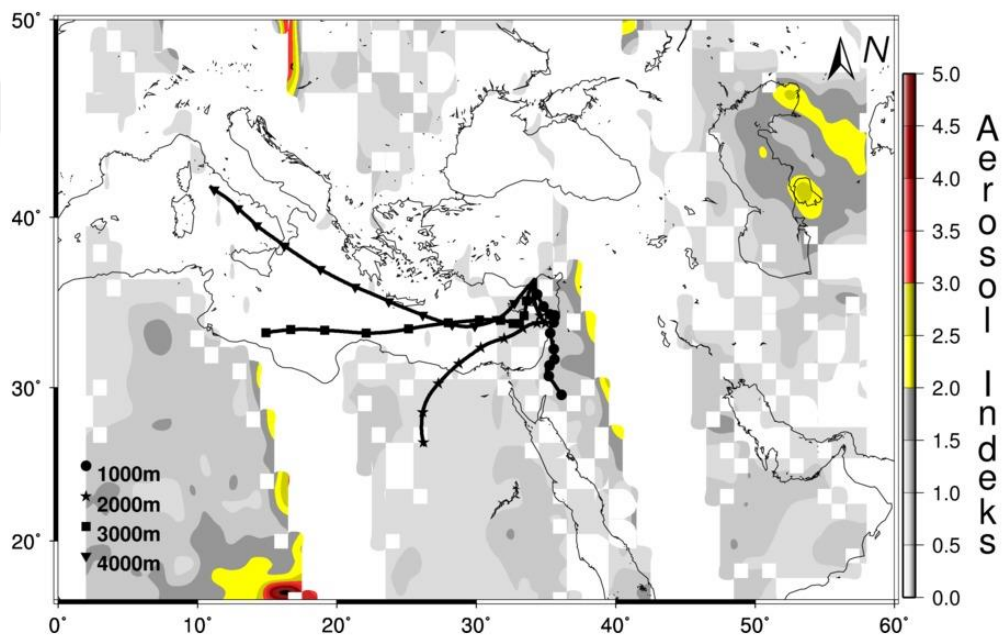


Figure 4. 21. 3-day air-mass back trajectories arriving at 1, 2, 3 and 4 km and OMI-AI corresponding to 24th of February 2014.

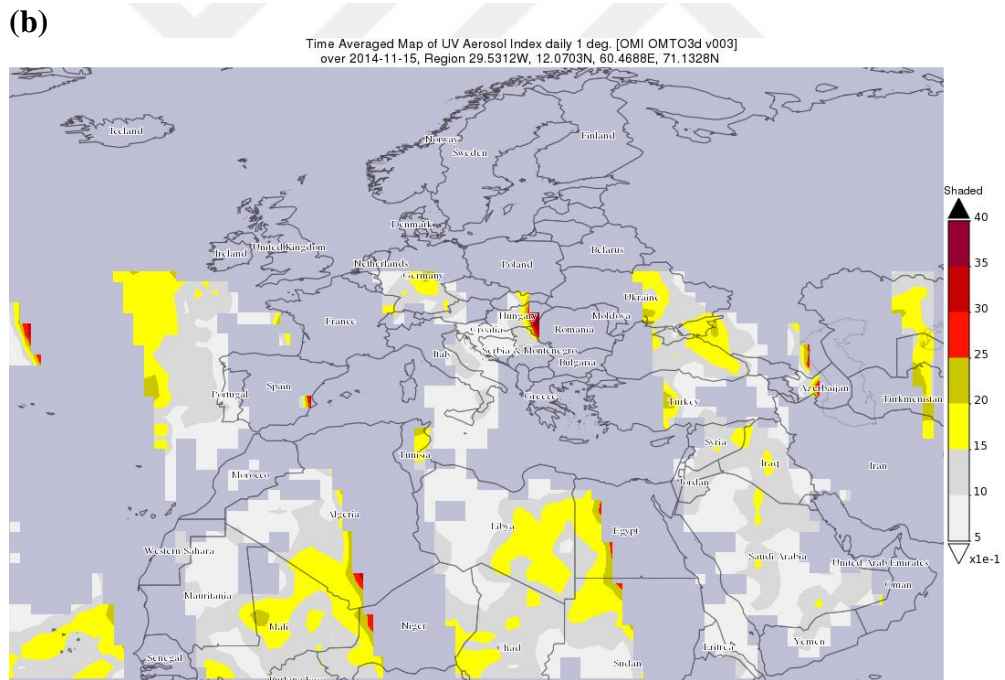
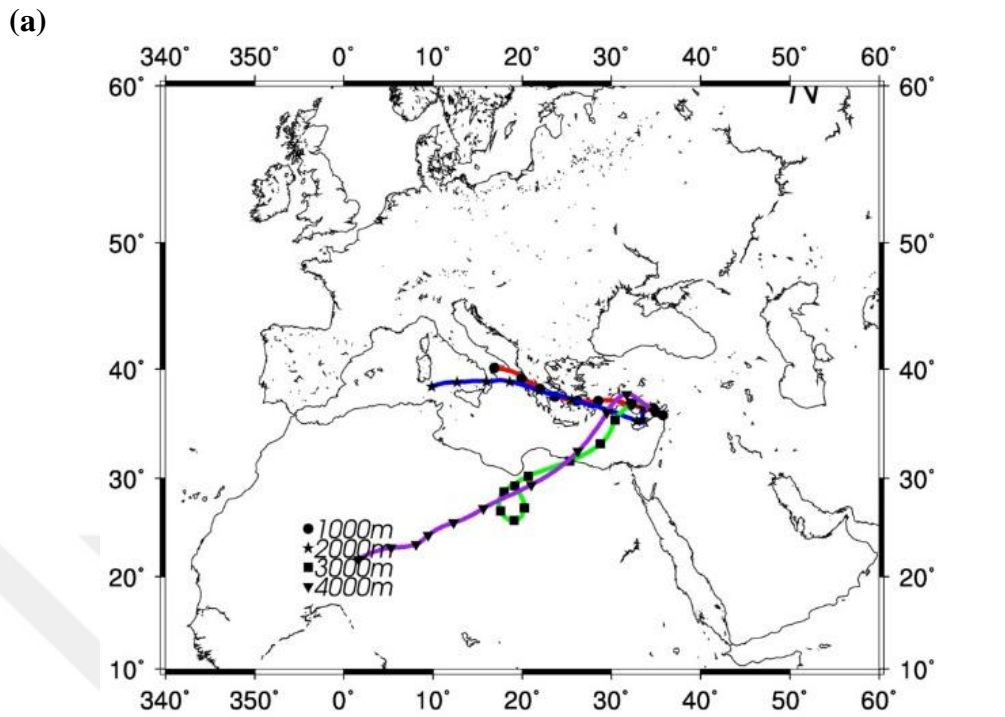
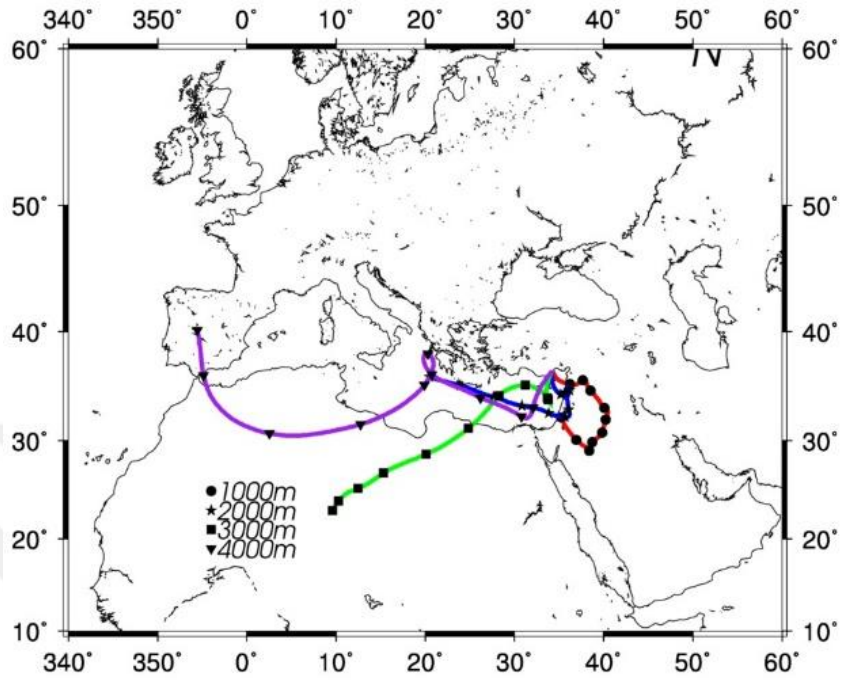


Figure 4. 22. (a) 3-day air-mass back trajectories arriving at 1, 2, 3 and 4 km and (b) OMI-AI for 15th of November 2014, (c) 3-day air-mass back trajectories arriving at 1, 2, 3 and 4 km and (d) OMI-AI for 16th of November 2014.

(c)



(d)

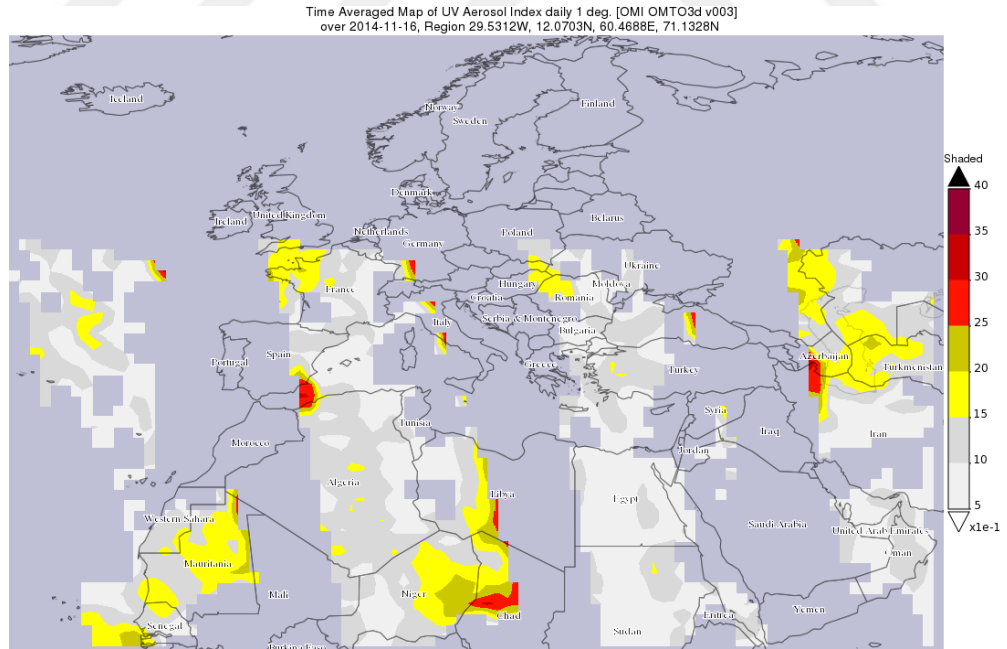


Figure 4.22. Continued.

The statistical summary of water-soluble nitrogen species and nssCa^{2+} for dust and non-dust days is presented in Table 4.6.a, and b. As can be seen from tables, except for ammonium, these species illustrated dramatic difference in their concentrations during dust and non-dust events. For instance, the crustally derived water-soluble nssCa^{2+} (3760 ng m^{-3}) for dust events was almost 4 times higher than that of observed for non-dust events. Water-soluble nitrate also showed similar behavior, being at least 2 times higher during dust events compared to non-dust events. This acidic species enriched on basic dust particles because of either homogeneous or heterogeneous reactions (Aymoz et al., 2004; Koçak et al., 2004a, 2007). As expected, ammonium did not show clear difference between dust and non-dust events. WSON and urea also denoted contrast for dust and non-dust events. During dust episodes, WSON exhibited an increase in its concentration around 30% whilst urea indicated an increase in its concentration around 200%. The strongest mineral dust episode was observed on 2nd of March 2014. The concentration of nssCa^{2+} exceeded 17.000 ng m^{-3} while the WSON and urea concentrations were reached up to 66 nmol N m^{-3} and 20 nmol N m^{-3} , respectively. The mineral dust not only influence concentration of WSON and urea but also impact the relative contribution of fine and coarse mode aerosol. For example, more than 80% of both WSON and urea were derived from coarse mode aerosols on 2nd of March 2014.

Table 4. 6. The statistical summary of aerosol species for (a) dust events (b) non-dust events at Erdemli.

(a)

Aerosol *	WSON	Urea	Ca ²⁺	NO ₃ ⁻	NH ₄ ⁺
PM₁₀					
Mean	29.3	7.8	3760.6	26.2	37.9
Std	22.1	5.3	2718.5	23.5	22.9
Median	28.8	8.0	2838.0	16.0	36.7
Minimum	-27.9	0.006	2037.3	1.5	1.7
Maximum	79.0	19.8	17319.8	83.0	88.4
PM_{10-2.5}					
Mean	17.4	5.1	3164.9	0.8	34.8
Std	12.3	4.0	2528.7	1.1	22.3
Median	15.2	4.7	2237.3	0.4	31.5
Minimum	0.3	0.006	1329.4	0.1	1.7
Maximum	56.2	16.4	16089.9	6.6	86.4
PM_{2.5}					
Mean	17.2	2.7	595.8	25.4	3.1
Std	16.2	2.2	360.6	23.4	2.9
Median	14.1	2.0	518.3	15.2	2.0
Minimum	-20.9	0.006	174.7	1.1	0.1
Maximum	56.9	8.3	2094.3	82.4	10.4

*The unit for Ca²⁺ concentrations are in terms of ng m⁻³ whilst the unit for WSON, urea, NO₃⁻ and NH₄⁺ concentrations are in terms of nmol N m⁻³.

(b)

Aerosol *	WSON	Urea	Ca ²⁺	NO ₃ ⁻	NH ₄ ⁺
PM₁₀					
Mean	23.9	3.9	1035.8	22.8	15.2
Std	15.2	3.1	384.6	24.5	12.2
Median	21.8	3.2	999.5	15.8	12.4
Minimum	-17.4	0.006	242.9	0.5	0.2
Maximum	70.9	14.0	1955.3	164.4	68.9
PM_{10-2.5}					
Mean	15.4	2.3	828.8	0.9	13.1
Std	12.5	2.2	344.1	1.0	11.1
Median	12.7	1.9	785.4	0.5	10.4
Minimum	-23.4	0.006	129.8	0.1	0.1
Maximum	66.5	9.5	1834.0	6.9	64.0
PM_{2.5}					
Mean	8.6	1.6	207.0	22.0	2.1
Std	10.2	1.5	110.2	24.3	2.2
Median	8.2	1.3	188.3	14.8	1.4
Minimum	-40.2	0.006	7.3	0.1	0.1
Maximum	42.7	9.0	810.9	161.1	15.3

*The unit for Ca²⁺ concentrations are in terms of ng m⁻³ whilst the unit for WSON, urea, NO₃⁻ and NH₄⁺ concentrations are in terms of nmol N m⁻³.

4.6. Influence of Air Flow on Water-Soluble Nitrogen Species

The impact of mineral dust on chemical composition of water-soluble nitrogen was clarified in the previous section. In order to demonstrate the influence of air flow on chemical composition of water-soluble nitrogen species the considerable variability due to dust episodes should be removed from the data set. Thus, the dusty days were omitted from data set before assign the effect of air flow on water-soluble nitrogen species. The statistical summary of these species is illustrated in Table 4.7, according to air flow.

The lowest WSON concentration was associated with air masses originated from Russia whereas the highest values were observed airflow from the Middle East and North Africa. The calculated $PM_{10-2.5}/PM_{2.5}$ ratios of WSON for these airflows were higher than 1.15, indicating predominance of coarse fraction. The lowest urea concentrations were found when airflow originated from Russia, Northern Turkey and Middle East, with concentrations of 2.7, 2.9 and 2.3 $nmol\ N\ m^{-3}$, respectively. Yet, there was a difference between their $PM_{10-2.5}/PM_{2.5}$ ratio, implying airflow from Russia and Northern Turkey was equally influenced by fine and coarse particles whilst air masses from Middle East was chiefly dominated by coarse particles. It might be argued that airflow coming from Middle East had more natural sources compared to anthropogenic sources.

Table 4. 7. The statistical summaries for WSON and urea mean concentrations (nmol N m^{-3}) according to the origination of air masses for non-dust events.

Air mass	WSON (nmol N m^{-3})				Urea (nmol N m^{-3})			
	PM ₁₀	PM _{10-2.5}	PM _{2.5}	PM _{10-2.5} / PM _{2.5}	PM ₁₀	PM _{10-2.5}	PM _{2.5}	PM _{10-2.5} / PM _{2.5}
Western Turkey	20.5	11.4	10.7	1.07	4.2	2.5	1.7	1.47
Southern Europe	22.7	11.5	12.1	0.95	4.4	2.5	1.9	1.32
Eastern Europe	20.7	11.9	11.0	1.08	4.0	2.4	1.6	1.50
Russia	18.0	10.7	8.3	1.29	2.7	1.3	1.4	0.93
Northern Turkey	22.2	11.8	11.2	1.05	2.9	1.5	1.4	1.07
Middle East	26.1	14.4	12.3	1.17	2.3	1.4	0.9	1.56
North Africa	25.3	15.1	12.2	1.24	4.0	2.6	1.3	2.00

4.7. Correlation between Water-Soluble Nitrogen Species and Major Ions

Correlation between variables show the extent to which they vary together. Consequently, the strong correlation coefficients between aerosol species might be attributed to one or more of the following processes: (i) similar source, (ii) similar generation and/or removal mechanism and/or (iii) similar transport pathways.

The significance level of the correlation coefficient strictly related to the number of sample in the data set. Even a small correlation coefficients can be statistically significant due to a high number of samples. To this end, four distinct terminology were applied during the interpretation of correlation coefficients obtained from the present study: (a) $r = 0$; no correlation, (b) $r = 0-0.4$; weak correlation, (c) $r = 0.4-0.7$; moderate correlation and (d) $r = 0.7-1.0$; strong correlations.

Table 4.8.a, b show correlation coefficients for fine and coarse particles for dust episodes while Table 4.9.a, b depict correlation coefficients for fine and coarse particles for non-dust events.

(a) Dust Events-Coarse: As expected, sea salt originated water-soluble ions (Na^+ , Cl^- and Mg^{2+}) denoted strong correlation coefficients between one another, showing they were chiefly derived from sea spray. Water-soluble potassium and sulfate illustrated strong correlation coefficient ($r > 0.75$) both with crust derived calcium and sea salts, implying influence of crust and sea spray on their observed concentrations. Urea and crust derived calcium demonstrated strong correlation coefficients with a value high that 0.70. This relationship suggested the considerable impact of mineral dust on urea concentration. On the other hand, there was a significant correlation between urea and nitrate ($r = 0.76$), denoting probable reaction between basic urea and acidic nitrate during long range transport. Sea salt particles and crustal calcium also had strong correlations confidents. However, this does not mean that sea salt particles were influenced by mineral dust. On contrary, it shows enrichment of sea salt particles when the mineral dust is mainly associated with a frontal pressure system (Kubilay et al., 2000). Sulfate had strong ($r = 0.94$) and moderate ($r = 0.67$) correlation coefficients with calcium and urea, respectively (Table 4.8.a). Former relationship implies the heterogeneous and/or homogeneous reactions of acidic sulfate on the surface of alkaline dust particles (Aymoz et al., 2004, Koçak et al., 2004a, b and 2007). WSON

and calcium illustrated moderate correlation, suggesting at least some of the WSON was originated from mineral dust particles.

(b) Dust Events-Fine: As can be deduced from the Table 4.8.b, relationship between aerosol species in fine mode was completely different from coarse mode. Water-soluble ammonium had strong correlation coefficient with sulfate ($r=0.92$). As it is well known, acidic sulfate is neutralized by NH_4^+ (Bardouki et al., 2003). Potassium had strong correlation with aforementioned secondary aerosols. Previous studies have been shown that the potassium in fine mode is chiefly originated from burning of vegetation and usage of fossil fuels (Sciare et al, 2003; Koçak et al., 2007). It might be suggested that during dust events secondary aerosols were heavily influenced by from burning of vegetation and fossil fuels. There was a moderate correlation coefficient between urea and secondary aerosols ammonium and sulfate.

(a) Non-Dust Events-Coarse: Similar to dust events, sea salt derived water-soluble ions (Na^+ , Cl^- and Mg^{2+}) showed strong correlation coefficients between one another, indicating they were mainly came from sea spray. However, relationships among the other species changed drastically. For instance, the relationship of urea with calcium and nitrate deteriorated for non-dust events compared to dust events. There were moderate correlation coefficients, implying that crustal contribution and reactions became less important during non-dust events. Acidic species nitrate and sulfate had moderate correlation coefficients with sea salt and crustal particles due to acid-basic reactions. Potassium showed moderate correlation coefficients with sea salt particles, suggesting partial influence of sea spray (Table 4.9.a).

(b) Non-Dust Events-Fine: Once more, sea salt derived water-soluble ions (Na^+ , Cl^- and Mg^{2+}) demonstrated strong correlation coefficients between one another, indicating they were primarily resulted from sea spray. As foreseen, there was a strong correlation coefficient between ammonium and sulfate ($r=0.94$, for more details see above). Nitrate had moderate correlation coefficients with sea salt particles, repeatedly suggesting acid-base reactions. Sulfate and ammonium had moderate correlation coefficients with potassium, referring considerable effect of biomass burning and fossil fuel combustion. Urea demonstrated moderate correlation coefficient with secondary aerosols ammonium and sulfate (Table 4.9.b).

Table 4. 8. Correlation coefficients for (a) coarse (PM_{10-2.5}) and (b) fine (PM_{2.5}) particles for dust episodes.

<i>(a)</i> PM _{10-2.5}	Na ⁺	Cl ⁻	Mg ⁺	K ⁺	SO ₄ ²⁻	Ca ²⁺	Urea	WSO _N	NO ₃ ⁻	NH ₄ ⁺
Na ⁺	1.00	0.97	0.94	0.86	0.77	0.70	0.62	0.51	0.27	-0.10
Cl ⁻	0.97	1.00	0.94	0.92	0.87	0.82	0.69	0.51	0.31	-0.15
Mg ⁺	0.94	0.94	1.00	0.91	0.87	0.86	0.69	0.52	0.34	-0.10
K ⁺	0.86	0.92	0.91	1.00	0.94	0.92	0.66	0.53	0.35	-0.02
SO ₄ ²⁻	0.77	0.87	0.87	0.94	1.00	0.94	0.67	0.52	0.40	-0.14
Ca ²⁺	0.70	0.82	0.86	0.92	0.94	1.00	0.71	0.50	0.45	-0.21
Urea	0.62	0.69	0.69	0.66	0.67	0.71	1.00	0.31	0.76	-0.29
WSO _N	0.51	0.51	0.52	0.53	0.52	0.50	0.31	1.00	0.15	0.01
NO ₃ ⁻	0.27	0.31	0.34	0.35	0.40	0.45	0.76	0.15	1.00	-0.33
NH ₄ ⁺	-0.10	-0.15	-0.10	-0.02	-0.14	-0.21	-0.29	0.01	-0.33	1.00

Table 4.8. Continued.

(b)PM_{2.5}	Na⁺	Cl⁻	Mg⁺	K⁺	SO₄²⁻	Ca²⁺	Urea	WSON	NO₃⁻	NH₄⁺
Na⁺	1.00	0.46	0.74	-0.03	-0.05	0.11	-0.38	-0.11	0.41	-0.31
Cl⁻	0.46	1.00	0.43	-0.11	-0.32	0.39	-0.24	-0.24	0.61	-0.39
Mg⁺	0.74	0.43	1.00	0.01	0.03	0.62	-0.39	-0.35	0.45	-0.25
K⁺	-0.03	-0.11	0.01	1.00	0.75	0.18	0.41	0.30	-0.37	0.69
SO₄²⁻	-0.05	-0.32	0.03	0.75	1.00	0.11	0.61	0.31	-0.40	0.92
Ca²⁺	0.11	0.39	0.62	0.18	0.11	1.00	-0.19	-0.26	0.33	-0.04
Urea	-0.38	-0.24	-0.39	0.41	0.61	-0.19	1.00	0.26	-0.29	0.68
WSON	-0.11	-0.24	-0.35	0.30	0.31	-0.26	0.26	1.00	-0.37	0.29
NO₃⁻	0.41	0.61	0.45	-0.37	-0.40	0.33	-0.29	-0.37	1.00	-0.53
NH₄⁺	-0.31	-0.39	-0.25	0.69	0.92	-0.04	0.68	0.29	-0.53	1.00

Table 4. 9. Correlation coefficients for (a) coarse (PM_{10-2.5}) and (b) fine (PM_{2.5}) particles for non-dust events.

<i>(a)PM_{10-2.5}</i>	Na ⁺	Cl ⁻	Mg ⁺	K ⁺	SO ₄ ²⁻	Ca ²⁺	Urea	WSON	NO ₃ ⁻	NH ₄ ⁺
Na ⁺	1.00	0.89	0.85	0.55	0.49	0.05	0.37	0.01	0.36	-0.09
Cl ⁻	0.89	1.00	0.73	0.45	0.39	0.04	0.32	-0.06	0.12	-0.16
Mg ⁺	0.85	0.73	1.00	0.56	0.42	0.13	0.32	0.06	0.35	-0.03
K ⁺	0.55	0.45	0.56	1.00	0.55	0.28	0.09	0.07	0.18	0.17
SO ₄ ²⁻	0.49	0.39	0.42	0.55	1.00	0.44	0.22	0.09	0.38	0.24
Ca ²⁺	0.05	0.04	0.13	0.28	0.44	1.00	0.24	-0.02	0.40	0.08
Urea	0.37	0.32	0.32	0.09	0.22	0.24	1.00	0.08	0.55	-0.30
WSON	0.01	-0.06	0.06	0.07	0.09	-0.02	0.08	1.00	-0.14	0.03
NO ₃ ⁻	0.36	0.12	0.35	0.18	0.38	0.40	0.55	-0.14	1.00	-0.12
NH ₄ ⁺	-0.09	-0.16	-0.03	0.17	0.24	0.08	-0.30	0.03	-0.12	1.00

Table 4.9. Continued.

(b)PM_{2.5}	Na⁺	Cl⁻	Mg⁺	K⁺	SO₄²⁻	Ca²⁺	Urea	WSON	NO₃⁻	NH₄⁺
Na⁺	1.00	0.81	0.91	0.04	0.11	0.20	0.00	0.00	0.64	-0.07
Cl⁻	0.81	1.00	0.77	-0.04	-0.19	0.17	-0.11	-0.04	0.39	-0.29
Mg⁺	0.91	0.77	1.00	0.02	0.07	0.30	-0.10	-0.02	0.56	-0.13
K⁺	0.04	-0.04	0.02	1.00	0.53	0.36	0.31	0.19	-0.22	0.53
SO₄²⁻	0.11	-0.19	0.07	0.53	1.00	0.27	0.59	0.17	-0.04	0.94
Ca²⁺	0.20	0.17	0.30	0.36	0.27	1.00	0.06	0.17	0.01	0.13
Urea	0.00	-0.11	-0.10	0.31	0.59	0.06	1.00	0.29	-0.07	0.59
WSON	0.00	-0.04	-0.02	0.19	0.17	0.17	0.29	1.00	-0.23	0.10
NO₃⁻	0.64	0.39	0.56	-0.22	-0.04	0.01	-0.07	-0.23	1.00	-0.14
NH₄⁺	-0.07	-0.29	-0.13	0.53	0.94	0.13	0.59	0.10	-0.14	1.00

4.8. Application of PMF to Determine the Sources of WSON and Urea

Table 4.10, presents results obtained from PMF analysis. The first factor explained 77 % and 26 % of the WSON and urea, respectively. This factor also elucidated 27 %, 27 %, 10 % and 9 % of the K^+ , Ca^{2+} , SO_4^{2-} and Mg^{2+} , correspondingly. These water-soluble ions are used as nutrient during agricultural practices, hence, this factor might be ascribed to re-suspension of cultivated soil. Second factor accounted 86 % and 51 % of the ammonium and sulfate, therefore, it might be identified as secondary aerosol source. This factor clarified 2 % of the WSON. Correspondingly, third factor refined 63 % and 49 % of the nitrate and urea, illustrating reaction between these two species. The last factor heavily loaded with sea salt originated particles and described 10 % of the WSON.

Table 4. 10. The results of PMF analysis that is used to determine the origins of WSON and urea.

Species	F1	F2	F3	F4
WSON	0.77	0.02	0.00	0.10
Urea	0.26	0.00	0.49	0.00
Cl ⁻	0.04	0.00	0.00	0.86
SO ₄ ²⁻	0.10	0.51	0.12	0.11
Na ⁺	0.03	0.02	0.07	0.70
K ⁺	0.27	0.21	0.05	0.25
Mg ²⁺	0.09	0.02	0.18	0.50
Ca ²⁺	0.27	0.14	0.21	0.12
NO ₃ ⁻	0.00	0.13	0.63	0.06
NH ₄ ⁺	0.04	0.86	0.00	0.00

4.9. Atmospheric Depositions of N-Species and Implications Regarding Marine Production

The atmospheric dry and wet deposition fluxes of WSON, NO_3^- and NH_4^+ and WSTN January 2014 and April 2015 are demonstrated in Table 4.11. The atmospheric depositions of NH_4^+ ($14.3 \text{ mmol N m}^{-2} \text{ yr}^{-1}$) was dominated by wet deposition, elucidating 92 % of the total atmospheric nitrogen fluxes. Whereas, the atmospheric flux of NO_3^- was mostly influenced by dry ($10.0 \text{ mmol N m}^{-2} \text{ yr}^{-1}$) deposition mode which covers 48 % of the total atmospheric nitrogen fluxes. Taking into account the values presented in Table 4.11, $57.8 \text{ mmol N m}^{-2} \text{ yr}^{-1}$ was calculated

in the study area. If one assumes that all N are bioavailable to primary producers for primary production and if a Redfield N/C ratios of 106/16 is applied, it would be estimated that atmospheric N depositions can support new production 7.95 g C yr⁻¹, respectively. According to recent study which has been shown that annual primary production for coastal and open waters of Cilician Basin were around 413 mg C m⁻² d⁻¹ and 179 mg C m⁻² d⁻¹, respectively (Yücel, 2013). It has been noted that f- ratio, defined as ratio between new and total production, may vary from 0.05 to 0.16 in oligotrophic seas such as Mediterranean (Estrada, 1996 and references therein). For instance, mean value of 0.16 was applied by Estrada (1996) to assess the amount of new production in the Eastern Mediterranean.

If the f-ratio of 0.16 is applied, the annual new production for coastal and open waters of Cilician Basin would be 24.12 g C yr⁻¹ and 10.45 g C yr⁻¹ respectively. Based on observed new production in the surface waters of the Eastern Mediterranean, the atmospheric water-soluble nitrogen flux was found to sustain 33 and 76 % of the new production in coastal and open waters, respectively (Figure 4.23). The observed new production between June and October was found to be around 2 mg C m⁻² d⁻¹. During this period, atmospheric nitrogen can support new production in the Cilicia Basin up to 6 times.

Table 4. 11. Summary of the WSON, NO₃⁻, NH₄⁺ and WSTN fluxes (F_d) in PM10 samples and WSON, NO₃⁻, NH₄⁺ contributions to WSTN in dry and wet depositions at Erdemli during the period of January 2014 and April 2015.

Aerosol	F_d (mmol N m⁻² yr⁻¹)	RC*
WSON	9.76	46
NO ₃ ⁻	9.97	47
NH ₄ ⁺	1.27	6
WSTN	21.0	
Rainwater	F_d (mmol N m⁻² yr⁻¹)	RC*
WSON	10.73	29
NO ₃ ⁻	11.67	32
NH ₄ ⁺	14.33	39
WSTN	36.73	

*RC refers to relative contribution of corresponding species to water-soluble total nitrogen in terms of percentages.

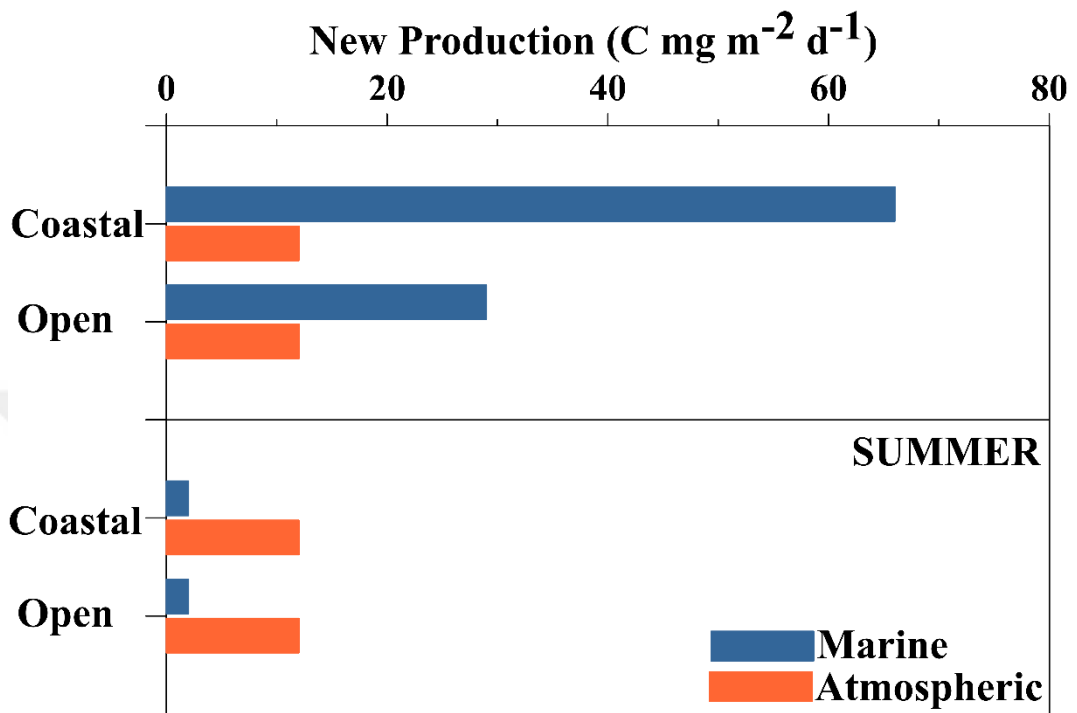


Figure 4. 23. The possible impacts of atmospheric nitrogen to the new production in the coastal and open marine environment.

5. CONCLUSION AND RECOMMENDATIONS FOR FUTURE RESEARCH

The soluble, bio-available fractions and sources of atmospheric water-soluble nitrogen species with the possible impacts of these species on coastal and open waters of the Eastern Mediterranean were investigated at a coastal rural site in the northeastern.

The results obtained from this study have shown that WSON was dominant water-soluble nitrogen species in aerosol with an arithmetic mean concentration of $24.6 \text{ nmol N m}^{-3}$. It was followed by NH_4^+ ($23.3 \text{ nmol N m}^{-3}$) and NO_3^- ($17.9 \text{ nmol N m}^{-3}$). WSON (61 %) and NO_3^- (88%) were primarily found in coarse particles. However, the majority of NH_4^+ (96 %) was associated with fine particles. The current study has shown that WSON was an important contributor to WSTN whilst urea elucidated significant portion of WSON in both aerosol and rainwater samples. WSTN was almost equivalently influenced by NO_3^- (49.8 %) and WSON (47.6 %) in coarse particles whereas, it was dominated by NH_4^+ in fine particles, explaining 65.5 %. The relative contributions of WSON to WSTN were 47.6 % in coarse particles, 28.1 % in fine particles and 29.3 % in rainwater samples. The mean concentration of urea was $4.4 \text{ nmol N m}^{-3}$. The majority urea was originated from coarse fraction (65 %) and the remaining part was associated with fine fraction (35 %). The relative contributions of urea to WSON were considerable over the Eastern Mediterranean atmosphere since it accounted around 18 % of WSON in atmospheric particles and 6 % of WSON in rainwater samples. Furthermore, Urea had a considerable contribution to WSTN; being 9 % in coarse mode aerosols, 5 % in fine mode aerosols and 2 % in rainwater samples. Sharp decrease (up to 50 %) was observed in the concentrations of secondary aerosols from 2001 to 2015. This dramatic decrease might be attributed to reduction on the usage of fertilization and abatement in NO_x emission.

Water-soluble nitrogen species exhibited an order of magnitude change from day to day and the concentrations of these species were highly influenced by meteorological parameters, chemical reactions, history of air mass back trajectories and emission strength. Determined concentrations of WSON and urea indicated lowest values in rainy days which verified that the particles were removed efficiently from atmospheric compartment with rain. One of the highest WSON ($66.1 \text{ nmol N m}^{-3}$) and

urea ($19.8 \text{ nmol N m}^{-3}$) concentrations were observed on March 2, 2014 when the air mass back trajectories associated with south/south westerly airflow. Not only back trajectories but also OMI-AI indicated that the sampling site was under the influence of mineral dust plume originating from desert regions such as Middle East and North Africa. During this dust episode, WSON (85 %) was enriched in coarse particles, dictating the mineral dust as a main source of WSON.

The arithmetic mean concentrations of water-soluble nitrogen species illustrated a complex seasonality. In general, the highest values of WSON and urea were observed in the summer season due to the absence of rain and resuspension of soil. During summer, WSON and urea were mainly associated with coarse mode aerosol however, WSON was mainly affiliated with fine mode in winter. The seasonality of NH_4^+ and NO_3^- were similar to those observed for WSON and urea, the lowest mean concentrations were observed in the winter season. Taking into account seasonal contributions of coarse and fine particles, more than 90 % of NH_4^+ was dominated by fine mode aerosols and more than 80 % of NO_3^- was related with coarse particles.

The influence of temperature and rain on the seasonal variability of water-soluble nitrogen were also investigated. In coarse particles, WSON concentrations were sharply decreased as rain amount and temperature increased. On the one hand there was no relationship between rain amount and WSON concentrations on the other hand there was an inverse relationship between temperature and WSON concentrations in fine particles. Similar relationships were observed for urea in coarse mode aerosols. There was no relationship between rain amount/temperature and urea for fine mode aerosols. An inverse relationship was observed between rain amount and NH_4^+ and NO_3^- concentrations in PM_{10} , indicating efficient removal of these particles from the atmospheric compartment via precipitation. As temperature increased, NH_4^+ and NO_3^- concentrations were also increased. There was a strong correlation coefficient between NH_4^+ and temperature with a value of 0.85 whilst there was a weak correlation between NO_3^- and temperature with a value of 0.39. The strong correlation coefficient between NH_4^+ and temperature revealed gas to particle conversion of NH_4^+ by photochemistry.

For the whole sampling period, 45 dusty days were identified by a sharp increase in the concentration of nssCa^{2+} . nssCa^{2+} values fluctuated between from of 2000 ng m^{-3} and 19000 ng m^{-3} , demonstrating a large variability of the dust events. Except for NH_4^+ , the dramatic influence of mineral dust episodes on the aerosol composition of water-soluble nitrogen species was demonstrated by comparing dust and non-dust events. During dust events, WSON and urea illustrated 30 % and 200 % increase in their concentrations, respectively, compared to those values of non-dust events.

Urea and crust originated Ca^{2+} had a strong correlation coefficient ($r = 0.71$) in coarse mode for dust events which indicated the noticeable impact of mineral dust on urea concentration. WSON and Ca^{2+} had a moderate correlation coefficient with a value of 0.50 in coarse mode for dust events suggesting at least some of the WSON was derived from mineral dust particles.

Based on cluster analysis, the air masses back trajectories were categorized into 7 groups namely: Western Turkey, Southern Europe, Eastern Europe, Russia, Northern Turkey, Middle East and North Africa. The lowest WSON concentration was associated with air masses originated from Russia while the highest values were observed airflow from the Middle East and North Africa. The calculated $\text{PM}_{10-2.5}/\text{PM}_{2.5}$ ratios of WSON for these airflows were higher than 1.15, denoting dominance of coarse fraction. The lowest urea concentrations were found when airflow derived from Russia, Northern Turkey and Middle East, with concentrations of 2.7, 2.9 and $2.3 \text{ nmol N m}^{-3}$, respectively. Whereas, there was a distinct difference between their $\text{PM}_{10-2.5}/\text{PM}_{2.5}$ ratio, suggesting airflow from Russia and Northern Turkey was equally influenced by fine and coarse particles whilst air masses from Middle East was mainly dominated by coarse particles. It might be argued that airflow originating from Middle East had more natural sources compared to anthropogenic sources.

Positive matrix factorization (PMF) analysis was applied to clarify sources of WSON and urea. Results denoted that 77 % and 10 % of the WSON was derived from the re-suspension of cultivated soil and sea-salt particles, respectively. Nevertheless, 27 % of the urea was held by re-suspension of cultivated soil while 49 % of urea was

found to be associated with nitrate, implying reaction between alkaline urea and acidic nitrate.

Annually, the atmospheric fluxes of WSON and nitrate were calculated 20.5 and 21.6 mmol N m⁻² yr⁻¹, respectively, whilst the atmospheric ammonium flux was found 15.6 mmol N m⁻² yr⁻¹. Based on detected new production in the surface waters of the Eastern Mediterranean, the atmospheric water-soluble nitrogen fluxes were calculated to sustain 33 % of the production in coastal waters and 76 % of the production in open waters.

In order to enhance our knowledge about WSON and urea, it is essential to:

- study organic nitrogen and urea isotopes to clarify the sources of WSON and urea,
- pinpoint which water-soluble nitrogen species might affect marine productivity positively and/or negatively,
- carry out real time measurements to reveal how organic nitrogen is affected by photochemical reactions.

REFERENCES

- Antia, N.J., Harrison, P.J., Oliveria, L., 1991. The role of dissolved organic nitrogen in phytoplankton nutrition, cell biology and ecology. *Phycologia* 30, 1–89.
- Arimoto, R., 2001. Eolian dust and climate: relationships to sources, tropospheric chemistry, transport and deposition, *Earth-Science Reviews*, 54, 29–42.
- Avila, A., Alarcon, M. and Queralt-Mitjans I., 1998. The chemical composition of dust transported in red rains its contribution to the biogeochemical cycle of a holm oak forest in Catalonia, Spain. *Atmospheric Environment*, 32, 179-191.
- Aymoz, G., Jaffrezo, J.L., Jacob, V., Colomb, A. and George, C., 2004. Evolution of organic and inorganic components of aerosol during a Saharan dust episode observed in the French Alps. *Atmospheric Chemistry and Physics*, 4, 2499–2512.
- Bardouki, H., Liakakou, H., Economou, C., Sciare, J., Smolik, J., Zdimal, V., Eleftheriadis, K., Lazaridis, M., Dye, C. and Mihalopoulos, N., 2003. Chemical composition of size resolved atmospheric aerosols in the eastern Mediterranean during summer and winter. *Atmospheric Environment*, 37, 195–208.
- Blanchard, D.C. and Cipriano, R.J., 1983. Sea spray production from bubbles. *Science*, 220, 1410.
- Borbely-Kiss, I., Koltay, E., Szabó, Gy., Bozó, L. and Tar, K., 1999. Composition and sources of urban and rural atmospheric aerosol in Eastern Hungary. *Journal of Aerosol Science*, 30, 369–391.
- Brody, L. R. and Nestor, M. J. R., 1980. Handbook for Forecasters in the Mediterranean, Part 2. Regional forecasting aids for the Mediterranean Basin. Naval Environmental Prediction Research Facility (Technical Report TR 80-10), pp. VII-1; VII-13. Monterey, California.
- Carbo, P., Krom, M.D., Homoky, W.B., Benning, L.G. and Herut, B., 2005. Impact of atmospheric deposition on N and P geochemistry in the southeastern Levantine basin. *Deep-Sea Research II*, 52, 3041–3053.
- Carlson, T.N. and Prospero, J.M., 1972. The large-scale movement of Saharan air outbreaks over the North Equatorial Atlantic. *Journal of Applied Meteorology*, 11, 283-297.
- Chen, H.Y. and Preston, M.R., 2004. Measurement of semi-volatile azaarenes in airborne particulate and vapor phases. *Anal. Chim. Acta* 501, 71–78.
- Chen, H.Y., Mills, S., Street, J., Golan, D., Post, A., Jacobson, M., Paytan, A., 2007. Estimates of atmospheric dry deposition and associated input of nutrients to Gulf of Aqaba seawater. *Journal of Geophysical Research*, 112, D04309, doi: 10.1029/2006JD007858.

Chen, H.Y., Chen, L., Chiang, Z., Hung, C., Lin, F., Chou, W., Gong, G., Wen, L., 2010. Size fractionation and molecular composition of water-soluble inorganic and organic nitrogen in aerosols of a coastal environment. *J. Geophys. Res. Journal of Geophysical Research*, 115(D22).

Choi, J.C., Lee, M., Chun, Y., Kim, J. and Oh, S., 2001. Chemical composition and source signature of spring aerosol in Seoul, Korea. *Journal of Geophysical Research*, 106, NO. D16, 18,067–18,074.

Collett Jr., J.L., Herckes, P., Youngster, S., Lee, T., 2008. Processing of atmospheric organic matter by California radiation fogs. *Atmos. Res.* 87, 232–241.

Cornell, S., A. Rendell, and T. Jickells, 1995. Atmospheric inputs of dissolved organic nitrogen to the oceans, *Nature*, 376, 243– 246.

Cornell, S., Jickells T., Thornton C., 1998. Urea in rainwater and atmospheric aerosol, *Atmospheric Environment*, 32, 1903-1910.

Cornell, S., K. Mace, S. Coeppicus, R. Duce, B. Huebert, T. Jickells, and L.-Z. Zhuang, 2001. Organic nitrogen in Hawaiian rain and aerosol, *J. Geophys. Res.*, 106(D8), 7983.

Cornell, S.E., Jickells, T.D., Cape, J.N., Rowland, A.P., Duce, R.A., 2003. Organic nitrogen deposition on land and coastal environments: a review of methods and data. *Atmos. Environ.* 37, 2173–2191.

Decesari, S., Facchini, M.C., Fuzzi, S., Tagliavini, E., 2000. Characterization of water-soluble organic compounds in atmospheric aerosol: a new approach. *J. Geophys. Res.* 105, 1481–1489.

Dentener, F., Carmichael, F., Zhang, Y., Lelieveld, J., Crutzen, P., 1996. “Role of mineral aerosol as a reactive surface in the global troposphere”. *Journal of Geophysical Research* 101, 22869–22889.

Dorling, S. R., Davies, T. D. and Pierce, C. E., 1992. Cluster analysis: A technique for estimating the synoptic meteorological controls on air and precipitation chemistry—Method and applications. *Atmospheric Environment*, 26A, 2575-2581.

Draxler, R.R., Rolph, G.D., 2003. HYSPLIT (HYbrid Single-Particle Lagrangian Integrated Trajectory), Model Access via NOAA ARL READY Website. NOAA Air Resources Laboratory, Silver Spring, MD. <http://www.arl.noaa.gov/ready/hysplit4.html>.

Duce R. A., J. LaRoche, K. Altieri, K. R. Arrigo, A. R. Baker, D. G. Capone, S. Cornell, F. Dentener, J. Galloway, R. S. Ganeshram, R. J. Geider, T. Jickells, M. M. Kuypers, R. Langlois, P. S. Liss, S. M. Liu, J. J. Middelburg, C. M. Moore, S. Nickovic, A. Oschlies, T. Pedersen, J. Prospero, R. Schlitzer, S. Seitzinger, L. L. Sorensen, M. Uematsu, O. Ulloa, M. Voss, B. Ward, L. Zamora, 2008. Impacts of Atmospheric Anthropogenic Nitrogen on the Open Ocean. *Science*, 320, 893.

Ediger, D., Tuğrul, S., Yılmaz, A., 2005. Vertical profiles of particulate organic matter and its relationship with chlorophyll-a in the upper layer of the NE Mediterranean Sea. *Journal of Marine Systems*, 55, 311-326.

Eklund, T.J., McDowell, W.H., and Pringle, C.M., 1997. Seasonal variation of tropical precipitation chemistry: La Selva, Costa Rica. *Atmospheric Environment* 31: 3903–3910.

EMEP programme (Co-operative Programme for Monitoring and Evaluation of the Long-range Transmission of Air pollutants in Europe) data online, <http://www.nilu.no/projects/ccc/emepdata.html>.

EMEP, 2013. Transboundary acidification, eutrophication and ground level ozone in Europe in 2011. Norwegian Meteorological Institute EMEP Rep. 1/2013, 205 pp.

EMEP, 2016.

Erduran, S. M. and Tuncel, S. G., 2001. Gaseous and particulate air pollutants in the Northeastern Mediterranean Coast., *Sci. Total Environ.*, 281, 205–215.

Estrada, M., 1996. Primary production in the northwestern Mediterranean. *Scientia Marina*, 60 (2), 55-64.

Finlayson-Pitts B. and Pitts, J. N., Jr., 2000. *Chemistry of the Upper and Lower Atmosphere: Theory, Experiments, and Applications*, Academic Press, San Diego, CA.

Glibert, P.M., Trice, T.M., Michael, B., Lane, L., 2005. Urea in the tributaries of the Chesapeake and coastal bays of Maryland. *Water Air Soil Pollut.* 160, 229–243.

Guerzoni, S., Malinaroli, E. and Chester, R., 1997. Saharan dust input to the western Mediterranean Sea: depositional patterns, geochemistry and sedimentological implications. *Deep-Sea Research II*, 44: 631-654.

Guerzoni, S., Chester, R., Dulac, F., Herut, B., Loye-Pilot, M. D., Measures, C., Migon, C., Molinaroli, E., Moulin, C., Rossini, P., Saydam, C., Soudine, A. and Ziveri, P., 1999. The role of atmospheric deposition in the biogeochemistry of the Mediterranean Sea. *Progress in Oceanography*, 44, 147-190.

Guo, J., Rahn, K.A. and Zhuang, G., 2004. A mechanism for the increase of pollution elements in dust storms in Beijing. *Atmospheric Environment*, 38, 855–862.

Güllü, G. H., Ölmez, I., Aygün, S. and Tuncel, G., 1998. Atmospheric trace element concentrations over the Eastern Mediterranean Sea: Factors affecting temporal variability. *Journal of Geophysical Research*, 103, D17, 21943-21954.

Hansell, D., 1993. Results and observations from the measurement of DOC and DON in seawater using a high-temperature catalytic oxidation technique. *Marine Chemistry*, 41, 195-202.

Hendry, C.D. and Brezonik, P.L., 1980. Chemistry of precipitation at Gainesville, Florida. *Environmental Science and Technology*, 14: 843–849.

Herut, B., Krom, M.D., Pan, G. ve Mortimer, R., 1999. Atmospheric input of nitrogen and phosphorus to the Southeast Mediterranean: sources, fluxes, and possible impact. *Limnology and Oceanography*, 44, 1683–1692.

Herut, B., Nimmo, M., Medway, A., Chester, R. and Krom, M.D., 2001. Dry deposition at the Mediterranean coast of Israel (SE Mediterranean): sources and fluxes. *Atmospheric Environment*, 35, 803-813.

Herut, B., Collier, R., and Krom, M. D., 2002. The role of dust in supplying nitrogen and phosphorus to the Southeast Mediterranean. *Limnol. Oceanogr.*, 47, 870–878.

Herut, B., Zohary, T., Krom, M.D., Mantoura, R. F. C., Pitta, P., Psarra, S., Rassoulzadegan, F., Tanaka, T. and Thingstad, T. F., 2005. Response of East Mediterranean surface water to Saharan dust: On-board microcosm experiment and field observations. *Deep-Sea Research II*, 52, 3024–3040.

Ho, K., Ho, S. S., Huang, R., Liu, S., Cao, J., Zhang, T., Chuang H., Chan C.S., Hu D., Tian, L., 2015. Characteristics of water-soluble organic nitrogen in fine particulate matter in the continental area of China. *Atmospheric Environment*, 106, 252-261.

Hopke, P. K., Xie, Y., Raunemaa, T., Biegalski, S., Landsberger, S., Maenhaut, W., Artaxo, P. and Cohen, D., 1997. Characterization of the Gent Stacked Filter Unit PM10 Sampler. *Aerosol Science and Technology*, 27, 726-735.

Huang, S., Rahn, K.A., Arimoto, R., 1999. Testing and optimizing two factor analysis techniques on aerosol at Narragansett, Rhode Island. *Atmospheric Environment*, 33, 2169–2185.

Jacobson, M.C., Hansson, H.C., Noone, K.J., Charlson, R.J., 2000. Organic atmospheric aerosols: review and state of the science. *Rev. Geophys.* 38, 267–294.

Jickells, 2006. The role of air-sea exchange in the marine nitrogen cycle. *Biogeosciences Discussions*, European Geosciences Union, 3 (1), 183-210.

Karakaş, D., I. Ölmez, S. Tosun, and G. Tuncel, 2004: Trace and Major Element Compositions of Black Sea Aerosol. *J. Radioanal. Nucl. Chem.*, 259, 187-192.

Keene, W., Montag, J., Maben, J., Southwell, M., Leonard, J., Church, T., Moody, J., Galloway, J., 2002. Organic nitrogen in precipitation over Eastern North America. *Atmospheric Environment*, 36(28), 4529-4540.

Kleanthous S., Vrekoussis M., Mihalopoulos N., Kalabokas P. and Lelieveld J., 2014. On the temporal and spatial variation of ozone in Cyprus, *Science of the Total Environment*, 476-477, 677-687.

Koçak M., Nimmo, M., Kubilay, N. and Herut, B., 2004a. Spatio-temporal aerosol trace metal concentrations and sources in the Leventine Basin of the Eastern Mediterranean. *Atmospheric Environment*, 38, 2133-2144.

Koçak, M., Kubilay, N. ve Mihalopoulos, N., 2004b. Ionic composition of lower tropospheric aerosols at a Northeastern Mediterranean site: implications regarding sources and long-range transport. *Atmospheric Environment*, 38, 2067-2077.

Koçak, M., Kubilay, N., Herut, B., Nimmo, M., 2005. Total and leachable atmospheric particulate fluxes of heavy metals (Al, Fe, Mn, Pb, Cd, Zn, Cu) over the Levantine Basin; a refined assessment. *Atmospheric Environment* 39, 7330–7341.

Koçak, M. 2006: Comprehensive chemical characterization of aerosols in the Eastern Mediterranean: Sources and Long range transport, Ph. D. thesis, Middle East Technical University, Institute of Marine Sciences, Erdemli, Turkey.

Koçak, M., Mihalopoulos, N., Kubilay, N., 2007. Chemical composition of the fine and coarse fraction of aerosols in the Northeastern Mediterranean. *Atmospheric Environment*, 41, 7351-7368.

Koçak, M, Mihalopoulos, N., Kubilay, N., 2009. Origin and source regions of PM10 in the Eastern Mediterranean atmosphere. *Atmospheric Research*, 92,464–474.

Koçak, M., Kubilay, N., Tuğrul, S., Mihalopoulos N., 2010. “Atmospheric nutrient inputs to the Northern Levantine basin from a long-term observation: sources and comparison with riverine inputs.” *Biogeosciences*, 7, 4037–4050.

Koçak, M., Theodosi, C., Zampas, P., Seguret, M.J.M., Herut, B., Kallos, G., Mihalopoulos, N., Kubilay, N., Nimmo, M., 2012. “Influence of mineral dust transport on the chemical composition and physical properties of the Eastern Mediterranean aerosol”. *Atmospheric Environment*, 57, 266-277.

Koçak, M., N. Mihalopoulos, E. Tutsak, C. Theodosi, P. Zampas, and P. Kalegeri, 2015. PM10 and PM2.5 composition over the Central Black Sea: Origin and seasonal variability. *Environ. Sci. Pollut. Res.*, 22, 18 076–18 092, doi: 10.1007/s11356-015-4928-2.

Koçak, M., N. Mihalopoulos, E. Tutsak, K., Violaki, C. Theodosi, P. Zampas and P. Kalegeri, 2016. Atmospheric Deposition of Macro Nutrients (DIN and DIP) onto the Black Sea and Implications on Marine Productivity. *J. Atmos. Sci.*, 73, 1727–1739, doi: 10.1175/JAS-D-15-0039.1.

Kouvarakis, G., Mihalopoulos, N., Tselepidis, A. and Stavrakaki, S., 2001. On the importance of atmospheric inputs of inorganic nitrogen species on the productivity of the eastern Mediterranean Sea. *Global Biogeochemical Cycles*, 15, 805–817.

Kouvarakis, G. and Mihalopoulos, N., 2002. Seasonal variation of dimethylsulfide in the gas phase and of methanesulfonate and non-sea-salt sulfate in the aerosols phase in the Eastern Mediterranean atmosphere. *Atmospheric Environment*, 36, 929-938.

Krom, M. D., Herut, B., and Mantoura, R. F. C. 2004. Nutrient budget for the Eastern Mediterranean: implications for P limitation, *Limnol. Oceanogr.*, 49, 1582–1592.

Krueger, B., Grassian, V., Cowin, J. and Laskin, A., 2004. Heterogeneous chemistry of individual mineral dust particles from different dust source regions: The importance of particle mineralogy. *Atmospheric Environment*, 38, 6253-6261.

Kubilay, N. and Saydam, C., 1995. Trace elements in atmospheric particulates over the Eastern Mediterranean: concentration, sources and temporal variability. *Atmospheric Environment*, 29, 2289-2300.

- Kubilay N., Nickovic S., Moulin C. and Dulac F., 2000. An illustration of the transport and deposition of mineral dust onto the eastern Mediterranean. *Atmospheric Environment*, 34, 1293-1303.
- Kubilay, N., Koçak, M., Çokacar, T. and Oğuz, T., 2002. "Influence of Black Sea and local biogenic activity on the seasonal variation of aerosol sulfur species in the eastern Mediterranean atmosphere". *Global Biogeochemical Cycles*, 16, NO. 4, 1079, doi: 10.1029/2002GB001880.
- Kubilay, N., Oğuz, T. and Koçak, M., 2005. Ground-based assessment of Total Ozone Mapping Spectrometer (TOMS) data for dust transport over the northeastern Mediterranean. *Global Biogeochemical Cycles*, 19, GB1022, doi: 10.1029/2004GB002370.
- Lee, E., Chan, C.K., Paatero, P., 1999. Application of positive matrix factorization in source apportionment of particulate pollutants in Hong Kong. *Atmospheric Environment*, 33, 3201–3212.
- Lewis WM Jr., 1981. Precipitation chemistry and nutrient loading in precipitation in a tropical watershed. *Water Resources Research*, 17: 169–181.
- Lowenthal, D.H., Chow, J.C., Mazzera, D. M., Watson, J.G. and Mosher, B.W., 2000. Aerosol vanadium at McMurdo Station, Antarctica: implications for Dye 3, Greenland. *Atmospheric Environment*, 34, 677-679.
- Loye-Pilot, M. D., J. M. Martin and J. Morelli, 1986. Influence of Saharan dust on the rain acidity and atmospheric input to the Mediterranean. *Nature*, 321, 427-428.
- Mace, K.A., Kubilay, N. and Duce, R.A., 2003a. Organic nitrogen in rain and aerosol in the eastern Mediterranean atmosphere: An association with atmospheric dust. *Journal of Geophysical Research*, 108, NO. D10, 4320, doi: 10.1029/2002JD002997.
- Mace, K.A., Duce R.A., Tindale N.W., 2003b. Organic nitrogen in rain and aerosol at Cape Grim, Tasmania Australia. *J. Geophys Res-Atmos*; 108:4338. *Atmospheric dust. Journal of Geophysical Research*, 108, NO. D10, 4320, doi: 10.1029/2002JD003051.
- Mace, K.A., Artaxo, P., Duce, R.A., 2003c. Water-soluble organic nitrogen in Amazon Basin aerosols during the dry (biomass burning) and wet seasons. *J. Geophys. Res.* 108, JD003557.
- Mamane, Y. and Gottlieb, J., 1989. Heterogeneous reactions of minerals with sulfur and nitrogen oxides. *Journal of Aerosol Science*, 20, 303-311.
- Mamane, Y. and Gottlieb, J., 1992. Nitrate formation on sea-salt and mineral particles-a single particle approach. *Atmospheric Environment*, 26A, 1763-1769.
- Markaki, Z., Oikonomou, K., Koçak, M., Kouvarakis, G., Chaniotaki, A., Kubilay, N., Mihalopoulos, N., 2003. "Atmospheric deposition of inorganic phosphorus in the Levantine Basin, eastern Mediterranean: spatial and temporal variability and its role in seawater productivity." *Limnology and Oceanography*, 48, 1557–1568.

Medinets, V. I., 1996. "Shipboard derived concentrations of sulphur and nitrogen compounds and trace metals in the Mediterranean aerosol". *The Impact of Desert Dust across the Mediterranean*, S. Guerzoni and R. Chester, Eds., Kluwer Academic Publishers, 359–368.

Medinets, S. and V. Medinets, 2012: Investigations of Atmospheric Wet and Dry Nutrient Deposition to Marine Surface in western Part of the Black Sea. *Turk. J. Fish. Aquat. Sci.*, 12, 497-505.

Mehta, A. and Yang, S., 2008. Precipitation Climatology over Mediterranean Basin from Ten Years of TRMM Measurements. *Journal of Advances in Geoscience*, 17, 87-91.

Mihalopoulos, N., Stephanou, E., Kanakidou, M., Pilitsidis, S. and Bousquet, P., 1997. "Tropospheric aerosol ionic composition in the E. Mediterranean region". *Tellus*, 49B, 1-13.

Mihalopoulos, N., Kerminen, V.-M., Kanakidou, M., Berresheim, H., Sciare, J., 2007. "Formation of particulate sulfur species (sulfate and methanesulfonate) during summer over the Eastern Mediterranean: a modelling approach". *Atmospheric Environment*, 41, 6860e6871.

Mishra, V.K., Kim, K.H., Hong, S. and Lee, K., 2004. Aerosol composition and its sources at the King Sejong Station, Antarctic peninsula. *Atmospheric Environment*, 38, 4069-4084.

Murphy, D.V., MacDonald, A.J., Stockdale, E.A., Goulding, K.W.T., Fortune, S., Gaunt, J.L., Poulton, P.R., Wakefield, J.A., Webster, C.P., Wilmer, W.S., 2000. Soluble organic nitrogen in agricultural soils. *Biol. Fertil. Soils* 30, 374–387.

Neff J., Holland E., Dentener F., McDowell W. and Russell K., 2002. "The origin, composition and rates of organic nitrogen deposition: A missing piece of the nitrogen cycle?" *Biogeochemistry*, 99-136.

O'Dowd C.D, Smith M.H, Consterdine I.E. and Lowe J.A., 1997. "Marine aerosol, sea-salt, and the marine sulfur cycle: A short review" *Atmospheric Environment*, 31, 73–80.

Özsoy, T. and Saydam, C., 2000. Acidic and alkaline precipitation in the Cilician Basin, north western Mediterranean sea. *The Science of the Total Environment*, 352, 93-109.

Paatero, P., 2007. User's Guide for Positive Matrix Factorization Programs PMF2 and PMF3, Part 1–2: tutorial. University of Helsinki, Helsinki, Finland.

Paatero, P., Tapper, U., 1994. Positive matrix factorization: a non-negative factor model with optimal utilization of error estimates of data value. *Environmetrics*, 5, 111–126.

- Paerl, H. W., 1993. Emerging role of atmospheric nitrogen deposition in coastal eutrophication: Biogeochemical and trophic perspectives. *Can. J. Fish. Aquat. Sci.* 50: 2254-2269.
- Paytan, A., Mackey, K.R.M., Mackey, Chen, Y., Lima, I.D., Doney, S.C., Mahowald, N., Labiosa, R., Post, A.F., 2009. "Toxicity of atmospheric aerosols on marine phytoplankton". *Proceedings of the National Academy of Sciences*, 106, 4601-4605.
- Peierls, B. J. and Paerl, H.W., 1997. Bioavailability of atmospheric organic nitrogen deposition to coastal phytoplankton. *Limnology and Oceanography* 42, 1819–1823.
- Pitta, P., Stambler, N., Tanaka, T., Zohary, T., Tselepides, A., and Rassoulzadegan, F., 2005. "Biological response to P addition in the Eastern Mediterranean Sea: the microbial race against time". *Deep-Sea Res. Pt. II*, 52, 2961–2974.
- Polissar, A., Hopke, P., Paatero, P., Malm, W. and Sisler, J., 1998. Atmospheric aerosol over Alaska 2. Elemental composition and sources. *Journal of Geophysical Research*, 103(D15), 19045-19057.
- Prospero, J.M., Barret, K., Church, T., Dentener, F., Duce, R.A., Galloway, J.N., Levy, H., Moody, J. and Quin, P., 1996. "Atmospheric deposition of nutrients to the North Atlantic Basin". *Biogeochemistry*, 25, 27-73.
- Raes, F., van Dingenen, R., Vignati, E., Julian Wilson, J., Putaud, J.P., Seinfeld, J.H. and Adams, P., 2000. "Formation and cycling of aerosols in the global troposphere." *Atmospheric Environment*, 34, 4215-4240.
- Ramanathan, V., Crutzen, P. J., Kiehl, J. T. and Rosenfeld, D., 2001. "Aerosols, climate, and the hydrological cycle". *Science*, 294, 2119–2124.
- Rendell, A.R., Ottley, C.J., Jickells, T.D., Harrison, R.M., 1993. The atmospheric input of nitrogen species to the North Sea. *Tellus* 45B: 53–63.
- Ridame, C. and Guieu, C., 2002. Saharan input of phosphate to the oligotrophic water of the open western Mediterranean Sea. *Limnology and Oceanography*, 47(3), 856–869.
- Rodriguez, S., Querol, X., Alastuey, A. Kallos, G. and Kakaliagou, O., 2001. Saharan dust contributions to PM10 and TSP levels in Southern and Eastern Spain. *Atmospheric Environment*, 35, 2433-2447.
- Rosenfeld, D., 2000. "Suppression of rain and snow by urban and industrial air pollution". *Science*, 287, 1793–1796.
- Russell, K.M., Galloway, J.N., Macko, S.A., Moody, J.L. and Scudlark, J.R., 1998. Sources of Nitrogen in Wet Deposition to the Chesapeake Bay Region. *Atmospheric Environment* 32: 2453–2465.
- Satheesh, S.K. and Moorthy, K. K., 2005. Radiative effects of natural aerosols: A review. *Atmospheric Environment*, 39, 2089–2110.

Saltzman, E.S., Savoie, D.L., Prospero, J.M. and Zika, R.G., 1986. Methanesulfonic acid and non sea salt sulfate in Pacific air: Regional and seasonal variations. *Journal of Atmospheric Chemistry*, 4, 227-240.

Savoie, D.L., Prospero, J.M., Arimoto, R. and Duce, R.A., 1994. Non sea salt sulfate and methanesulfonate at American Samoa. *Journal of Geophysical Research*, 99, No.D2, 3587-3596.

Saydam, A.C. and Senyuva, H.Z., 2002. Deserts: can they be the potential suppliers of bioavailable iron? *Geophysical Research Letters*, Vol. 29, No. 11, 10.1029/2001GL013562.

Sciare, J., Cachier, H., Oikonomou, K., Ausset, P., Sarda-Estève, R. and N., Mihalopoulos, 2003. Characterization of carbonaceous aerosols during the MINOS campaign in Crete, July–August 2001: a multi-analytical approach. *Atmospheric Chemistry and Physics Discussions*, 3, 3373-3410.

Seinfeld, J.H. and Pandis, S.N., 1998. *Atmospheric chemistry and physics: From pollution to climate change*. Wiley-Interscience, New York.

Seitzinger, S.P. and Sanders, R.W., 1999. Atmospheric inputs of dissolved organic nitrogen stimulate estuarine bacteria and phytoplankton. *Limnology and Oceanography* 44: 721–370

Simoneit, B., Kobayashi, M., Mochida, M., Kawamura, K., Huebert, B., 2004. Aerosol particles collected on aircraft flights over the northwestern Pacific region during the ACE-Asia campaign: composition and major sources of the organic compounds. *J. Geophys. Res.* 109, D19S09.

Spokes, L. J., Jickells, T. D. and Lim, B., 1994. Solubilisation of aerosol trace metals by cloud processing: A Laboratory study. *Geochimica Cosmochimica Acta*, 58, 3281-3287.

Tuomi, T.Y., Hopke, P. K., Paatero P., Basunia, M.S., Landsberger, S., Viisanen, Y. and Paatero, J., 2003. Atmospheric aerosol over Finnish Arctic: source analysis by the multilinear engine and the potential source contribution function. *Atmospheric Environment*, 37, 4381-4392.

Turley, C.M., 1999. The changing Mediterranean Sea — a sensitive ecosystem? *Progress in Oceanography*, 44, 387–400.

Underwood, G.M., Song, C. H., Phadnis, M., Carmichael, G.R. and Grassian, V.H., 2001. “Heterogeneous reactions of NO₂ and HNO₃ on oxides and mineral dust: A combined laboratory and modeling study”. *Journal of Geophysical Research*, 106(D16), 18,055– 18,066.

Usher, C. R., Michel, A. E. and Grassian, V. H., 2003a. Reactions on mineral dust. *Chemical Reviews*, 103, 4883-4939.

Viana, M., Pandolfi, M., Minguillon, M.C., Querol, X., Alastuey, A., Monfort, E.,

Celades, I., 2008. Inter-comparison of receptor models for PM sources apportionment: case study in an industrial area. *Atmospheric Environment*, 42, 3820–3832.

Violaki, K., Zarbas, P., Mihalopoulos, N., 2010. Long-term measurements of dissolved organic nitrogen (DON) in atmospheric deposition in the Eastern Mediterranean: fluxes, origin and biogeochemical implications. *Mar. Chem.* 120, 179-186.

Violaki K and Mihalopoulos N., 2010. Water Soluble Organic Nitrogen (WSO_N) in size-segregated atmospheric particles over the Eastern Mediterranean. *Atmospheric Environment.*, 44: 4339–45.

Violaki, K. and Mihalopoulos, N., 2011. Urea: An important piece of Water Soluble Organic Nitrogen (WSO_N) over the Eastern Mediterranean. *Science of the Total Environment*, 409(22), 4796-4801.

Violaki, K., Sciare, J., Williams, J., Baker, A.R., Martino, M. and Mihalopoulos, N., 2015. Atmospheric Water-Soluble Organic Nitrogen (WSO_N) over marine environments: A global perspective. *Biogeosciences*, 12, 3131-3140.

Vukmirovic, Z., Unkasevic, M., Lazic, L., Tomic, I., Rajsic, S. and Tasic, M., 2004. Analysis of the Saharan dust regional transport. *Meteorology and Atmospheric Physics*, 85, 265–273.

Wedyan, M., Fandi K. and Al-Rousan S. 2007. Bioavailability of Atmospheric Dissolved Organic Nitrogen in the Marine Aerosol over the Gulf of Aqaba. *Australian Journal of Basic and Applied Sciences*, 1(3), 208-212.

Wieprecht, W., Brüggemann, E., Müller, K., Acker, K., Spindler, G., ten Brink, H.M., Hitznerberger, R., and Maenhaut, W.: INTERCOMP2000: Ionic constitution and comparison of filter and impactor samples and its analysis, 2004, *Atmos. Environ.*, 38, 6477–6486.

Yang, X.H., Scranton, M.I., Lee, C., 1994. Seasonal variations in concentration and microbial uptake of methylamines in estuarine waters. *Mar. Ecol. Prog. Ser.* 108(3), 303–312.

Yücel, N., 2013. Monthly changes in primary and bacterial productivity in the north-eastern Mediterranean shelf waters. Ph. D. thesis, Middle East Technical University, Institute of Marine Sciences, Erdemli, Turkey.

Zamora, L. M., Prospero, J. M., & Hansell, D. A., 2011. Organic nitrogen in aerosols and precipitation at Barbados and Miami: Implications regarding sources, transport and deposition to the western subtropical North Atlantic. *J. Geophys. Res. Journal of Geophysical Research*, 116(D20).

Zhang, Y., Zheng, L., Liu, X., Jickells, T., Cape, N., Goulding, K., Fangmeier, A. and Zhang, F., 2008. "Evidence for organic N deposition and its anthropogenic sources in China." *Atmospheric Environment*, 42, 1035-1041.

Zohary, T., Herut, B., Krom, M., Mantoura, F., Pitta, P., Psarra, S., Rassoulzadegan, F., Stambler, N., Tanaka, T., Thingstad, F. and Woodward, M., 2005. P-limited bacteria but N and P co-limited phytoplankton in the Eastern Mediterranean—a microcosm experiment. *Deep-Sea Research II*, 52, 3011-3023.

